The Trace Metal Geochemistry of
Suspended Oceanic Particulate Matter

by

Robert M. Sherrell

B.A. Chemistry, Oberlin College

(1979)

SUBMITTED IN PARTIAL FULFILLMENT
OF THE REQUIREMENTS FOR THE DEGREE OF
DOCTOR OF PHILOSOPHY

at the

MASSACHUSETTS INSTITUTE OF TECHNOLOGY
and the
WOODS HOLE OCEANOGRAPHIC INSTITUTION

June, 1989

© Massachusetts Institute of Technology 1989

Signature of Author_____
      Department of Earth, Atmospheric and Planetary Sciences,
      Massachusetts Institute of Technology and the Joint Program in
      Oceanography, Massachusetts Institute of Technology/Woods Hole
      Oceanographic Institution, June, 1989

Certified by_____
      Edward A. Boyle, Thesis Supervisor

Accepted by_____
      Philip M. Gschwend, Chairman, Joint Committee for Chemical
      Oceanography, Massachusetts Institute of Technology/Woods Hole
      Oceanographic Institution

THE TRACE METAL GEOCHEMISTRY OF
SUSPENDED OCEANIC PARTICULATE MATTER

by
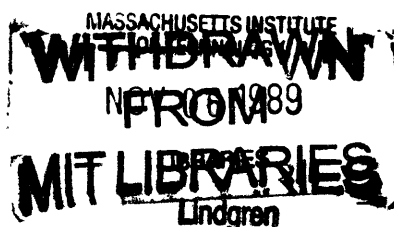
Robert M. Sherrell

Submitted to the Department of Earth, Atmospheric and Planetary Sciences
on May 5th, 1989 in partial fulfillment of the requirements for
the Degree of Doctor of Philosophy in Oceanography

ABSTRACT

Vertical profiles of suspended particulate trace metals were
measured in the Sargasso Sea near Bermuda and in the California Current,
northwest Pacific. Using a new in situ pump, sufficiently large samples
of particulate matter (order 10mg) were collected to allow measurement of
a suite of trace metals as well as major component elements, using
several different leaching techniques on separate subsamples.

Concentrations of particulate Cu, Zn, Co, Cd, Ni, and Pb near
Bermuda were determined to be substantially lower than estimates based on
previously published work. Concentrations of the more abundant elements
Al, Fe, and Mn were similar to previous estimates.

Vertical profiles of Mn, Co, Pb, Zn, Cu, and Ni (mol/l) at Bermuda
dispayed similar features: a relative depletion in surface waters, a
relative maximum in the upper thermocline, and relatively constant deep
water concentrations. The similarity in the vertical variations of
dissolved/particulate fractionation for these metals may be caused by
interaction of dissolved metals with authigenic Mn phases; the
fractionation is anti-correlated with other major particle components
(organic carbon, calcium carbonate, opal, and aluminosilicate). The
vertical profile of particulate Cd displayed a different form: enrichment
at the surface and decreasing concentrations through the thermocline to
constant deep water values.

These measurements were incorporated into a steady-state two-box
flux model for the Bermuda station. Estimates of the residence time of
small suspended particles suggest that metals associated with these
particles contribute less than half of the total flux observed in deep
ocean sediment traps. This result held for metals displaying a wide
variety of behaviors in their dissolved profiles, and suggests that
processes occurring in the upper ocean are more important determinants of
metal removal from the open ocean environment than dissolved/particulate
interactions in the deep ocean.

The interactions between suspended particulate and dissolved Pb were
investigated further by an analysis of the isotopic composition of Pb in
each pool. Profiles of particulate $Pb/^{210}Pb$ and $^{206}Pb/^{207}Pb$ were

virtually identical to contemporaneous seawater profiles for the same tracer ratios in the upper 2000m at Bermuda, indicating isotopic equilibration on a time scale which is rapid relative to the residence time of suspended particles in the water column (a few years), and to the time rate of change of the non-steady state dissolved profiles (years-decades). Analysis of the relative contribution of deep suspended particles to the total deep ocean downward flux suggests that the Pb isotopic composition of material delivered to the sediments will increasingly resemble that of deep ocean suspended matter as the anthropogenic input of Pb to the surface decreases over the next few years-decades. These results support a relatively rapid and reversible exchange of Pb between solution and particles.

The particulate metals distributions in the Sargasso Sea were compared with those observed at a station in the California Current, characterized by higher productivity, closer proximity to continental and hydrothermal particle sources, and the distinct dissolved metal distributions of the northwest Pacific. This provided an opportunity to observe the effect of bulk particle composition and dissolved metal concentration on dissolved/particulate metal fractionation. Although concentrations of non-aluminosilicate particulate metals were of the same order (generally within a factor of two) at the two stations, the differences are significant and are not generally proportional to differences in the dissolved distributions. Particulate contents of Mn, Co, and Cu are lower by a factor of 2-3 in mid-waters at the Pacific site, despite similar dissolved concentrations. In contrast, particulate concentrations of the nutrient-type elements Zn, Ni, and Cd were less than 50% greater at the Pacific station, although dissolved metal concentrations are several times higher. Of the metals investigated, only Pb showed similar dissolved/particulate fractionation at both stations. The evidence indicates that metal partitioning in the open ocean water column varies in response to factors which are outside the predictive capability of simple chemical exchange models.

ACKNOWLEDGMENTS

As I emerge from this thesis, and recover from what at times seemed like a solitary and arduous preoccupation, I feel especially grateful for the friends and family who saw me through it and lent support and guidance in more ways than I will be able to express here.

I thank Ed Boyle for being a demanding and caring teacher and advisor. After trying to follow his example for the last five (all right, six) years, I am finally getting an inkling as to how to be a good scientist. Thanks also to my committee members, Mike Bacon, Jim Bishop, Francois Morel, and Ed Sholkovitz for their interest and insight, especially in the final writing stages of this thesis. Mike made space for me to do the radiochemical analyses in his lab, where reside a particularly friendly and helpful crowd.

Thanks to everyone around the lab whose friendship and good cheer made up for the lack of windows. They are the real reason for coming in every day. Many helped as well in building and going to sea with the pumps, under conditions ranging from laborious to impossible. Gary Klinkhammer, John Trefry, Chris German, Erik Brown, Scott Doney, Phil Newton and Vernon Ross all gave invaluable assistance and good company at sea. Jim Bishop taught me everything I know about pumps, gave me some good design sense, and provided the impetus for starting this whole business. Mike Rhodes and Tony Sherriff were a great help on every trip to Bermuda, and finally, after about a dozen tries, found some nice weather to work in. John Edmond and Bill Simpson were very generous to invite me on their cruises and provide more than my share of deck time at sea.

Lex van Geen and I were office mates for most of this time, and kept each other company through the difficult periods. I've been impressed by his unique combination of motivation and joy, and enjoyed this time with him tremendously.

I thank my parents and my brothers for their support and confidence throughout this period. It was with my family that I learned the rudiments of oceanographic sampling, raking Irish moss in Cape Cod for three cents a pound (an hourly wage to which I aspire twenty years later).

The last year or so was brightened by the arrival of Maggie, who turns out to be a sporadic and inattentive seminar participant, but a lovely companion nevertheless.

Finally, I am forever grateful to Judy Storch, who stood by me with enthusiastic support and the warmest love during times which called only for toleration. She helped a great deal, as well, with the nitty-gritty of getting done, and with preserving a sense of fun which I think I can still match. I cherish the time we are together, and trust that there will now be more of it.

Dedicated to

J. A. S.

and to my parents

TABLE OF CONTENTS

LIST OF FIGURES

LIST OF TABLES

CHAPTER 1

INTRODUCTION

The influence of particles on the distribution of dissolved trace

metals in the ocean was recognized many years before the true

concentrations and the details of the distribution were known (Goldberg,

1954; Krauskopf, 1956). The concentrations of many minor elements were

known well enough at that time to determine that their concentrations

were lower than would be predicted based solely on the solubility of

their least soluble minerals. It was therefore proposed that interaction

with a constant rain of particulate matter through the oceanic water

column maintained the low concentrations by removing metals to the

sediments.

In the past 15 years, progress in determining accurate

concentrations of dissolved trace metals in the ocean has been rapid

(Bruland, 1983, and references therein). We now have a general knowledge

of the distribution of many trace metals between the surface and deep

waters, and between the major ocean basins (Wong et al., 1983). Broad

categories of elemental behavior have begun to emerge, all of which are

tied to interactions with oceanic particulate matter. Elements such as

Cd and Zn appear from their dissolved distributions to be strongly

influenced by processes which control the distributions of the major

nutrients (Boyle et al., 1976; Bruland et al., 1978; Bruland, 1980).

These "nutrient-type" metals are taken up by phytoplankton in surface

waters and are regenerated into solution at greater depths, where the

sinking biological material is decomposed. Other metals, such as Cu,

demonstrate strong interactions with particles at mid-depth, but are apparently returned to solution at the bottom. This causes the vertical profile of dissolved Cu to be concave upward in regions which are uncomplicated by additional sources introduced by horizontal advection (Boyle et al., 1977). A third group of metals are highly particle-reactive, and have residence times substantially shorter than the oceanic mixing time. Dissolved profiles of metals in this group, which includes Mn, Co, and Pb, do not display the bottom source evident for Cu, and are therefore thought to be removed on sinking particulate matter without substantial regeneration (Martin and Knauer, 1980; Knauer et al., 1982; Shaule and Patterson, 1981).

The major component phase composition and major element chemistry of the particles responsible for these behaviors is reasonably well known. Particulate matter in the open ocean is composed primarily of the organic and inorganic remains of surface-dwelling organisms, with a smaller lithogenic mineral component, and a very minor contribution from cosmogenic and anthropognic particles (Lal, 1977; Bishop et al., 1980). Major elements are thus Ca (as $CaCO_3$), Si (as opaline silica and lithogenic ordered silicates), and C (as organic compounds and carbonate). The minor element composition is not as well known. Accurate data exists on the particulate concentration and vertical flux of minor elements which are relatively abundant in oceanic particles, such as Al, Fe, Mn, and Ba (Orians and Bruland, 1986; Landing and Bruland, 1987; Bishop and Fleischer, 1987; Collier and Edmond, 1984; Bishop, 1988). However, very little is known about the concentration and distribution of less abundant trace metals on oceanic particulate matter. Measurements

of trace elements in surface plankton have been made in a few locations
(Martin and Knauer, 1973; Knauer and Martin, 1981; Collier and Edmond,
1984), and on sinking particles caught in sediment traps (Jickells et
al., 1984; Dymond and Collier, 1987; Martin and Knauer, 1986). However,
the trace element composition of suspended particles which comprise most
of the suspended mass and available surface area, and therefore might be
expected to dominate interactions with dissolved metals, is largely
unknown. A few studies have described the particulate distribution of
specific elements (e.g. V, Collier, 1984). One study, published ten
years ago, presented average intermediate and deep water particulate
metal concentrations, but no details of the distributions were reported
(Buat-Menard and Chesselet, 1979).

Much of what we know about interactions between dissolved and
particulate trace elements comes from studies of the partitioning of the
natural radionuclides ^{210}Pb, ^{210}Po, and the Th isotopes (Thomson and
Turekian, 1976; Bacon et al., 1978; Cochran et al., 1983; Bacon et al.,
1985). The distribution of dissolved and particulate Th, for example, is
consistent with a reversible exchange model where dissolved Th is
repeatedly taken up and released by suspended particles as the particles
are carried toward the sediments by large, fast-sinking aggregates (Bacon
and Anderson, 1982; Bacon et al., 1985). The extent to which Th serves
as an analog for the behavior of other trace metals is not clear from
available evidence. The mechanism by which dissolved/particulate
exchange occurs is also not well understood. While many investigators
have considered dissolved/particulate interactions to be surface chemical
processes (adsorption/desorption)(Balistrieri et al., 1981; Honeyman et

al., 1988), other types of interactions, such as ion exchange, (co-)precipitation, incorporation into insoluble mineral phases, and active biological uptake, may be equally important.

The goal of this research was to investigate dissolved/particulate interactions of trace metals by accurately determining suspended particulate trace metal distributions in distinct oceanic environments. Five broad questions form a framework for this research.

(1) What is the concentration and vertical distribution of suspended particulate trace metals in the open ocean?

(2) What controls the partitioning of trace metals between dissolved and suspended phases?

(3) What is the quantitative relationship between suspended particulate trace metals in the deep ocean and the total flux of metals observed in deep water sediment traps?

(4) How rapidly does exchange between dissolved and suspended particulate trace metals occur, relative to the residence time of the particles?

(5) How does trace metal partitioning vary with oceanographic regime?

To address these questions, I present detailed profiles of suspended particulate Al, Fe, Mn, Co, Zn, Cu, Ni, Cd, and Pb for stations in the Sargasso Sea and in the northeast Pacific. These studies required the development of a new particle sampling device, which is described in Chapter 2, along with the methods of analysis. The results of five occupations of station near Bermuda in the Sargasso Sea are presented in Chapter 3. This section defines the first accurate profiles of

particulate concentrations of many of these elements, and suggests

mechanisms by which the vertical particulate metal profile is maintained.

Particulate metal distributions are considered in light of known fluxes

of metals in deep water at this site in order to investigate particle

interactions in the deep ocean and the source of metals which are

transported to the bottom on fast-sinking particles. Chapter 4 reports

the dissolved and particulate distributions of stable Pb isotopes and the

ratio of Pb to ^{210}Pb at the Bermuda station. The results demonstrate

rapid isotopic equilibration between dissolved and suspended particulate

Pb. In Chapter 5, the Sargasso Sea results are compared to particulate

metal distributions measured at a station in the northeast Pacific in

order to understand factors which control the partitioning of trace

metals in these two distinct oceanographic regimes. Preliminary

investigation of suspended particulate trace metals in a transect of

stations extending from the contintental shelf to Bermuda, and in a

dispersed hydrothermal plume on the mid-Atlantic Ridge are presented in

Chapter 6. A brief concluding chapter summarizes the findings and

presents the implications of this work for the continuing investigation

of oceanic scavenging mechanisms.

REFERENCES

Bacon, M.P., Spencer, D.W. and Brewer, P.G. (1978) Lead-210 and
    polonium-210 as marine geochemical tracers: Review and discussion of
    results from the Labrador Sea. In: <u>Natural Radiation Environment III</u>
    (T.F. Gesell and W.F. Lowder, eds.), Vol. 1, pp. 473-501, U.S. Dept.
    Energy Report CONF-780422.

Bacon, M.P., Anderson, R.F., (1982) Distribution of thorium isotopes
    between dissolved and particulate forms in the deep sea, J. of
    Geophys. Res. 87, 2045-2056.

Bacon, M.P., Huh, C.-A., Fleer, A.P., Deuser, W.G. (1985) Seasonality in
    the flux of natural radionuclides and plutonium in the deep Sargasso
    Sea, Deep-Sea Res. 32, 273-286.

Balistrieri, L., Brewer, P.G., Murray, J.W., (1981) Scavenging residence
    times of trace metals and surface chemistry of sinking particles in
    the deep ocean, Deep-Sea Res. 28A, 101-121.

Bishop, J.K.B., Collier, R.W., Ketten, D.R., and Edmond, J.M. (1980) The
    chemistry, biology, and vertical flux of particulate matter from the
    upper 1500m of the Panama Basin, Deep-Sea Res. 27A, 615-640.

Bishop, J.K.B. and Fleisher, M.Q. (1987) Particulate manganese dynamics
    in gulf stream warm-core rings and surrounding waters of the N.W.
    Atlantic. Geochim. Cosmochim. Acta 51, 2807-2827.

Collier, R.W. (1984) Particulate and dissolved vanadium in the North
    Pacific Ocean. Nature 309, 441-444.

Collier, R. and Edmond, J. (1984) The trace element geochemistry of
    marine biogenic particulate matter. Prog. Oceanog. 13, 113-199.

Cochran, J.K., Bacon, M.P., Krishnaswami, S. and Turekian, K.K. (1983)
    Po-210 and Pb-210 distributions in the central and eastern Indian
    Ocean. Earth Planet. Sci. Lett. 65, 433-452.

Dymond, J. and Collier, R. (1987) Nares Abyssal Plain sediment flux
    studies. In: Subseabed disposal project annual report, physical
    oceanography and water column studies, S.L. Kupferman, ed., Sandia
    National Laboratories, Livermore CA pp B1-B24.

Goldberg, E.D. (1954) Marine geochemistry 1. Chemical scavengers of the
    sea. J. Geol. 62, 249-265.

Honeyman, B.D., Balistrieri, L.S., Murray, J.W., (1988) Oceanic trace
    metal scavenging: the importance of particle concentration, Deep-Sea
    Res. 35, 227-246.

Jickells, T.D., Deuser, W.G. and Knap, A.H. (1984) The sedimentation
    rates of trace elements in the Sargasso Sea measured by sediment
    trap. Deep-Sea Res. 31, 1169-1178.

Knauer, G.A.and Martin, J.H. (1981) Phosphorus-cadmium cycling in
    northeast Pacific waters. J. Mar. Res. 39, 65-78.

Knauer, G.A., Martin, J.H. and Gordon, R.M. (1982) Cobalt in north-east
    Pacific waters. Nature 297, 49-51.

Krauskopf, K.B., Factors controlling the concentration of thirteen rare
    metals in sea water, Geochim. Cosmochim. Acta 9, 1-32, 1956.

Lal, D. (1977) The oceanic microcosm of particles. Science 198,
    997-1009.

Landing, W.M. and Bruland, K.W. (1987) The contrasting biogeochemistry of
    iron and manganese in the Pacific Ocean. Geochim. Cosmochim. Acta,
    51, 29-43.

Martin, J.H. and Knauer, G.A. (1973) The elemental composition of
    plankton. Geochim. Cosmochim. Acta 37, 1639-1653.

Martin, J.H. and Knauer, G.A. (1980) Manganese cycling in northeast
    Pacific waters. Earth Planet. Sci. Lett. 51, 266-274.

Martin, J.H. and Knauer, G.A. (1986) VERTEX: Distributions and fluxes of
    Ag, Al, Ba, Cd, Co, Cr, Cu, Fe, Mn, Mo, Ni, Pb, V, and Zn in
    sub-oxic waters off Mexico. Earth Planet. Sci. Lett. unpublished
    manuscript.

Orians, K.J. and K.W. Bruland (1986) The biogeochemistry of aluminum in the Pacific Ocean. Earth Planet. Sci. lett. 78, 397-410.

Schaule, B.K. and Patterson, C.C. (1981) Lead concentrations in the Northeast Pacific: evidence for global anthropogenic perturbations. Earth Planet. Sci. Lett. 54, 97-116.

Wong, C.S., Boyle, E., Bruland, K.W., Burton, J.D. and Goldberg, E.D. (1983) Trace Metals in Sea Water, NATO Conference Series, Plenum Press, New York.

CHAPTER 2

METHODS: COLLECTION OF SUSPENDED OCEANIC PARTICULATE MATTER

FOR TRACE METAL ANALYSIS USING A NEW IN SITU PUMP

2.1. INTRODUCTION

The interaction between dissolved chemical constituents and fine

particles suspended in the ocean is an important control on the minor

element composition of seawater. In order to understand this

interaction, it is necessary to accurately sample and analyze both

seawater and suspended particles. Techniques for collection and analysis

of seawater samples for trace elements have advanced rapidly in the last

15 years, and we now have a basic knowledge of the concentration and

distribution of many trace metals dissolved in the world's oceans

(Bruland, 1983). The distribution of particulate trace metals, which

generally comprise a small fraction of the dissolved concentration, is

not as well known (Buat-Menard and Chesselet, 1979). Accurate knowledge

of the partitioning of trace metals between dissolved and particulate

forms at several representative oceanic stations would lead to a better

understanding of transformations between these two phases, and the

processes which result in vertical flux of metals out of the oceanic

system (Jickells et al., 1984; Dymond and Collier, 1987). This paper

describes a new device for collecting relatively large uncontaminated

samples of suspended oceanic particulate matter, and a procedure for

analysis of the particles for major constituent elements and trace

metals.

One of the difficulties to be overcome in collection of open ocean
suspended matter for chemical analysis is the low mass concentration and
consequent need to sample large volumes of seawater. The most commonly
used technique is ship-board filtration of a few to a few tens of liters
of water collected with conventional Niskin bottles (Brewer et al.,
1976). When clean room-type precautions and Go-Flo bottles are used in
sample handling, this procedure has been shown to work very well for
analysis of relatively abundant metals such as Al, Fe, and Mn (Landing
and Bruland, 1987; Orians and Bruland; 1986) and for some more
contamination-prone metals such as Zn (Bruland, pers. comm. 1989). The
disadvantage of this technique is that sample sizes are limited to a few
hundred micrograms at typical deep ocean particle concentrations,
restricting the number of different analyses or dissolution procedures
that can be carried out on each sample. In addition, bottle artifacts
(such as incomplete sampling due to rapid settling of particles in the
samplers, Gardner, 1977; Calvert and McCartney, 1979) can be minimized
(bottle inversion, re-orientation of sampling orifice) but are difficult
to evaluate. The rationale behind the design of the current sampler was
to increase sample size by 1-2 orders of magnitude over the bottle
technique, and to avoid ship-board contamination sources and possible
bottle artifacts by filtering the particles in situ with a submersible
pump.

The use of pumps as oceanographic sampling devices is not new.
Deck-mounted pumps have been used for some time for sampling particles in
the upper water column by sucking water through various lengths of tubing
(Beers et al., 1967; Lisitzin, 1972; Lenz, 1972; Jeffrey et al., 1973).

In situ pumps capable of collecting particles in the deep ocean have also been used to study the biological, mineralogical, chemical and radiochemical composition of suspended matter (Laird et al., 1967; Spencer and Sachs, 1970; Beer et al., 1974; Bacon and Anderson, 1982; Winget et al., 1982). Some of these devices are powered from the surface by means of an electro-mechanical cable and are capable of filtering up to 25,000 liters of seawater (Bishop and Edmond, 1976; Bishop et al., 1985). Another instrument couples battery-powered filtration with sensors which relay temperature, depth, light transmission and particle size fractionation data to the ship as the instrument is deployed (Simpson et al., 1987). The current design was conceived as a relatively simple sampling device which could be used on any vessel equipped with a standard hydrographic winch, incorporating design elements intended to minimize trace metal contamination of the particulate sample.

Here I present a detailed description of the new pump, called the Rotating Automatic Pump for Particulate Inorganics Determination (RAPPID), and a procedure for analysis of oceanic particulate matter for major elements (Ca, Al, Fe), phosphorus, opaline silica, the trace metals Mn, Co, Cu, Zn, Ni, Cd, and Pb, and the radionuclides ^{210}Pb and ^{210}Po. Three of these devices have been constructed and used successfully on seven oceanographic cruises to collect over 50 samples of particulate matter from volumes of 200-1500 liters to depths of 4000m. Results of the chemical analyses indicate that concentrations of particulate metals are, for several elements, much lower than previously estimated (see Chapter 3). Moreover, the observed variations with depth and

oceanographic regime clarify the role of suspended matter in geochemical cycling and removal of metals in the open ocean (Chapters 3-5).

2.2. INSTRUMENTATION

Two key features distinguish the new pump as a design especially suited for trace metal studies: (1) the entire unit mounts on a standard hydrowire so that it pivots like a weathervane, such that the filter holder and intake are oriented upstream of any particulate contamination from the wire or the metal components of the pump itself; (2) the filter holder and its mounting struts are constructed of plastics which have been shown to contribute minimal metal blanks in dissolved trace metal studies. The main components of the pump are mounted within a double box-shaped aluminum frame (Fig. 2.1 and 2.2). These consist of the battery unit, pump and motor unit, electronics pressure case, flow meters and, for certain configurations, stainless steel counterweights. The filter holder is mounted on plexiglas struts on the front of this frame, so that the intake is located about one meter laterally distant from the hydrowire. A large plastic and aluminum vane mounted on the back end serves to orient the intake into the ambient current. When the pump is turned on, water is sucked through the filters, passes through two flow meters, into the pump impeller, and is exhausted at the rear.

This section describes each of these components and outlines the deployment procedure. A summary of the performance specifications is given in Table 2.1.
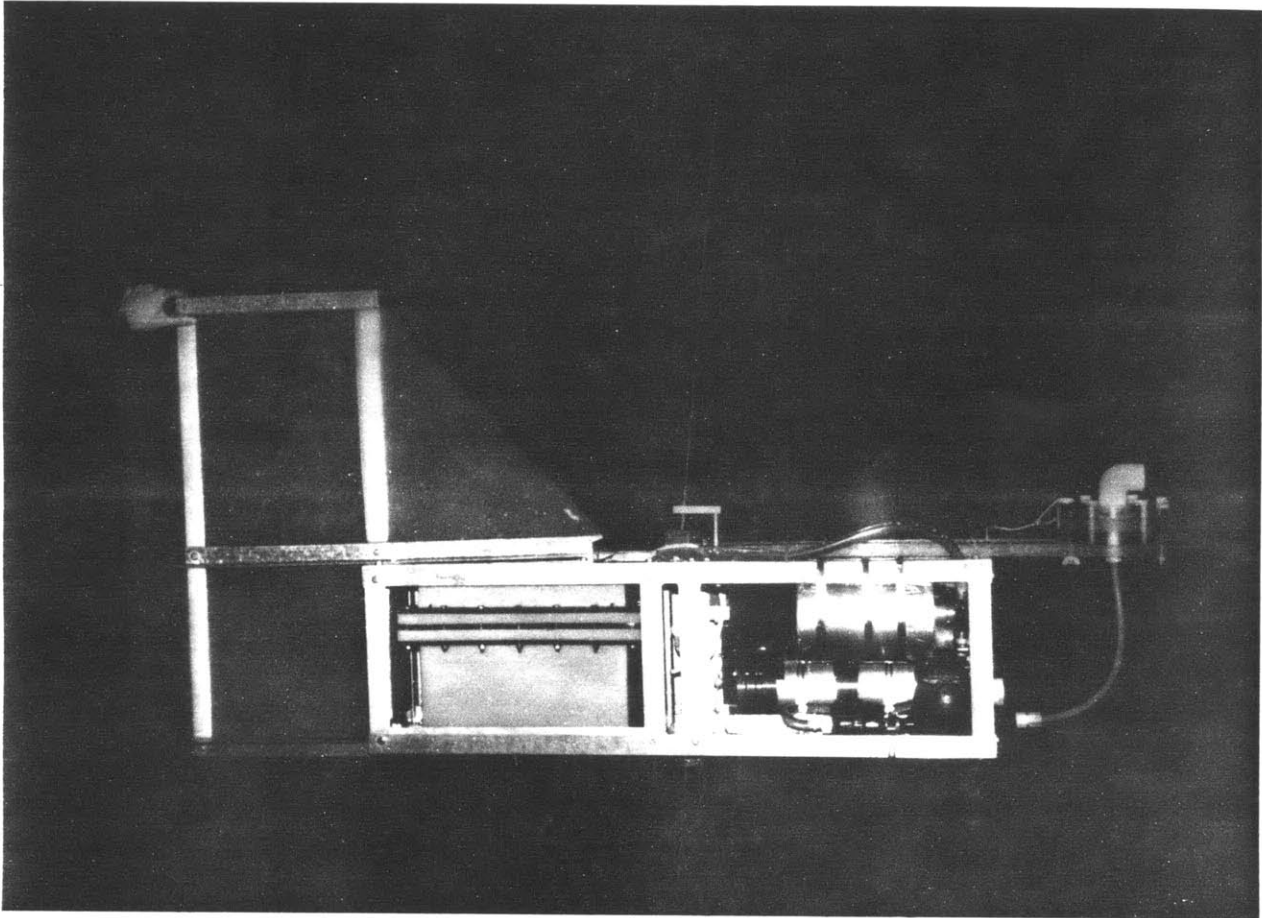
Fig. 2.1. Photograph of _in situ_ pump mounted on hydrowire.

FLOWMETERS   ┌─ HDPE WIRE SURROUNDS

└ ELECTRONICS PRESSURE CASE

◄─────── 190 cm ───────►

MESSENGER RELEASE

FILTER HOLDER

COUNTERWEIGHTS

VANE

PUMP →

38 cm

BATTERY

TEFLON BUSHING   STOP BLOCK
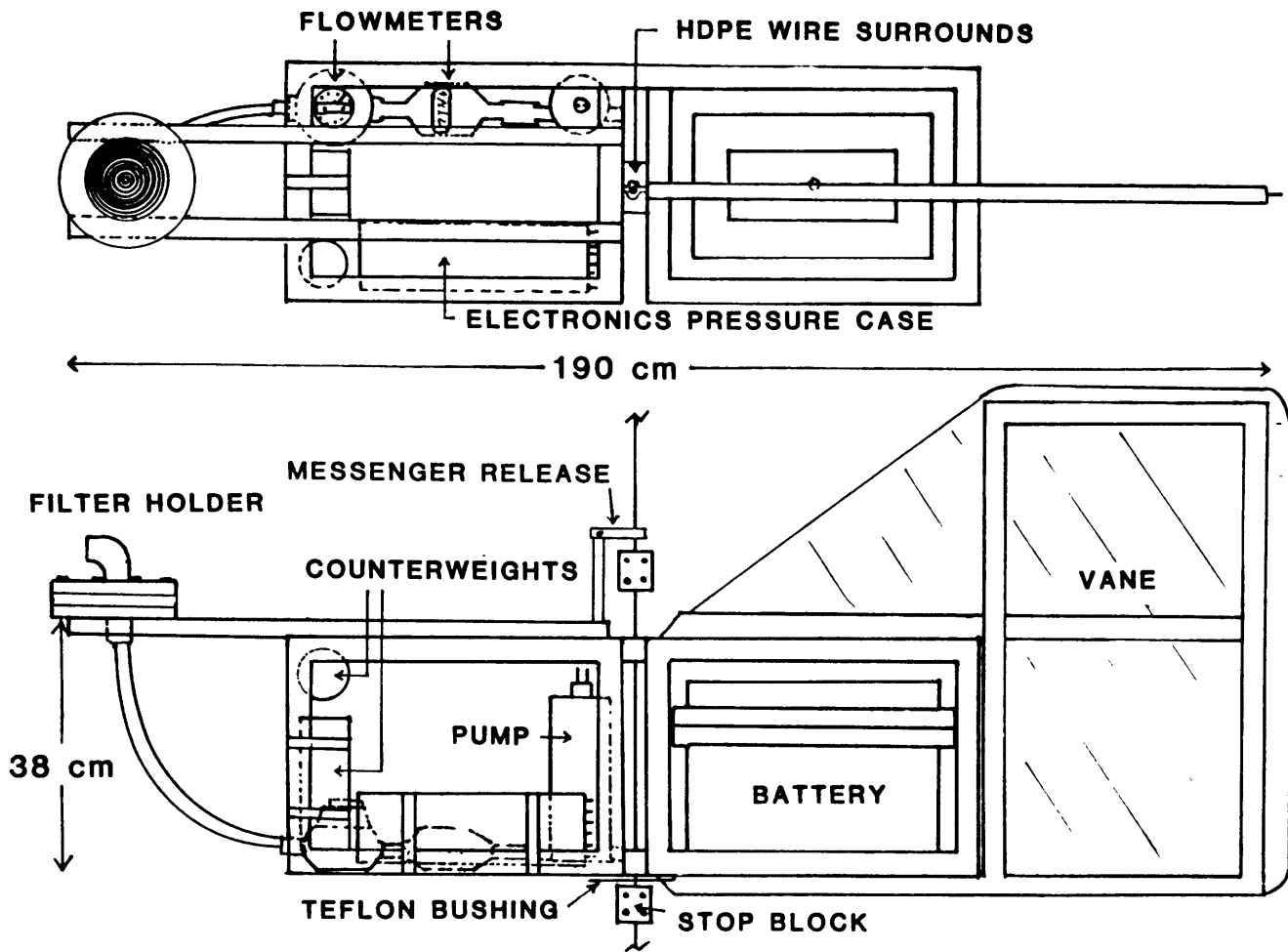
Fig. 2.2.   Schematic of pump construction and principal components.

Table 2.1. RAPPID performance specifications.

Weight: 80kg in air

Filter: 142mm, 127mm effective diameter

Maximum flow rate: ~7.5 1/min

Maximum face velocity: 1.0 cm/sec

Battery: 12V, 76AH or 24V, 38AH
         ~6 hrs pumping per charge cycle
         3 year battery life span

Maximum deployment depth: 6500m (limited by pressure housing)

Winch speed: 50 m/min

Structure and mounting. The frame consists of two symmetrical box-shaped units constructed of 1.5 x 1/8" structural aluminum (6061-T6 alloy) bolted together with 1/4" x 20 tpi stainless steel bolts (316 alloy). These are joined along one side and at the longitudinal axis, creating a lateral slot into which the hydrowire is positioned on mounting (Fig. 2.2). The wire is held at this central axis by four high-density polyethylene blocks, two of which are structural members in the frame, the other two being held in place with 1/4" toggle bolts which are inserted once the pump is in position. Stainless steel stop blocks are bolted firmly to the wire above and below the pump. The entire pump rests on the bottom block, with a Teflon sheet bushing in between to decrease pivoting friction and minimize abrasion of the aluminum frame. The upper block prevents the pump from riding up the wire during lowering or heavy ship roll. In water, the pump is dynamically balanced about the central wire, minimizing resistance to rotation so that orientation can be achieved even in slow currents.

Power. The RAPPID pump is powered by a pressure-compensated SeaBattery (Deep-Sea Power and Light, San Diego, California). This unit consists of two 12V, 38AH lead-acid suspended electrolyte batteries mounted in a rugged polyethylene box with a flexible, transparent polyurethane diaphragm in the lid. The box is filled with high-viscosity mineral oil for pressure compensation. Power is brought out through doubled conductors in an underwater connector which passes through the diaphragm. Two versions of the pump have been used, based on 12V or 24V wiring configurations. The battery is charged with 12V, 10A automotive chargers, used singly for the 12V application or wired in series for

charging the batteries in the 24V configuration. Line voltage to the chargers is controlled with a Variac transformer, allowing the charging amperage to be manually adjusted during the charge cycle. Charging is stopped when current falls below 1.0A, or when gas is observed emanating from the cells. A typical charging cycle took eight hours (for near full discharge), and was sufficient for 2-3 pump deployments.

Pump/Motor Unit. Two different pump/motor combinations have been used. The first is a 12V unit which runs in Bray oil and is fitted with a Jabsco flexible vane pump head (Pelagic Electronics, Falmouth, MA). A more recent version uses a 24V motor, pressure compensated with aviation-type hydraulic oil, mated to a rotating-disk positive displacement adjustable flow-rate pump head (Flotec) by means of an anodized aluminum housing with ceramic shaft seal (Oceanic Industries, Monument Beach, MA). These pumps have similar flow rate versus pressure differential characteristics, but the latter has proved somewhat more efficient (55VA vs. 75VA at full load) and more durable. Stainless steel counterweights are hose-clamped to the pump frame when the lighter 12V pump/motor is used, in order to maintain the fore/aft balance of the entire unit.

Flow meters. Two flow meters mounted in series downstream of the filter holder record total volume sampled and flow rate versus time data. The first (Kent Meters, model C-700, Ocala, FL) was modified to send electrical pulses to the electronics unit by mounting a small magnet on the rotating central spindle of the index, and fixing a matching reed switch to the index face (T. Hammar, pers. comm.). Flow through the

meter caused the switch to make and break a circuit to the control unit.
These pulses are recorded by the computer at the rate of 200 state
changes per gallon (52.8/liter). Flow rate decreases quasi-exponentially
with time due to filter loading (Fig. 2.3). The record of flow rate
evolution provides an indication of pump performance during the
deployment, serves as a diagnostic tool for locating pump failures, and
guides subsequent sampling so that the pump interval can be set to
optimize sample volume within ship time constraints.

The second flow meter was a different design (Kent Meters, model PSM
190, Ocala, FL) which was not readily adapted for telemetering but had
the advantage of a lower stall rate (1/8 gal/min vs. 1/4 gal/min). The
two meters provided replicate measurements of sample volume, and gave
equivalent results within the manufacturer's stated precision ($\pm$1.5%, at
flow rates exceeding stated stall rate). Discrepancies between the two
were noted only when flow rate fell below 1 l/min. In these cases,
volume indicated by the PSM 190 was assumed correct.

Electronic control. The pumping interval is controlled by an
independently powered Hewlett-Packard 41CX handheld computer mated to a
small input/output/control unit (CMT-200 Data Acquisition and Control
Unit, Corvallis Microtechnology, Corvallis, OR). The computer is pre-set
for on/off times by programming control alarms actuated by the built-in
time function in the HP 41CX. After some experience, the time required
for deployment can be estimated to within 20 minutes, so that little ship
time is lost. To save battery power, the computer is on only during the
pump interval, using a "wake-up" function actuated by the control alarm.
The control unit powers a relay, also contained within the pressure
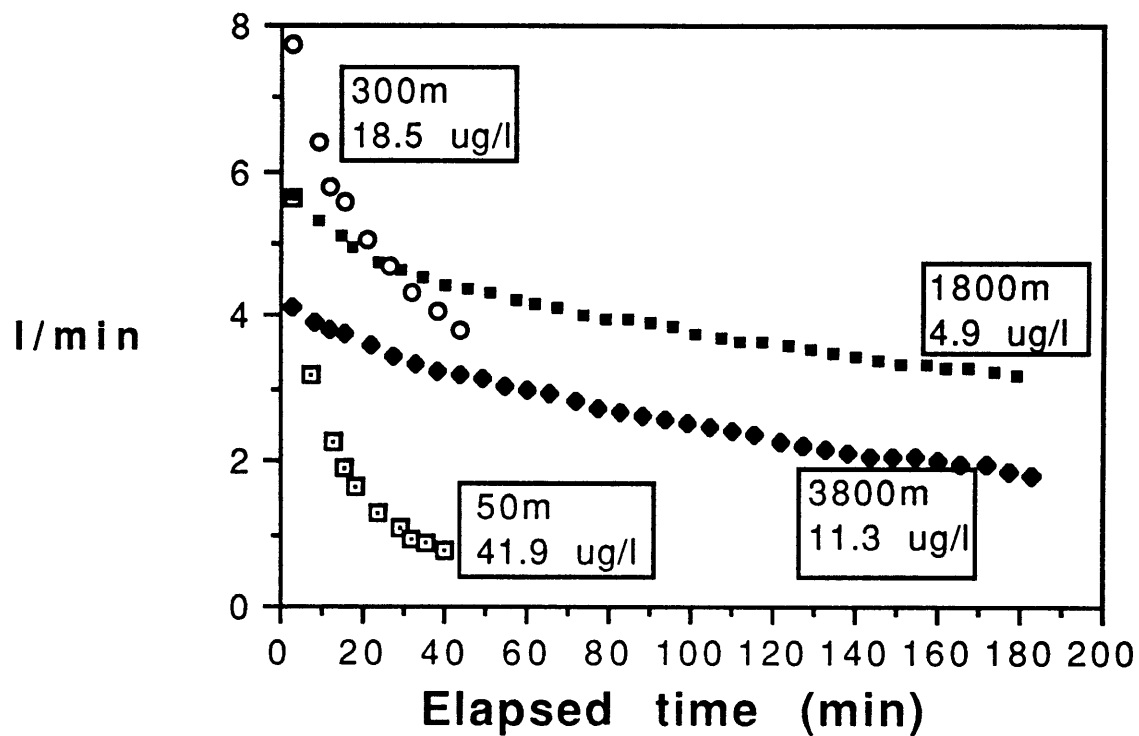
Fig. 2.3. Typical flow rate versus time curves for samples collected at various depths and <53 μm particle concentrations in the Sargasso Sea. Flow rate is a function of filter loading and the state of charge of the battery. The 3800m sample is in the nepheloid layer, approximately 400m above the bottom.

vessel, which carries primary current from the battery. An input channel on the control unit is connected to the flow meter circuit, and pulses are sub-totaled after a specified time interval (~5 min for a typical deployment) and recorded in data storage registers in the computer (Fig. 2.3). All of these functions are controlled by an operation program stored in computer memory. Upon retrieval of the pump, the pressure case is opened, and a data reduction program transfers recorded data (flow counts for each time interval, total counts, time on, time off) to a compatible thermal printer (Hewlett-Packard model 22143A).

Filter Holder. The RAPPID system is designed to be used with 142mm diameter filters, which were judged to be large enough to collect sufficient sample in a reasonable length of time while avoiding the handling difficulties of a larger standard size filter (e.g. 293mm). The filter holder is custom designed to optimize effective filter area and to minimize use of potentially contaminating materials. The two-stage holder consists of three acrylic plastic sections (Fig. 2.4). The base supports the primary filter on a 35 μm pore-size sintered polyethylene disk insert (Bel-Art). The middle section is simply an open ring which supports a prefilter, held only by tension around its perimeter. The top section incorporates a flow expansion chamber and a PVC intake elbow, with a 15.2 cm^2 orifice facing horizontally so that the pump does not act as a trap for rapidly sinking particles.

Silicone o-rings sit in glands machined in the upper faces of the bottom two pieces, such that they project 0.25 mm above the face of the holder. All three pieces are bolted together with six 1/2" Nylon bolts, and tightened with custom-made Lexan polycarbonate wrenches so that all

top section
(acrylic)

prefilter

prefilter support
(acrylic)

primary filter

sintered polyethylene support

silicone o-ring

primary filter support
(acrylic)
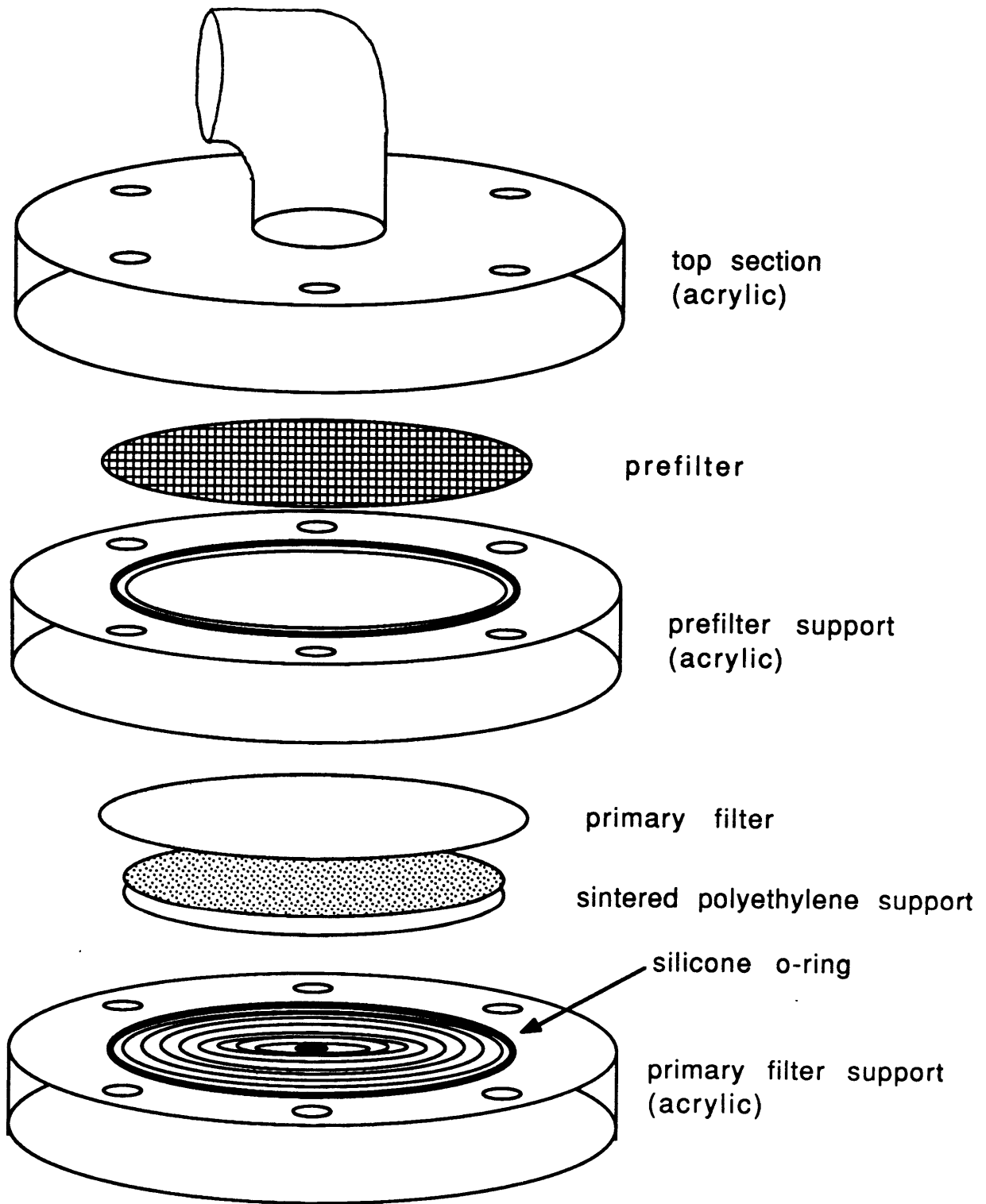
Fig. 2.4. Schematic of filter holder design.

faces contact firmly. This establishes a crisp edge to the sample area, so that subsamples can later be cut as accurate fractions of the total sample. Tightening also compresses the o-rings slightly, and water leakage is prevented by the o-ring's position on the low-pressure side of the primary filter. Effective filter area is 126.7 cm^2 (80% of total filter area). The assembled filter holder is connected to the flow meters by 1/2" polyethylene tubing and polypropylene compression fittings (Jaco).

In preparation for use, all parts of the filter holders are carefully washed, thoroughly rinsed, soaked in dilute HCl at 35°C for several days, and rinsed in distilled, deionized water. During use at sea, filter holders are rinsed between deployments with distilled, deionized water in a polyethylene squeeze bottle, using polyethylene gloves for all stages of handling .

Deployment procedure. The RAPPID is designed to be used in multiple-pump casts, so that several-depth profiles can be obtained in one cast. Up to three pumps have been deployed simultaneously in seas up to 6m high without undue difficulty. In calmer weather, it is expected that several more pumps could be deployed on a single cast, increasing sampling efficiency.

In preparation for a cast, filter holders are loaded with clean filters in a laminar flow clean bench, bolted together, sealed with a clean polyethylene plug inserted in the intake, and stored temporarily in clean zip-lock polyethylene bags. Computers are set for pump interval and sealed inside the pressure cases, which are purged with compressed Freon to prevent condensation of water vapor on the electronic

components. Pressure cases are attached to the pump frames, initial flow meter readings are recorded, and the bottom stop block is affixed to the hydrowire. When the pump is ready for deployment, the filter holder is removed from its storage bag, attached to the struts with acid-cleaned Nylon wing-bolts, connected to the pump plumbing, and re-covered with a larger polyethylene bag. The weight of the pump (over 50% of which is due to the battery) requires it to be lifted into position on the wire using a block and tackle. The wire is captured in position by fixing the removable plastic blocks in place, and the lifting tackle is removed. The top stop block is bolted to the wire, and a messenger is attached to a release mechanism on the pump frame (Fig. 2.2).

To minimize the possibility of airborne contamination reaching the filters, the protective plastic bag and intake plug are removed only moments before the pump is submersed. Winch speed is limited to 50 m/min to avoid kiting, although faster speeds have occasionally been used without mishap.

The pumping interval varies from 40 minutes to 3 hours, depending on anticipated particle concentration and filter clogging rate. Sampling depth is estimated by use of reversing thermometers attached to Niskin bottles which are mounted 10m above or below the pumps. These are tripped by dropping a messenger at the mid-point of the pumping interval. Additional bottles have been mounted at other depths to combine water and particle collection in a single cast. Upon retrieval, the plastic intake plugs are replaced immediately as the pumps emerge from the water, and the pumps are removed from the wire. Filter holders are immediately removed for disassembly in a laminar flow clean bench, the flow meter

indexes are read, the pressure cases are removed and opened, and computers are withdrawn for data retrieval.

2.3. SAMPLE HANDLING AND ANALYSIS

Filter cleaning, drying and weighing. The filters used in this work are chosen for an optimum combination of low metal blank, low water absorption (for precise mass determination), and reasonably high flow rate. The standard filters used are a 1.0 μm pore size 142mm diameter Nuclepore polycarbonate primary filter, and a 53 μm mesh size square weave polyester prefilter cut from bulk material (Pecap, #7-53/2, Tetko, Briarcliffe Manor, NY). Control of trace metal blank levels requires that they be carefully cleaned and handled only with acid-cleaned Teflon forceps and polyethylene gloves in a laminar flow clean bench.

Filters are cleaned in batches of 25 by placing them in 1 liter polyethylene bottles, filling with ~1 N HCl (reagent grade, in distilled deionized water), and heating in an oven at 60°C overnight. The acid is then decanted to waste, and the bottles filled with distilled deionized water and allowed to sit for ~1 hour. This solution is then decanted to waste, and the filters are rinsed five times in the bottles with distilled deionized water, swirling and inverting the bottles each time. The filters are then removed to a large, clean polyethylene beaker in a laminar flow clean bench and allowed to sit in additional distilled deionized water. They are then removed, drip-dried, and transferred one at a time to acid-cleaned 150mm diameter polystyrene Petri dishes. The lids are placed loosely ajar on the dishes and the filters are allowed to dry overnight at room temperature in the laminar flow clean bench.

Dried filters are weighed to constant weight ($\pm$0.1mg) using an analytical balance (Mettler H31), controlling electrostatic interactions with two α-source anti-static strips positioned in the weighing cabinet. Filters are prevented from contacting the stainless steel weighing pan by placing a 152mm diameter acid-cleaned Teflon mesh disk on the pan. Typical mass for primary and prefilter is 180 and 640 mg, respectively. Filters are returned to the labeled Petri dishes, which are then sealed individually in zip-lock polyethylene bags, and in batches in larger bags for tranporting to sea.

Shipboard procedures. At sea, filters are carefully mounted in the filter holders immediately before use. Upon recovery, filter holders are rid of excess seawater using a vacuum line attached to a clean length of polyethylene tubing. Within three hours of recovery, the holders are disassembled and the filters rinsed to remove residual seawater. For the primary filters, this is accomplished by attaching the filter holder base, with the filter left in position, directly onto a vacuum rinsing apparatus by means of a short piece of clean polyethylene tubing. The filter is rinsed with ~125ml of pH 8.3 distilled water (adjusted with pre-cleaned NaOH), which is gently dripped through the filter in a repeating spiral fashion under moderate vacuum, so that the entire surface is uniformly rinsed. The rinse solutions run into acid-cleaned 250ml polyethylene bottles mounted within the rinsing apparatus. These solutions are then acidified with 0.5 ml 3x Vycor-distilled 6 N HCl, and treated as dissolved trace element samples. Any loss of metal from the particulate matter during rinsing can be determined by analysis of these "rinsates" (Appendix C).

The prefilters are then placed on the same holder base and rinsed in the same manner, still within the laminar flow bench. Both filters are then returned to their original Petri dishes and allowed to dry for several hours in the laminar flow bench before being sealed as before. During transport back to the laboratory, samples are kept level to prevent dislodging of particulate material from the filter surface.

Laboratory filter handling. Upon return to the laboratory, the filters are re-dried for several days in a desiccator. Filters are rapidly transferred from the desiccator (placed in a laminar flow bench) to the balance, and sample weights are determined by re-weighing the filters as before (this time in a desiccated weighing cabinet). Blank filters are carried through the entire operation, and average differences between pre- and post-sampling weights for these filters were used to correct final weights for changes in the mass of the filter material itself due to water absorption. This correction was less than ± 0.2 mg for Nuclepore filters, but was larger (± 1.0mg) for the more absorbent pre-filters. This method was used instead of equilibration with ambient room air to prevent erroneously high sample dry weights due to water absorption by the particles or by residual seasalt. Within each weighing batch, several filters are re-weighed to determine reproducibility. Corrections for the mass of residual seasalt were made by analyzing filter sub-samples for Na (see below), and assuming seawater major ion composition. Salt corrections are generally less than 5% of particle mass and are often negligible (<1%). Typical sample masses were 4.0 - 18.0 $\pm$ 0.2 mg of <53μm material, and 0.5-2.0 $\pm$ 0.5 mg of >53μm material.

These studies are concerned with the composition of small, slowly sinking particles rather than the larger, rarer, fast-sinking particles, represented by the >53 μm prefilter fraction. Therefore the purpose of the prefilter in this study was to separate the larger fraction from the smaller particles which were the primary interest. Only the <53 μm fraction, which comprised 75-94% of total particulate mass, was prepared for chemical analysis. Analysis of the >53μm fraction would enable a better understanding of exchange of metals among particle size classes, but blank levels are too high to allow accurate analysis of any but the most abundant elements (e.g. Al and Fe), unless a method of quantitatively removing the particles from the filter could be devised (Table 2.2). The primary filter was subsampled by using a small polystyrene template and a stainless steel scalpel to cut known-area squares for various treatments. One contribution to the total uncertainty of the analyses is therefore associated with the homogeneity of particle distribution across the face of the filter. Sub-sampling repoducibility was estimated at $\pm10\%$, based on analyses of replicate sub-samples, subtracting the analytical error determined by replicate analyses of single sub-sample digest solutions. Occasionally, visible redistribution of the particles occurred during pump retrieval, and replicates on these samples gave $\pm25\%$ subsampling reproducibility.

Analytical procedures. Filter sub-samples were prepared for chemical analysis using several different dissolution procedures. For trace metals, Ca, Al, Fe, ^{210}Pb, and ^{210}Po analyses, two subsamples (8.3% of total filter area, cut from radially opposed positions on the filter face) were placed in a 7 ml flat-bottom screw-cap Teflon PFA vial

Table 2.2. Filter blanks, reagent blanks and analytical
           precision.

Element	Filter blank[a]		Reagent blank[b] (as nmol/filter)	Analytical[c] precision
	Primary (nmol/filter)	Prefilter		
Ca	ND	--	40	1%
Al	20	--	20	4%
Fe	5	2.0	5	5%
Mn	0.1	--	0.1	2%
Co	0.04	--	0.04	4%
Zn	0.4	1.0	0.1	10%
Cu	0.3	--	0.3	4%
Ni	1.6	--	0.1	3%
Cd	0.001	0.003	ND	4%
Pb	0.03	0.04	0.02	3%

a) Primary is mean for unused Nuclepore 142mm 1.0μm pore size, acid
    cleaned. Prefilter is mean for unused 142mm 53μm mesh Pecap
    polyester.

b) combined acid plus procedural blank, expressed as equivalent per
    filter.

c) estimated percent uncertainty, based on replicate analyses of single
    digest solutions, primary filter only.

ND = not detectable

-- = not determined

(Savillex). Acid-cleaned Teflon forceps were used to maneuver the filter squares within the vial such that they adhered by electrostatic attraction to opposite walls of the vial, particle side inward. With the filter pieces so positioned, 0.5ml of 3x Vycor-distilled concentrated HNO_3 was added in 100 μl aliquots, dripping these down the faces of the filter to initiate dissolution and further adhere the filters to the wall. To assure complete dissolution of refractory mineral phases, 20 μl of sub-boiling distilled concentrated HF was then added. The vials were tightly capped, weighed, and placed on a hotplate to fume/reflux for 4 hours. With proper temperature regulation, refluxing down the faces of the filter pieces did not lead to total destruction of the polycarbonate matrix, simplifying subsequent handling. After cooling, vials were re-weighed to correct for loss of acid (generally <0.5%), and were diluted with 2.0 ml of distilled, deionized water.

The dilution step was adopted after the discovery of a precipitate phase apparently present in some undiluted digest solutions. The precipitate was never visible, but its presence was suspected when poor reproducibility was noticed during analysis of replicate aliquots for Al. To test this possibility, digest solutions were transferred to an acid-cleaned 1.5 ml microcentrifuge tube and spun for a few minutes. Small aliquots (10μl) were then removed from the solution surface and from the conical bottom of the tube, where a pellet would be located if one were visible. These were analyzed for Al again. Al concentrations in the pellet aliquot were >10 times higher than the supernatant aliquot, which had an Al concentrations roughly equivalent to that of a dipped blank. Subsequent aliquots pipetted from the bottom of the same tube

gave lower concentrations, appoaching that of the supernatant. Analysis of calcium in the "pellet" aliquots indicated Ca/Al ratios of ~3.5 mol/mol, more than an order of magnitude higher than the ratio for aluminosilicates. This suggested that the solid phase was not the result of incomplete dissolution of refractory mineral particles. It was concluded that Al was probably adsorbing to a fine precipitate, most likely CaF_2. Dilution by a factor of five apparently caused a sufficient decrease in the solubility product to redissolve the solid. The centrifuge test on diluted solutions gave equal aluminum concentrations for "pellet" and "supernatant" aliquots.

Diluted digest solutions were analyzed for Na, Al, Fe, Mn, Co, Cu, Zn, Ni, Cd and Pb by graphite furnace atomic absorption spectroscopy, using additional dilutions as necessary and standardizing by the method of standard additions. Most analyses were carried out on a Perkin-Elmer 5000 equipped with with continuum source background correction, HGA 400 furnace controller, and AS-40 autosampler. A Perkin-Elmer Zeeman/5000 with HGA 500 furnace controller was used for Co and some Zn determinations because furnace blanks were lower for these elements on this particular instrument (not because Zeeman effect background correction was necessary). Ca was determined by diluting $100\mu l$ of digest solution to 5.0ml in dilute HCl/HNO_3 (La added as an ionization suppressant), and analyzing against matrix-matched standard solutions using flame atomic absorption spectrophotometry (Perkin-Elmer 403). Long-term secondary standards were maintained throughout this work. Analytical precision was determined by replicate analyses of single solutions. Blanks were determined on unused filters and on "dipped"

blanks, filters which were treated identically to a normal sample, including submergence on a pump, but had not had water drawn through them. On two occasions, additional "dipped" blanks were inadvertantly collected as a result of an electrical failure in the pump. A summary of analytical precision and blank values is given in Table 2.2.

For ^{210}Po and ^{210}Pb determination, portions of digest solutions from three separate subsample pairs, equivalent to 20% of the total sample, were pooled, spiked with ~10 dpm ^{209}Po yield monitor and 4.0 ml 70% $HClO_4$, and heated to near dryness in a Teflon beaker. After redissolution in 2.0M HCl, ^{210}Po and ^{209}Po were autoplated on silver disks following the method of Fleer and Bacon (1984). Alpha counting of the plated Po isotopes was performed on an alpha spectrometer fitted with low-background detectors. ^{210}Pb was determined after 6-12 months ingrowth by measuring the ingrown daughter ^{210}Po. Because ^{210}Po activity on oceanic particulate matter is generally several times greater than ^{210}Pb activity (Bacon et al., 1978), counting times of 1-2 days were sufficient to accumulate >500 counts on the first plating. For the ingrown ^{210}Po determination, however, 3-5 days counting time was required to obtain adequate counting statistics. Uncertainty due to counting statistics was <5%, except for a few low-Pb surface samples. Stable Pb was determined on each digest solution before pooling, so that accurate $Pb/^{210}Pb$ ratios could be determined.

Particulate phosphorus and opaline silica were determined on separate, smaller pairs of subsamples (2.4% of total sample). Phosphorus was liberated as inorganic phosphate by wet oxidation in perchloric acid using a micro adaptation of the procedure of Strickland and Parsons

(1968). Amorphous silica was selectively dissolved by leaching in 0.7M Na_2CO_3 at 90°C for four hours (Eggimann et al., 1980). This treatment should leave ordered silicates largely undissolved. Leachates were neutralized and analyzed colorimetrically in a narrow 1 cm cell, using a micro adaptation of the standard seawater method (Strickland and Parsons, 1968).

2.4. SUMMARY

A new in situ pump has been designed which filters trace metal-clean particulate samples from volumes of the order of 1000 liters. It is reliable and simple to use, requiring ordinary oceanographic deck hardware, and can be deployed to full ocean depth. Three such RAPPID pumps have been built, and have been used to collect >50 particulate samples from the North Atlantic and North Pacific oceans.

These samples have been analyzed for a suite of trace metals, as well as major constituent elements, using wet digestion techniques combined with atomic absorption and UV/VIS spectrometry. This new technique has enabled the first accurate determination of the suspended particulate concentrations of several trace metals in the open ocean. The results and implications of this work are presented in the following chapters.

REFERENCES

Bacon, M.P., D.W. Spencer, and P.G. Brewer (1978) Lead-210 and
    polonium-210 as marine geochemical tracers: Review and discussion of
    results from the Labrador Sea. In: Natural Radiation Environment III
    (T.F. Gesell and W.F. Lowder, eds.), Vol. 1, pp. 473-501, U.S. Dept.
    Energy Report CONF-780422.

Bacon, M.P.and R.F. Anderson (1982) Distribution of thorium isotopes
    between dissolved and particulate forms in the deep sea. J. Geophys.
    Res. 87, 2045-2056.

Beer, R.M., J.P. Dauphin and T.S. Sholes (1974) A deep-sea in situ
    suspended sediment sampling system. Marine Geol., 17, M35-M44.

Beers, J.R., G.L. Stewart and J.D.H. Strickland (1967) A pumping system
    for sampling small plankton. J. Fish. Res. Bd. Canada, 24,
    1811-1818.

Bishop, J.K.B. and J.M. Edmond (1976) A new large volume filtration
    system for the sampling of oceanic particulate matter. J. Marine
    Res. 34, 181-198.

Bishop, J.K.B., D. Schupack, R.M. Sherrell and M.H. Conte (1985) A
    multiple unit large volume in-situ filtration system (MULVFS) for
    sampling oceanic particulate matter in mesoscale environments. In:
    Mapping Strategies in Chemical Oceanography, A. Zirino, ed.,
    Advances in Chemistry Series, American Chemical Society, Vol. 29,
    pp. 155-175.

Brewer, P.G., D.W. Spencer, P.E. Biscaye, A. Hanley, P.L. Sachs, C.L.
    Smith, S. Kadar and J. Fredricks (1976) The distribution of
    particulate matter in the Atlantic Ocean. Earth Planet. Sci Lett.
    32, 393-402.

Bruland, K.W. (1983) Trace elements in sea-water, in Chemical
    Oceanography Vol. 8, J.P. Riley, R. Chester, eds., Academic Press,
    pp.158-220.

Buat-Menard, P., R. Chesselet (1979) Variable influence of the
    atmospheric flux on the trace metal chemistry of oceanic suspended
    matter. Earth Planet. Sci. Lett. 42, 399-411.

Calvert, S.E. and M.J. McCartney (1979) The effect of incomplete recovery
    of large particles from water samplers on the chemical composition
    of oceanic particulate matter. Limnol. Oceanogr. 24, 532-536.

Cochran, J.K., H.D. Livingston, D.J. Hirschberg, L.D. Surprenant (1987)
    Natural and anthropogenic radionuclide distributions in the
    northwest Atlantic Ocean. Earth Planet. Sci. Lett. 84, 135-152.

Dymond, J. and R. Collier (1987) Nares Abyssal Plain sediment flux studies. In: Subseabed disposal project annual report, physical oceanography and water column studies, S.L. Kupferman, ed., Sandia National Laboratories, Livermore CA pp B1-B24.

Eggimann, D.W., F.T. Manheim and P.R. Betzer (1980) Dissolution and analysis of amorphous silica in marine sediments. J. Sediment. Petrol. 50, 215-225.

Fleer, A.P. and M.P. Bacon (1984) Determination of Pb-210 and Po-210 in seawater and marine particulate matter. Nuc. Instrum. Meth. Phys. Res. 223, 243-249.

Folsom, T.R., N. Hansen, T.J. Tatum and V.F. Hodge (1975) Recent improvements in methods for concentrating and analyzing radiocesium in seawater. J. Radiation Res., 16, 19-27.

Gardner, W.D. (1977) Incomplete extraction of rapidly settling particles from water samples. Limnol. Oceanog. 22, 764-768.

Hess, F.R. (1977) Stream powered, large volume deep ocean sampler. Woods Hole Oceanogr. Inst. Invention Disclosure 214-ERDA Docket S-47, 453.

Jeffrey, L.M., A.D. Fredericks and E. Hillier (1973) An inexpensive deep-sea pumping system. Limnol. Oceanog. 18, 336-340.

Jickells, T.D., W.G. Deuser, A.H. Knap (1984) The sedimentation rates of trace elements in the Sargasso Sea measured by sediment trap. Deep-Sea Res. 31, 1169-1178.

Laird, J.C., D.P. Jones and C.S. Yentsch (1967) A submersible batch filtering unit. Deep-Sea Res., 14, 251-252.

Landing, W.M. and K.W. Bruland (1987) The contrasting biogeochemistry of iron and manganese in the Pacific Ocean. Geochim. Cosmochim. Acta, 51, 29-43.

Lenz, J. (1972) A new type of plankton pump on the vacuum principle. Deep-Sea Res., 19, 453-461.

Lisitzin, A.P. (1972) Sedimentation in the world oceans. S.E.P.M. Spec. Publ. 17, 218pp.

Orians, K.J. and K.W. Bruland (1986) The biogeochemistry of aluminum in the Pacific Ocean. Earth Planet. Sci. lett. 78, 397-410.

Simpson, W.R., T.J.P. Gwilliam, V.A. Lawford, M.J.R. Fasham and A.R. Lewis (1987) In situ deep water particle sampler and real-time sensor package with data from the Madeira Abyssal Plain. Deep-Sea Res., 34, 1477-1497.

Spencer, D.W. and P.L. Sachs (1970) Some aspects of the distribution, chemistry, and mineralogy of suspended matter in the Gulf of Maine. Marine Geol. 9, 117-136.

Strickland, J.D.H. and T.R. Parsons (1968) A Practical Handbook of Seawater Analysis. Bull. 167, Fisheries Research Board of Canada, Ottowa.

Winget, C.L., J.C. Burke, D.L. Schneider and D.R. Mann (1982) A self-powered pumping system for in situ extraction of particulate and dissolved materials from large volumes of seawater. Woods Hole Oceanog. Inst. Technical Report WHOI 82-8, Woods Hole, Mass., 16pp.

CHAPTER 3

TRACE ELEMENT COMPOSITION OF SUSPENDED PARTICULATES IN THE NORTHWEST

ATLANTIC OCEAN

3.1. Introduction

The interaction of dissolved trace metals with particles suspended

in seawater, and removal of these particles into sediments, exerts a

major control on the concentration and distribution of metals in the

world's oceans [1-4]. Vertical and horizontal variations in dissolved

trace metal concentrations result from the interaction of particle

formation, decomposition, and transport with physical processes of mixing

and advection. A predictive understanding of metal behavior under

different oceanographic regimes therefore requires detailed quantitative

understanding of dissolved/particulate fractionation and movement of

particles through the water column. Unfortunately, few open ocean

measurements of trace element concentrations on suspended particles have

been made.

Advances in sampling and analysis of trace metals in the past 10-15

years have provided a fundamental understanding of the distribution of

many dissolved trace metals in the major ocean basins [5]. More

recently, measurements of metals in particulate matter collected with

sediment traps have enabled quantification of vertical fluxes of metals

under certain oceanographic conditions [6-11]. The reservoir of fine

particles which sink very slowly (and therefore comprise the bulk of

suspended matter) is a critical link between dissolved and sinking

particulate metals. Because of the abundance of these particles and their large available surface area, it has been suggested that they control exchange with the dissolved reservoir. Several studies have described the distribution of metals which are relatively abundant in suspended particulate matter (e.g. Mn [12,13], Al [14,15], Fe [13]), and the metal content of large and small particles collected from the surface ocean has been reported [16-19]. Other workers have presented average particulate concentrations for a large group of elements in North Atlantic intermediate and deep waters [20], but whole water column suspended particulate profiles in well characterized open ocean regions are not available.

The dearth of particulate metal data results in part from the difficulty in obtaining these measurements by conventional sampling techniques. Typically, water samples of the order of ten liters are filtered from sampling bottles on board ship. At particle concentrations found in the open ocean, this limits sample sizes to about 100 μg. Filter and handling blanks and possible bottle artifacts [21,22] make accurate metal determinations difficult. Small sample sizes also limit the number of other analyses which can be carried out to characterize the sample and provide geochemical context. In the present study, I endeavored to minimize these limitations by collecting much larger samples by _in situ_ filtration.

The principal goals of this work are (1) to determine accurate full water column profiles of suspended particulate trace metals in an open ocean regime, (2) to identify factors controlling particulate metal content, e.g. bulk particle composition, dissolved metal distribution,

and water column hydrography, and (3) to understand the role of fine, slowly sinking particles in determining the flux of metals through the deep ocean.

Here I present suspended particulate concentrations of Al, Fe, Mn, Co, Zn, Cu, Ni, Cd and Pb at a Sargasso Sea station near Bermuda. The data demonstrate that for most of these metals, concentrations are substantially lower than previous estimates, and that sinking of fine particles below the thermocline is a minor contributor to the total deep ocean flux for these elements.

3.2. Sampling and Analysis

Samples were collected from depths of 10 to 4000m on five occasions at a cluster of stations centered near Station "S", ~50km southwest of Bermuda in the Sargasso Sea (Table 3.1). Particles were filtered from seawater using an in situ pump developed for the project and described in detail elsewhere (Chapter 2). Briefly, this device is a self-contained battery-powered unit which attaches to a normal hydrowire in such a way that it is free to pivot. A vane on one end orients the intake upstream in the ambient current, away from particulate contamination associated with the hydrowire or the metal components of the pump itself. A small computer controls the pre-set pumping period (typically 2-3 hours), and provides a record of flow rate and total volume sampled. A single pump was deployed repeatedly to obtain the samples on the earlier two cruises. In the later work, three pumps were deployed simultaneously in a single cast.

Table 3.1. Sargasso Sea (Bermuda) pump sampling stations

Date	Station	Vessel/Cruise
22-33 September, 1986	31°50'W, 64°08'W	Endeavor 148
14-16 March, 1987	31°49'N, 64°16'W	Endeavor 157
3-4 September, 1987	32°22'N, 64°17'W	Weatherbird
12-13 March, 1988	32°12'N, 64°28'W	Weatherbird
10 April, 1988	32°07'N, 64°23'W	Oceanus 197

Particles were collected on a 142mm diameter 53 μm mesh size polyester (PeCap, Tetko, Inc., Briarcliffe Manor, N.Y.) prefilter and a 142mm diameter, 1.0 μm pore size Nuclepore polycarbonate primary filter. Both filters were acid-cleaned, dried, and pre-weighed before mounting in a similarly cleaned custom-made filter holder made of acrylic, silicone rubber and sintered polyethylene. No prefilter was used for the September, 1986 and March, 1987 samples. A 0.4 μm Nuclepore filter was substituted for the standard primary filter on one occasion as a test of recovery efficiency using the larger pore-sized filter. Sampled volumes ranged from 120 to 1530 liters, depending on pumping time and filter clogging rate, yielding 3.1 to 10.6 mg total dry weight of particulate matter.

Within 2 hours of recovery, excess seasalt was rinsed from the samples by dripping pH adjusted distilled deionized water (pH 8.3 by addition of trace element clean NaOH) through each filter under mild vacuum in a laminar flow clean bench. Filtrates were saved to evaluate the possible loss of material during rinsing (Appendix C). Filters were transferred to acid-cleaned 150mm Petri dishes and dried for several hours under class 100 conditions in a clean bench. Petri dishes were then closed, sealed within several layers of polyethylene bags, and transported upright to the laboratory. The filters were then re-dried in a desiccator and re-weighed to ± 0.1 mg on an analytical balance. Precision of the sample mass, determined from replicate weighings, was $\pm 4\%$ for the <53 μm fraction, but ~20% for the >53 μm fraction due to uncertainties in sample loss during rinsing and to the hygroscopicity of the filter material.

Subsamples for various analyses were cut from the primary filters using a polystyrene template and a stainless steel scalpel on an acid-cleaned acrylic cutting board. For metal analysis, subsamples (8% of total) were digested for 4 hours at ~100°C in 0.5ml concentrated nitric acid and 1.2M hydrofluoric acid, effecting a complete dissolution of the particulate material. This was done by adhering the filter pieces to the inside walls of a tightly closed 7 ml Teflon FEP screw-cap vial (Savillex) which was placed on a hot plate, allowing the acid to fume and reflux down the sample face of the filter. Digest solutions were cooled, weighed to check for evaporative loss, and diluted to 2.5 ml with distilled deionized water. These solutions were analyzed for Al, Fe, Mn, Co, Zn, Cu, Ni, Cd, Pb and Na by graphite furnace atomic absorption spectrometry (Perkin-Elmer 5000 with continuum or Zeeman background correction) using the method of standard additions. Sodium concentrations were used to estimate residual seasalt as a correction to the mass and particulate calcium determinations. Calcium was determined using flame atomic absorption (Perkin-Elmer 403) and matrix-matched standards.

Reproducibility of the analyses of replicate subsamples depends on (1) homogeneity of particle distribution across the face of the filter and (2) analytical procedures. In general, these factors contributed about equally, for an overall precision of ±15% or better. Blanks were determined on both unused filters and process blanks which were treated identically to samples, including submersion on a non-operating pump. Blanks were generally less than 10% of sample signals, often on the order of 1%, but occasionally exceeded 50% for Zn, Cu and Ni in near-surface

samples. Rinsing losses were 0-10% for Zn and 15-50% for Cd (very high

values were rejected as contamination suspects, Appendix C). Rinse

solutions were not analyzed for other elements, and all values disscussed

in the text are uncorrected for losses. Prefilters caught a small

fraction of total suspended matter, and were analyzed for mass only.

Separate subsamples (2.4% of total) were subjected to a wet

oxidation in perchloric and nitric acid and analyzed for P

spectrophotometrically in a modification of the procedure of Strickland

and Parsons [23]. Other subsamples (2.4% of total) were leached in 0.7M

sodium carbonate at 90° for four hours to selectively dissolve amorphous

silica, leaving ordered silicates largely undissolved [24]. Leachates

were neutralized and analyzed for silicate by a micro adaptation of the

standard seawater technique [23]. Organic carbon content could not be

determined directly, but was estimated by difference between total weight

and summed inorganic components, assuming carbon is 50% of the total

residual weight'

3.3. SUSPEENDED PARTICLE COMPOSITION

3.3.1. Suspended mass

The composite suspended mass profile (Fig. 3.1) is similar to those

observed in other open ocean sites. Relatively high values (26-42 μg/l)

are observed in the near-surface layer of highest biological production;

concentrations decrease rapidly through the thermocline to low and nearly

constant values of ~6 μg/l in the intermediate and deep water column. A

small increase to ~11 μg/l in the deepest samples (~200-400m above the
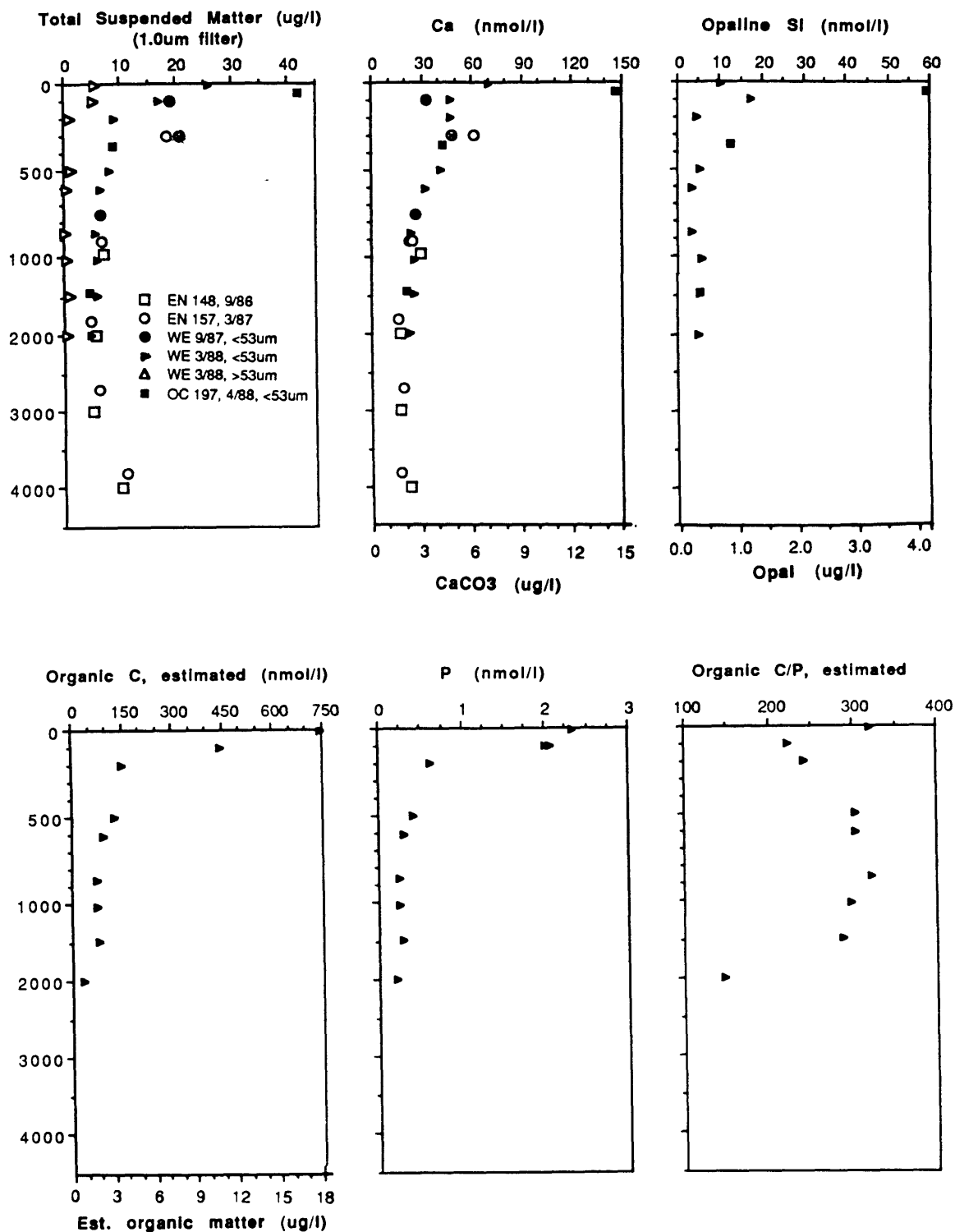
Fig. 3.1.   Profiles of suspended particulate mass and major constituent
elements. Depths in meters; note change in vertical scale at 1000m.   Open
circle with cross indicates replicate sample collected using 0.4 μm
filter (see text).

sediment surface) is caused by sediment resuspension, as discussed below. The >53 μm fraction comprises 6-25% of total suspended mass, the highest percentage being at the base of the euphotic zone (100m). Previous measurements of suspended mass in the Sargasso Sea have produced somewhat higher and more variable results than were determined here. Brewer et al. [27] reported a range of approximately 2-20 μg/l for the depth interval 500-3000m, with a mean of approximately 10 μg/l and a standard deviation of 5 μg/l (based on replicate samples) at GEOSECS Station 120 (33°15'N, 56° 34'W). Similar results were obtained at Parflux Station S (31°31'N, 55°03'W) by Spencer et al. [8], who reported 5.5-14.4 μg/l (9.0±2.2 μg/l, 1σ, n=13) for the same depth interval. These previous studies were based on filtration of 4-30 liter Niskin bottle samples through 0.4 or 0.6 μm Nuclepore filters. My in situ pump results for 500-3000m at Station S range from 4.7 to 7.3 μg/l (6.1±0.9, 1σ, n=13). While natural oceanographic variability may account for the 30% discrepancy in mean mass concentration between this and the Parflux findings, failure to adequately correct for residual seasalt, or even the hydroscopicity of the particulate matter itself may have given results which were too high in the previous study. Differences in filter pore size may also contribute to the discrepancy, but a single experiment comparing mass concentrations obtained on 0.4 μm vs. 1.0 μm Nuclepore filters in consecutive pump samples at 300m (EN 157) indicated only 12±5% more mass retained on the 0.4 μm filter. This suggests that undersampling of the smallest particles is unlikely to be a major source of error. However, Bishop and Fleisher [12] observed that particulate Mn values increased 40% with a 3-fold increase in pumped sample volume in

the upper water column of a 1982 Warm Core Ring. They interpreted this result as an effect of filter loading on the efficiency with which particles near the nominal pore size are sampled by quartz fiber filters. No comparable effect was observed for the single comparison just described, but it should be kept in mind that particulate concentrations are operationally defined. The contributions of the <1.0 μm size fraction to the individual elemental distributions (as distinct from suspended mass) has not been rigorously quantified.

No temporal variability in mass concentration was discernable for samples below 200m (~ the top of the main thermocline) with the exception of the 300m sample in March, 1987. Suspended mass for this sample was about twice the values at bracketing depths in March and April, 1988. Hydrographic data indicates an unusually deep convective mixed layer in early Spring, 1987 [26], which probably mixed surface-produced particles into the upper thermocline.

3.3.2. Biogenic components: CaCO$_3$, opaline silica, organic matter, and phosphorus

In order to determine whether trace metal content correlates with any aspect of bulk composition, I analyzed suspended particles for the dominant components. These results are interesting in their own right, because although these components are relatively easy to analyze compared to the trace metals, very little comparable data exists for open ocean Atlantic waters. This is due, in part, to sample size limitations when ≤30 liters are filtered. Because different dissolution procedures are required for various major component determinations, previous

investigators have been obliged to limit analyses to a chosen subset. The current study was not limited by sample size, although direct determination of organic carbon was sacrificed for the low metal blank obtainable with polycarbonate filters.

The vertical distribution of suspended particulate Ca resembles the total mass profile (Fig. 3.1). Concentrations are maximum in near-surface waters. The 50m value in April 1988 is more than twice the particulate Ca concentration at 10 or 100m one month earlier (146 vs. 47-71 nmol/l), suggesting substantial vertical or temporal variability during the period of the spring phytoplankton bloom. Below the surface layer, concentrations decrease with constant slope through the thermocline, decrease more gradually from 1000-2000m, and are approximately constant at 20 ± 5 nmol/l in deep water. These values are within the range reported for other open ocean environments. For example, Jickells [27] reported a four-year average suspended Ca in the upper 100m at Station S to be 75 nmol/l. Mean particulate Ca for the 0-100m depth range near Bermuda were seasonally variable in the range 15-150 nmol/l, with highest concentrations corresponding to early spring productivity maxima [28]. Bishop and Fleischer [12] found values of 30-40 nmol/l in the upper 700m of a station in the northwest Sargasso Sea, approximately equal to values in the upper 400m of the eastern equatorial Atlantic [29]. Sub-thermocline values in the current study closely matched those observed in the eastern Sargasso Sea (GEOSECS Sta. 29 [30]) and in the Panama Basin [31]. These are apparently several times higher than deep water values in the tropical northwest Atlantic (GEOSECS Sta. 31 [30]).

Calcium carbonate accounts for >90% of particulate Ca through most
of the water column. The remainder is associated with refractory
lithogenous material (estimated from suspended Al and average crustal
Ca/Al ratios of Taylor [32]; see discussion below) and there may be a
small contribution from non-skeletal cellular Ca in near-surface waters
[29]. In the nepheloid layer samples, lithogenous Ca contributes ~40% of
the total. The decrease in particulate Ca with depth in the upper water
column is caused by the interaction of $CaCO_3$ production in near-surface
water, and the incorporation of suspended Ca into sinking particles
occurring throughout the upper 2000m.

Like calcium carbonate, opaline silica is relatively high and
variable in surface waters, but decreases to low and constant values
within the upper thermocline (Fig. 3.1). This may reflect rapid removal
and substantial dissolution just below the seasonal mixed layer [33].
Opal was greatly enriched at 50m in April 1988, indicating that siliceous
as well as calcareous plankton species were abundant. Below 500m, opal
concentrations are 3-7 nmol/l. These values are much lower than in the
Panama basin (40-700 nmol/l, upper 1500m, [31]), the upper 400m of the
equatorial east Atlantic (15-30 nmol/l, [29]), or the midwaters of the
Antarctic circumpolar current (35-110 nmol/l, [34]). At the Bermuda
station the refractory mineral Si, estimated from particulate Al and
average Si/Al in crustal materials [32], exceeds measured opaline Si by a
factor of three in sub-thermocline waters. Thus dissolution of a
fraction of the refractory Si could lead to over-estimates of biogenic
silica. To avoid this problem, rigorous dissolution techniques
(concentrated NaOH, Na_2CO_3 fusion) were avoided, and the relatively mild

leaching treatment of Eggiman et al. [24] was employed. Honjo et al. [35], using a similar dissolution procedure, determined opal content for sinking particles in the Sohm Abyssal Plain (31°33'N, 55°55'W) which were comparable to my values for suspended matter.

Particulate organic carbon (estimated by difference) and particulate phosphorus (measured) decrease by about an order of magnitude from relatively high values in surface waters (POC = 750nmol/l, PP = 2.3 nmol/l) to very low concentrations (POC = 71 nmol/l, PP = 0.26 nmol/l) in thermocline and deep waters (Fig. 3.1). Values throughout the sub-surface water column are lower than have been observed in the equatorial and tropical eastern North Atlantic [29,36] but are of similar magnitude to values observed in the northwest Sargasso Sea [12]. The estimated C/P molar ratio exceeds the Redfield ratio (106:1 [37]) by a factor of 2-3, as has been observed previously in oligotrophic waters [29,36]. An increase with depth is observed in the upper thermocline (100-500m), consistent with rapid remobilization of P relative to C [16]. The C/P ratio is then constant at 300 mol/mol from 500-1500m. The reason for the relatively high surface value (320 at 10m) or the decrease from 300 to 150 mol/mol between 1500 and 2000m is not known.

3.3.3. Lithogenic components: Al and Fe

Profiles of particulate aluminum and iron parallel each other throughout the water column, suggesting that both elements are contained largely in the same phases (Fig. 3.2). Aluminum concentrations increase linearly from ~1 nmol/l in the upper 200m, to 3.5 nmol/l at 1000-3000m. Iron concentrations increase from 0.25 to 1.2 nmol/l in the same depth
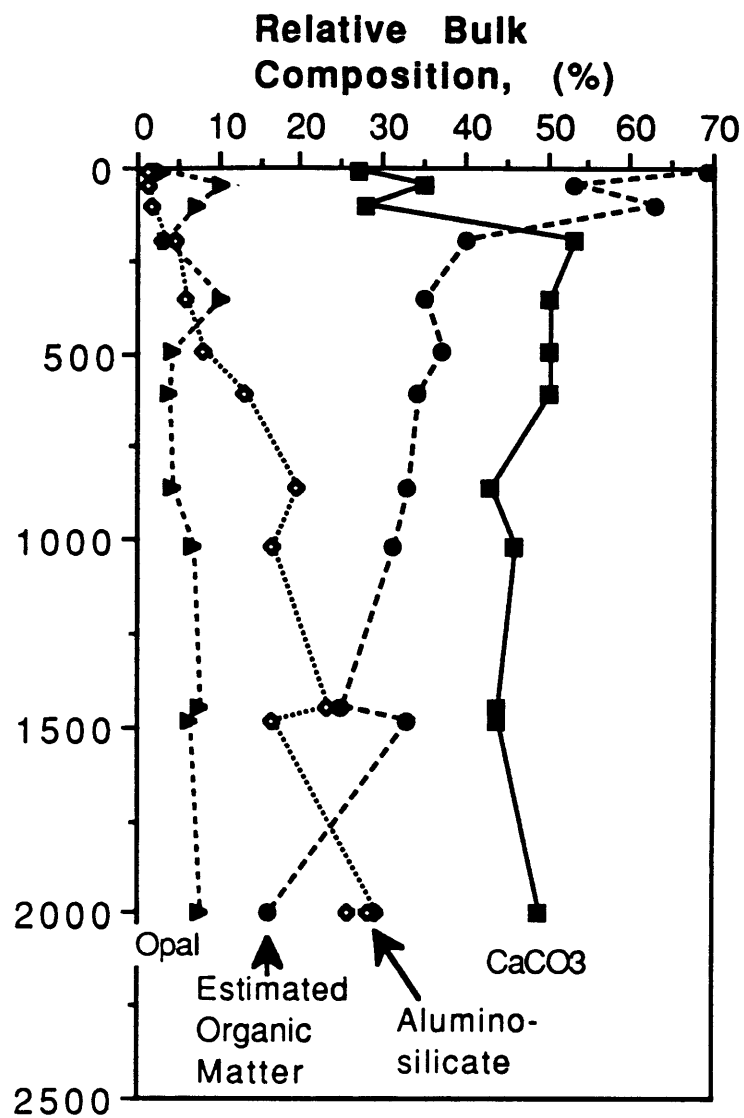
Fig. 3.2.   Bulk particle composition, upper 2000m (3/88 and 4/88 samples). Percentages calculated as described in text.

range. Both elements are greatly enriched in the near-bottom samples, where sediments enriched in detrital phases are resuspended to at least several hundred meters above the bottom. The presence of a benthic nepheloid layer is expected in this region because of its proximity to high-energy western boundary currents [38]. Particle mass and aluminum concentrations over an order of magnitude larger than those observed here have been reported for bottom waters at other locations in the northwest Atlantic [39].

Aluminum concentrations below 1000m are similar to previously reported values for North Atlantic intermediate and deep values [20,30]. Low surface concentrations and a linear increase through the thermocline have not been previously described. The surface concentrations are several times lower than published mean particulate Al concentrations for North Atlantic surface waters [18,20] and are approximately equal to the lowest values observed by Krishnaswami and Sarin [17] (Table 3.2).

Molar Fe/Al ratios throughout the water column (Fig. 3.2) cluster within 40% of the average crustal ratio of 0.33 [32]. Ratios in atmospheric aerosols collected near Bermuda [40] and across the N. Atlantic [41] also fall, on average, within 30% of the crustal value. Similar ratios have been observed for suspended particles in the North and South Pacific as well [13,15,42]. Other workers have found North Atlantic suspended particulate Fe/Al averaging 1.0-1.3 mol/mol (mean N.W. Atlantic, 3°N-42°N and mean N.E. Atlantic, 15°N-40°N), approaching the crustal ratio only in nepheloid layers <500m above bottom where aluminosilicates constituted more than 50% of total particulate mass [20,39]. Enrichment over crustal values suggested that

Table 3.2. Suspended particulate trace metals in Atlantic surface
waters

Element	Sargasso Sea, Bermuda, 0-100m 4 samples (This work)		Subtropical N. Atlantic 2 samples (Krishnaswami and Sarin, 1976 [17])	Sargasso Sea, Bermuda 4 samples (Wallace et al. 1977 [18])	Atlantic 4 samples (Buat-Menard and Chesselet, 1979 [20])	Sargasso Sea, Bermuda, 0-100m 146 samples (Jickells, et al., 1989, [27])
	mean	range	mean	mean	mean	mean
Al	1.22	0.5-2.2	2.5	3.0	2.9	6.7
Fe	.32	0.25-0.45	2.2	1.1	4.0	
Mn	34.00	9.0-59	58.0	29.0	64.0	110.0
Cd	.93	0.65-1.0				
Pb	1.20	0.8-1.8		5.4	22.0	
Zn	5.20	3.1-7.3		34.0	240.0	
Cu	6.30	3.7-8.0	50.0	40.0	57.0	
Ni	5.80	4.9-7.2	34.0	18.0	31.0	
Cd	.30	0.19-0.39		.4		

non-aluminosilicate phases constitute a substantial fraction of total particulate Fe, although the identity of these phases was unclear [43]. In contrast, my data suggest that particulate Fe is dominated by detrital minerals at all depths, in agreement with the Sargasso Sea surface particulate data of Wallace et al., [18]. Observation of nanomolar quantities of particulate Fe liberated by weak acid leaching in the upper water column of the equatorial Atlantic [29] suggest that authigenic Fe phases may be important under some conditions and may be subject to the sampling efficiency for the smallest particles, as discussed above. Additional data on the particulate distribution of Fe would augment our poor understanding of Fe cycling in the water column, and set limits on estimates of non-refractory particulate Fe reservoirs (oxides, hydroxides, organics, or adsorbed) which may be important host phases for some trace metals [19,44,45].

The bulk composition of suspended particles near Bermuda (WE 3/88 and OC 197, March-April, 1988) is presented in Figure 3.3. Mass fractions for calcium carbonate, opaline silica, aluminosilicates, and organic matter were calculated from elemental concentrations using the following equations:

$$\%CaCO3 = 100g/40g \times [Ca - (Ca/Al)_{crust} \times Al] \times 100/(wt) \qquad (1)$$

$$\% \ Opal = 70g/28g \times Si \times 100/(wt) \qquad (2)$$

$$\% \ Aluminosilicate = 10 \times Al \times 100/(wt) \qquad (3)$$

$$\% \ Organic \ matter = 100 - (\%CaCO3 + \%opal + \% \ aluminosilicate) \qquad (4)$$

where (wt) is total dry weight and all elemental quantities are expressed as μg per sample. Estimate of aluminosilicate-bound Ca is based on average Ca/Al for shales, rather than average crust, as the crustal value includes a carbonate rock contribution [79](Table 3.3). Conversion factors used in equations (2) and (3) assume that opaline silica contains some hydration water not removed during drying [46], and that aluminosilicates comprise 10% Al (by mass), somewhat higher than the crustal average [32] but consistent with the relatively Al-enriched clays found in low-latitude nepheloid layers in the Atlantic (Ref. [43] and references therein).

At this station, calcium carbonate dominates suspended particle mass, comprising ~50% of the total mass except in surface waters, where organic matter dominates. Organic matter content decreases rapidly as remineralization occurs in the upper water column, while terrigenous material increases from less than 1% in surface waters to ~25% at 2000m. Opaline silica is a minor phase comprising $\leq$10% of suspended mass throughout the water column.

3.3.4. Trace metal composition

Concentrations of particulate trace metals vary smoothly with depth and, except for Cd, have similar profile shapes (Fig. 3.4). Particulate Mn, Co, Pb, Zn, Cu and Ni are depleted to varying degrees in surface water, increase to relative maxima at ~500m and, except for Cu, decrease to relatively constant values in the 1000-3000m depth range. Cu is relatively constant from 500-4000m compared with the other metals. The distribution of particulate Cd is distinct from the other metals and

Fig. 3.3.   Particulate Al, Fe, and Fe/Al ratio.   Symbols as per Fig.
3.1.   Replicate symbols at a single depth represent replicate analyses of
separate subsamples of a single filter.   Note change of scale on both
axes.

Al (nmol/l) Fe (nmol/l) Fe/Al (mol/mol)
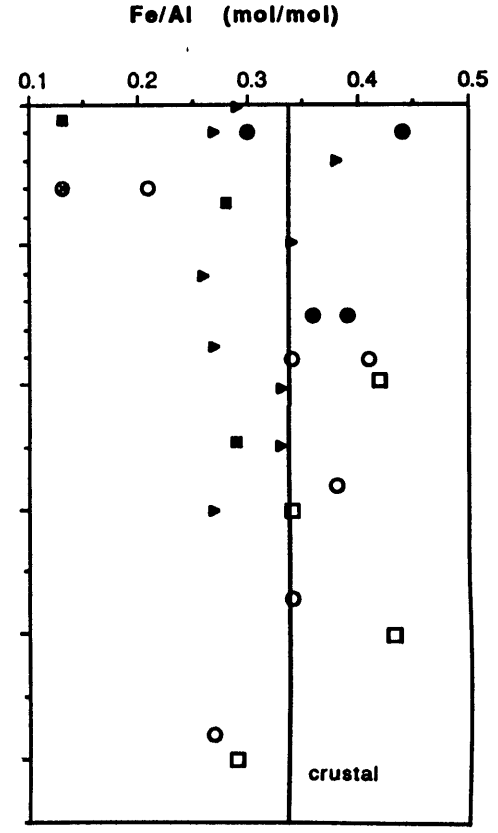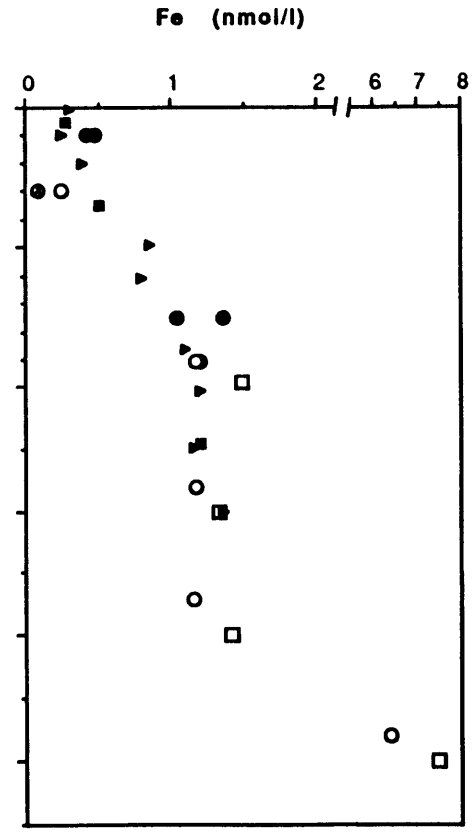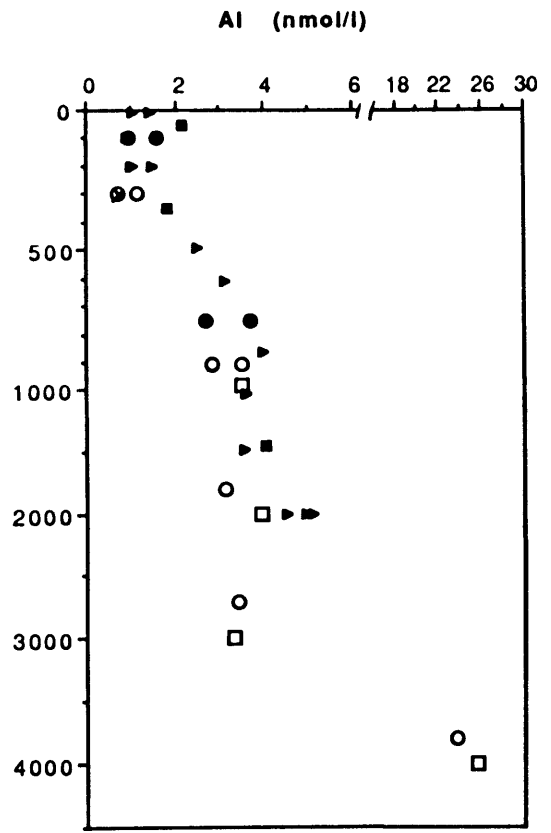
Table 3.3. Metal to alumimum ratios (mol/mol) in average crustal material
and in nepheloid layer particles, Sargasso Sea.

Element/Al	Average crustal[a]	Average nepheloid suspended particles[b]
Fe/Al	0.33	0.28
Mn/Al	5.7×10^{-3}	8.1×10^{-3}
Co/Al	1.4×10^{-4}	1.2×10^{-4}
Zn/Al	3.5×10^{-4}	5.6×10^{-4}
Cu/Al	3.1×10^{-4}	5.7×10^{-4}
Ni/Al	4.2×10^{-4}	--
Cd/Al	5.9×10^{-7}	1.6×10^{-6}
Pb/Al	2.0×10^{-5}	6.0×10^{-5}
Ca/Al	0.19[c]	0.8
Si/Al	3.3	--

(a) From Taylor, 1964 [32].
(b) Average of 4000m (EN 148, September, 1986) and 3800m (EN 157, March, 1987) samples, this work.
(c) Average for shales from Turekian and Wedepohl, 1961 [79].
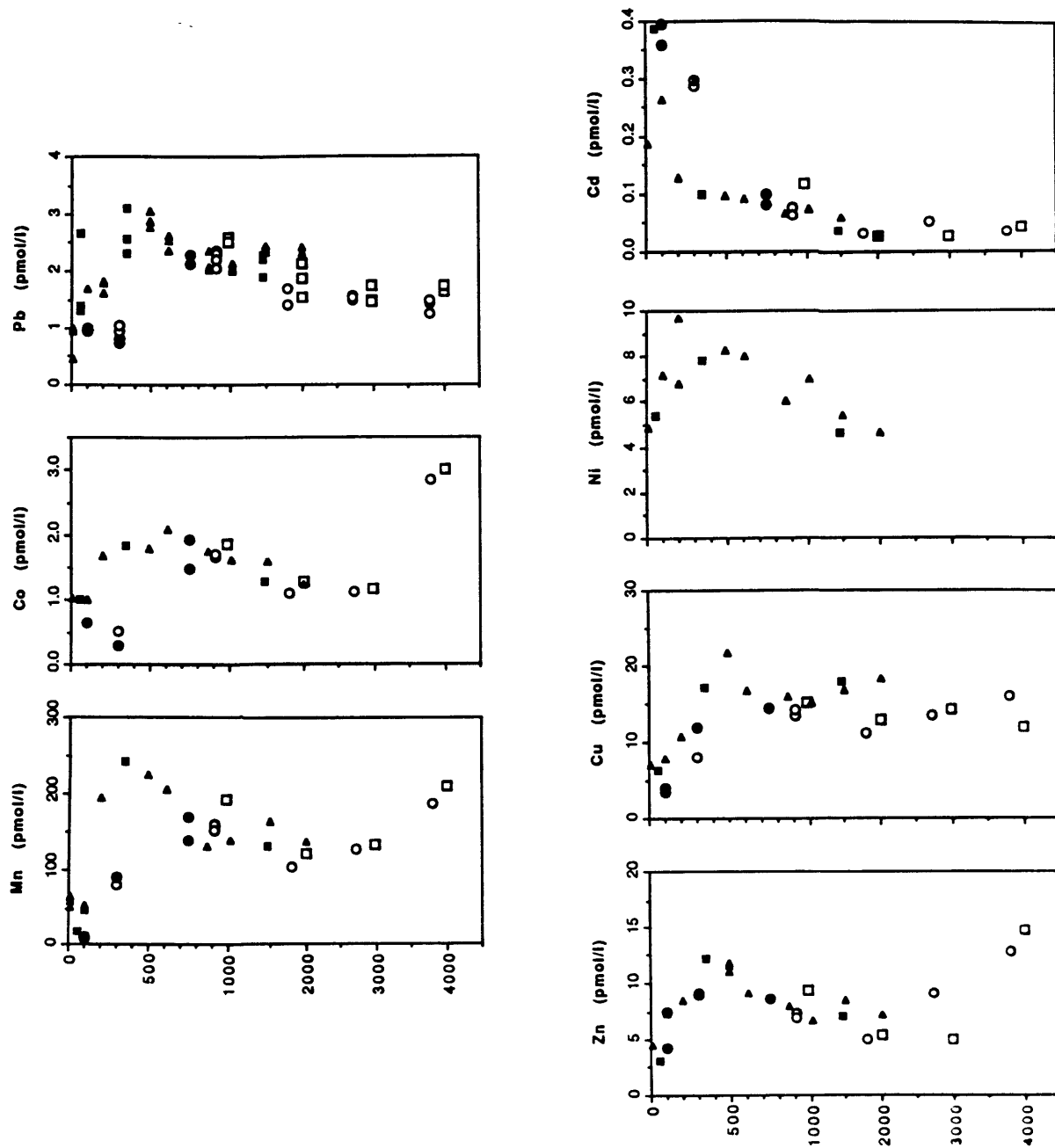
Fig. 3.4.   Particulate trace metal profiles.   Symbols as per Fig. 3.1.
Replicate symbols as per Fig. 3.3.   Note change of depth scale at 1000m.

Table 3.4. Suspended Particulate Metal Concentrations: Intermediate and Deep Water Means

	Al	Fe	Mn	Cu	Zn	Co	Cd	Pb	Ni
	(nmol/l)		----------(pmol/l)--------------						
Sargasso Sea (this study, 500-3000m)	3.6	1.2	146	15	7.4	1.5	.06	2.1	5.9
N. Atlantic (Buat-Menard & Chesselet, 1979, [20])	4.1	3.6	87	47	230	3.9		42	34
N.W. Atlantic (Lambert et al., 1984 [39])	5.2	6.3	140						
N.W. Sargasso (Bishop & Fleischer, 1987 [12])			200						

resembles P in being greatly enriched in surface waters, decreasing monotonically to very low levels at depth. Nepheloid layer samples are enriched in Mn, Co, and Zn because of the contribution of resuspended clays to the total metal content. Clays also contribute >50% of Cu and Co, indicating a depletion in non-aluminosilicate content of these metals in the deepest samples relative to those in the overlying water column. Clays contribute only ~30% of nepheloid layer particulate Cd and Pb content. The clay component is estimated from average crustal metal/Al ratios, which are tabulated with corresponding ratios for the nepheloid layer samples in Table 3.3. Because no differences were detected between earlier samples of total suspended matter (EN 148 and EN 157) and later determinations on the <53 μm fraction, it is assumed that the profiles are representative of total suspended metals. This assumption has not been verified in the upper water column (<1000m) where sample coverage is adequate only for the <53 μm samples. In addition, because no temporal variability was observed between station occupations at depths >300m, I will discuss the distributions as single composite profiles.

Mean concentrations of Fe, Cu, Zn, Co, Pb and Ni in intermediate and deep waters (500-3000m) are lower than previously reported North Atlantic values by a factor of 3 (Fe, Co) to 30 (Zn) (Table 3.4). Moreover, previous workers' data showed no systematic trends in concentration from 300-5000m [20]. Discrepancies with previous values are greatest for Zn and Pb, elements known to be especially subject to contamination during sample collection and processing [47,48]. In contrast, results for Al and Mn, which are relatively abundant in suspended matter, are in good agreement. Concentrations for 0.4 versus 1.0 μm filter deployments

described above were equal within measurement precision (Fig. 3.4).
Therefore, the use of 1.0 μm filters in this study is unlikely to produce
substantial underestimates of particulate metal concentrations. These
observations suggest that earlier values were subject to contamination
artifacts and that the present results represent real particulate metal
distributions.

In near-surface waters, particulate metal concentrations vary
between station occupations, but even the highest values are considerably
lower than previously reported surface values, except for Al, Mn, and Cd,
which are in reasonable agreement (Table 3.2). Decreasing atmospheric
input of anthropogenic Pb since the earlier studies [49] may explain the
factor of 4.5 difference between my Pb results and those determined on
1974 samples by Wallace [18]. Temporal variability in particulate mass
and composition in surface waters is caused by seasonal variations in
biological productivity, intermittent inputs of atmospheric aerosols,
changes in mixed layer depth, and passage of inhomogeneous water masses
[49]. It is unlikely, however, that the near-surface sampling dates
(September, 1987, March, 1988, April, 1988) all fell during periods of
anomalously low particulate metal concentration. Exclusion of the >53 μm
fraction from the pump samples may contribute to differences, but metal
contents in >44 μm Pacific plankton samples collected in waters with
dissolved metal and nutrient concentrations similar to the Bermuda
station were substantially greater only for Zn and Cd (Pb and Co not
analyzed [16]). These two metals were enriched by about an order of
magnitude (mol/g dry weight) over my <53 μm particles. Thus it is
possible that the excluded size fraction, although contributing <25% of

total mass, might contain a substantial fraction of total particulate Cd and Zn. Therefore, upper water column values for these elements must be considered as representative only of the <53 μm fraction. Discrepancies between this work and previous workers' values for surface particulate Fe, Cu, and Ni are difficult to reconcile on the basis of large particle exclusion, and may be contamination artifacts in the earlier studies.

This comparison of the present results with existing data suggests that concentrations obtained using the in situ pump are, in general, at least several-fold lower than results obtained previously by filtration of isolated water samples. When combined with the earlier sediment trap measurements of Jickells, et al. [6], the profiles presented here therefore enable the first realistic assessment of the role of suspended particles in controlling the distribution and removal of metals in the North Atlantic.

3.4. CONTROL OF PARTICULATE TRACE ELEMENT DISTRIBUTIONS: THE ROLE OF MANGANESE

The vertical distribution of trace metals in suspended particulate matter is the net result of several processes, including (1) variations in the concentration of individual mineral phases, in which metals are incorporated by solid solution or by occlusion within the mineral lattice, (2) re-distribution of the total suspended particle population or some fraction thereof by association with rapidly-sinking but numerically rare large particles, and (3) exchange of metals between particulate and dissolved forms, controlled by chemical sorption or precipitation on particle surfaces or by active biological uptake or

efflux of metals within living cells. Through some combination of these three processes, metals are scavenged from the water column and eventually delivered to the sediments. Some understanding of the relative importance of each of these contributing factors can be gained by consideration of particulate metal distribution in its geochemical context. In addition to the suspended mass and major element composition data described here, existing knowledge of dissolved metal distributions can be considered [5]. In the following discussion, I argue that some of these processes are of minor importance, and that the data suggests that the major determinants of the overall profile shapes (except Cd) are enhanced metal uptake on inorganic Mn phases and decreasing particulate mass concentration with depth.

The most striking aspect of the particulate metal distributions shown in Figure 3.4 is that profiles for Mn, Co, Pb, Zn, Cu, and Ni all have the same general shape, in contrast to the varying profile shapes of the dissolved metals (Fig 5.7). The similarity of the profile shapes is demonstrated more clearly when plotted on the same scale in smoothed "cartoon" form (Fig. 3.5). Surface values are generally depleted relative to deep, and all show a relative maximum in the upper thermocline. The similarity of distributions suggests control by a common phase or process, but examination of the vertical variations in major components reveals no similar pattern. Al and Fe profiles, representative of refractory terrigenous material, increase through the thermocline with no apparent anomalous feature at the metal maximum. Elements associated with biogenic inorganic phases ($CaCO_3$, opaline silica) and organic matter (organic carbon, phosphorus) all decrease

Mn (pmol/l)

Co, Pb, Ni, Zn, Cu, Cd (pmol/l)
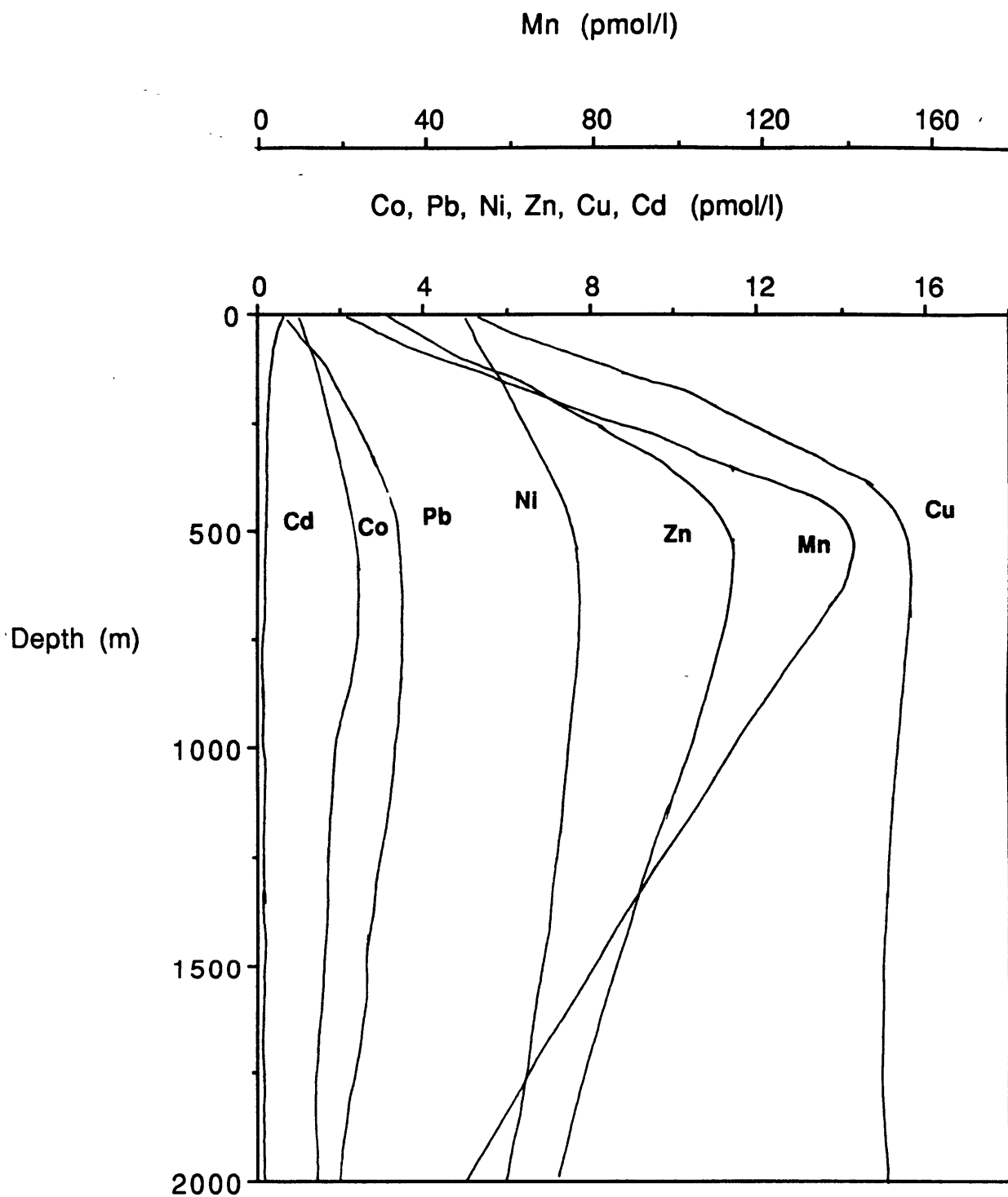
Fig. 3.5.   Smoothed representation of suspended particulate metal profiles at Bermuda, showing similarity of all profiles except Cd to particulate Mn distribution.   Note scale for Mn is compressed one order of magnitude.

Table 3.5. Estimated percent of total particulate metal carried in
mineral lattice of major component phases.

Element	Aluminosilicate[a]		Calcium carbonate[b]		Opaline silica[b]	
	100m	3000m	100m	3000m	100m	3000m
Al	100	100	.05	.003	.05	.005
Fe	~100	~100	.07	.003		
Mn	80	15	.13	.006		
Co	28	42				
Zn	7	13	10	5	7.8	1.7
Cu	10	7	1.0	.07	1.1	.13
Ni	5	60	.8	.16	.4	.13
Cd	1	11	.6	.16		
Pb	2	4				

(a) Estimates based on average crustal metal/Al ratios of Taylor, 1964
[32].
(b) Upper limit estimates based on measurements in cleaned forams and
unwashed diatoms (Collier and Edmond, 1984 [16]).

regularly through the upper water column. The lack of correlation with the metal distributions suggests these phases are not directly responsible for the observed profiles. Estimates of the contributions of lattice-bound metals in aluminosilicates, $CaCO_3$, and opal corroborate this result (Table 3.5). Only the aluminosilicate contribution to Co and Ni (and Mn at 100m) constitutes more than 15% of total particulate metals. This indicates that in general, either organic matter or a relatively minor inorganic phase are the most likely host phases for the group of metals considered here.

If a minor particle type were enriched in trace metals, a particulate metal maximum could be generated simply by the vertical distribution of this phase. If the phase were sufficiently metal-rich, one could hypothesize that aggregation/sinking/disaggregation processes might accumulate such a phase in a particular depth zone without substantially altering the suspended mass profile. Such a hypothesis would require a source of such particles to the surface ocean. Atmospheric aerosols, the major exogenous particle source to Sargasso Sea surface waters, are the most obvious candidate. However, the water column distribution of aluminosilicate materials, the major component of atmospheric dust, does not match that of the particulate trace metals. It is difficult to imagine another metal-rich particle type sufficiently resistant to dissolution to maintain its metal content after vertical transport from the surface. Lack of an obvious candidate suggests that particle transport processes acting on discrete phases are unlikely to be the cause of the particulate metal maxima.

The explanations considered thus far have focused on the distribution of particular phases with reasonably well known and presumably stable metal composition, ignoring any dependence on dissolved metal distributions. Interaction of suspended particles with the much larger reservoir of trace metals dissolved in seawater will now be considered. Control of particulate metal contents by exchange with dissolved metals implies that particle surfaces, the composition of which might not be represented by the bulk composition, are the important variable.

Metal scavenging has been considered by many authors to be a surface-chemical process [50-52], but the nature of oceanic particulate surfaces is not well understood [53]. Balistrieri et al. [54] modeled metal scavenging as a surface-complexation process, and suggested that organic coatings on suspended particles control sorptive removal of metals from seawater. Others have suggested control by inorganic surfaces such as Mn oxyhydroxides [55]. The sorptive behavior of Mn oxides has been demonstrated in laboratory studies using single minerals [56] and natural sediments [57]. In the open ocean, Mn may form as oxide coatings on carbonate particles [58] or in association with encapsulated bacteria [59]. Little is known about its effect on trace metal distributions in natural suspended matter.

In Bermuda waters, particulate Mn contents are 1-2 orders of magnitude greater than for other metals, presenting substantial sorptive surface if present in the form of a fine-grained authigenic mineral. The observed correlation of trace metal concentrations with Mn (Fig. 3.6), and lack of correlation with organic carbon (Figs. 3.1 and 3.4, and as

Fig. 3.6.   Metal to manganese regressions, Bermuda upper 2000m. Data
from March, 1988 (open symbols) and April, 1988 (closed symbols). Total
metal concentrations (no correction for aluminosilicate fraction) are
plotted.
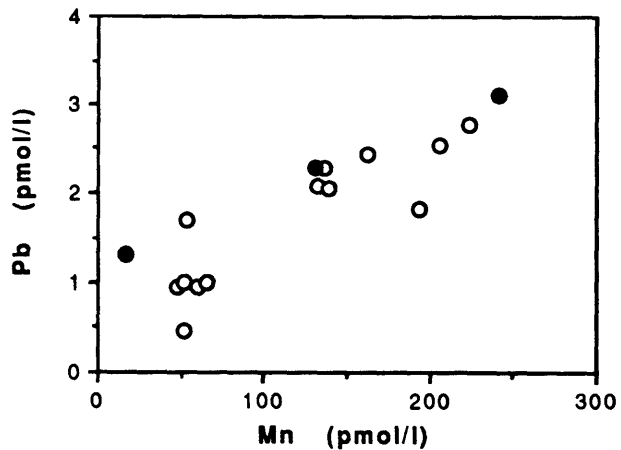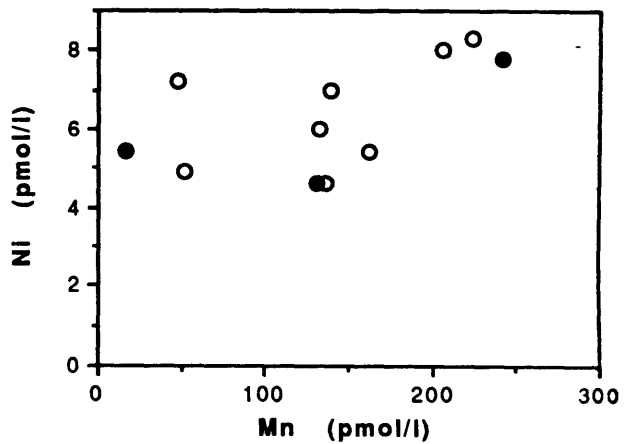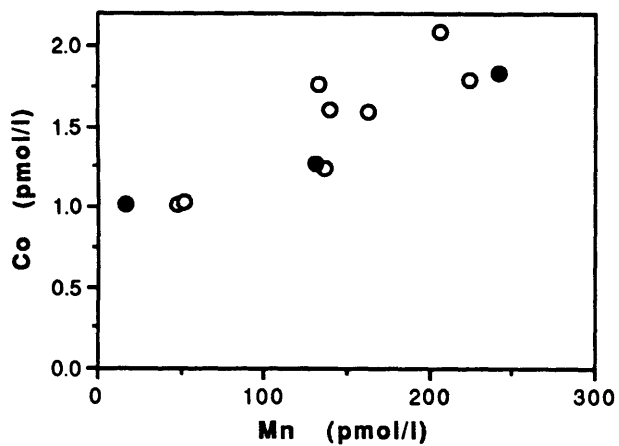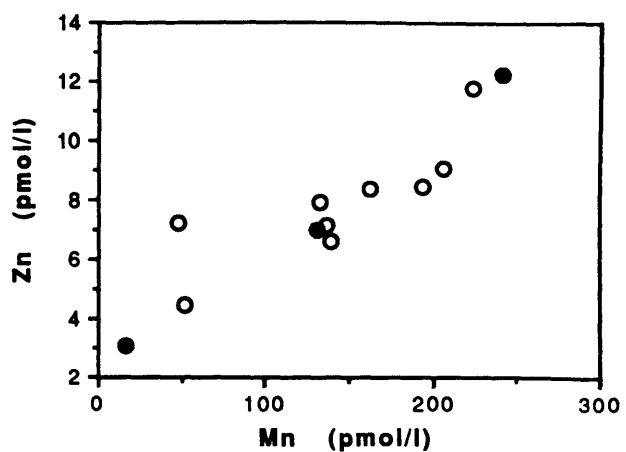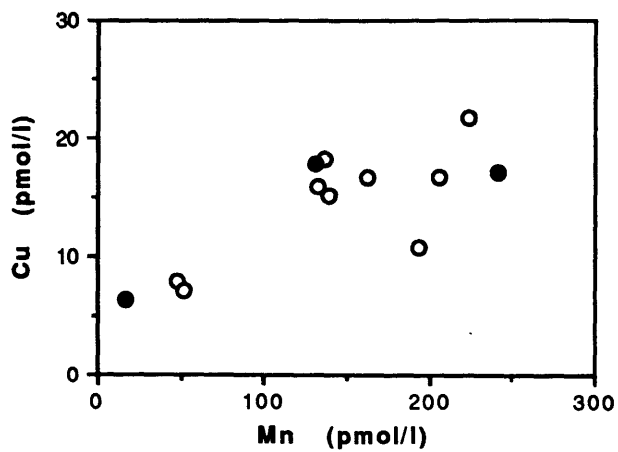
noted by Bishop and Fleisher, 1987 for Mn [12]), suggests that sorptive uptake of dissolved metals onto recently oxidized Mn solids may be an important control on particulate metal contents. Understanding processes which control the formation and distribution of particulate Mn in the upper water column may thus shed light on the distribution of other metals as well. Fortunately, there exists sufficient data on dissolved and particulate Mn in the northwest Atlantic to test several hypotheses of Mn distribution near Bermuda. In particular, it should be possible to propose a reasonable explanation for the particulate Mn maximum at 300-500m.

The observation of an upper thermocline particulate Mn maximum in the Atlantic is consistent with the upper 700m profile of Bishop and Fleisher [12] from the northwest Sargassso, and may by a ubiqitous feature of Sargasso Sea waters at temperate latitudes. Subsurface authigenic particulate Mn maxima have been observed previously in the Pacific [10,13] but these have generally been associated with oxygen minima (<100umol/kg) and coincident dissolved Mn maxima. The Sargasso Sea Mn maximum is not associated with an oxygen minimum and appears to occur 100-200m deeper than the base of the Mn-enriched near-surface waters (0-200m) observed throughout the Sargasso Sea [60-63] (Fig. 5.7).

The particulate Mn maximum occurs in the depth range of the subtropical mode water (18° water, centered about 300m). Because water at this depth is ventilated by winter convective mixing events [64] or mixing along isopycnals which outcrop at higher latitudes [65], high Mn surface waters could provide a source for in situ oxidation to particulate Mn. Ventilation along outcropping isopycnals has been shown

to be an important source of dissolved Pb in the thermocline at this station [49]. However, Sargasso Sea Mn profiles demonstrate that dissolved Mn at 500m is not appreciably higher than deep water concentrations [62,63] (Fig. 5.7). This suggests that oxidation of surface-derived dissolved Mn to particulate Mn has occurred very rapidly. The Mn residence time at the depth of the maximum can be estimated by assuming no dilution of the surface Mn during convection, Mn concentration equal to 2 nmol/kg in surface water and 0.5 nmol/kg at 500m, and a ventilation time for water at this depth of 10 years [65]. This calculation yields a first-order half-removal time of 5 years, considerably shorter than reported estimates of scavenging residence times for Mn in the deep ocean (25-75y, [13,66]). This source of dissolved Mn to the upper thermocline depends upon elevated dissolved/particulate Mn ratios in surface waters. Such ratios are maintained, apparently throughout the western North Atlantic [61], by a mostly dissolved atmospheric input (wet deposition > dry deposition [67]), by low active uptake of Mn by plankton [16,19], and by photo-chemically mediated Mn(IV) reduction [68].

Horizontal advection must also be considered as a potential source of Mn to the particulate maximum. Horizontal advection from ocean margins has been invoked as a major influence on dissolved Mn maxima observed in the thermocline near Hawaii [10,13]. It has been suggested that the source of this Mn could be near-shore Mn enrichments observed along the west coast of the United States and presumed to occur along other North Pacific continental margins. However, concentrations of dissolved Mn in sub-surface waters are low and uniform throughout the

sub-tropical North Atlantic [62,63]; no gradient of decreasing concentration with distance from the continents is observed. Horizontal particulate Mn transport is also possible. Bishop and Fleisher [12] reported 1-53 μm suspended Mn profiles in Gulf Stream and adjacent Sargasso Sea stations with concentrations in upper thermocline waters (200-500m) of about 200 pmol/kg, very similar to Bermuda suspended Mn for the same depth range. The similarity of the profiles suggests that particulate Mn distribution in the western Sargasso may be influenced by advection from the Gulf Stream/slope water system, perhaps in association with mesoscale eddies. However, the apparent lack of a particulate Mn gradient suggests that lateral transport is unlikely to occur by eddy diffusion alone, unless the horizontal eddy diffusion rate is sufficiently large to eliminate an observable gradient.

Although the cause of the particulate Mn maximum cannot be proven with the current data set, given the evidence at hand, it seems likely that physical transport of dissolved Mn-enriched surface waters into the upper thermocline, followed by in situ oxidation to particulate Mn, is a major influence on the particulate Mn distribution near Bermuda. Below the maximum, the Mn content (per mass particles) remains approximately constant, but particulate Mn (per volume seawater) decreases with decreasing mass concentration, thereby inducing the upper thermocline concentration maximum.

The influence of particulate Mn on the particulate content of Co, Pb, Zn, Cu, and Ni is illustrated by comparing the partitioning of metals between particulate and dissolved forms. Empirically defined metal distribution coefficients (K_d) for surface water and upper thermocline

Table 3.6. Log K_d[a] and (percent total)[b] for suspended particles in surface water and upper thermocline, Bermuda

Depth	Al	Fe	Mn	Co	Ni	Cu	Zn	Cd	Pb
100m	--	--	5.7	6.0	5.2	5.3	6.1	6.4	5.7
	(5%)	(50%?)	(1%)	(2%)	(0.3%)	(0.4%)	(2.5%)	(5%)	(1%?)
500m	--	--	7.5	6.9	5.5	6.3	6.4	5.3	6.5
	(10%)	(50%?)	(25%)	(8%)	(0.3%)	(2.0%)	(2.5%)	(0.2%)	(3%)

(a) K_d defined as mol/g of particles divided by mol/g water, calculated using "excess" metal (total minus estimated aluminosilicate fraction) for Mn and Co, and total particulate metal (~ =excess metal) for other elements. Dissolved metal data from references [49,60,63].

(b) calculated as percent of total (dissolved + particulate) metal.

(--) insufficient "excess" metal data

(?) dissolved metal data questionable

waters are examined in Table 3.6. The results indicate that particles in the Mn maximum (500m) have a higher affinity (Kd) for most metals than particles in surface waters (upper 100m). For example, Kd's increase from a factor of 2 (Zn, Ni) to 10 (Cu) over this depth range. This was not obvious from the particulate profiles alone, since dissolved concentrations of nutrient-type trace elements [5,60] are also depleted in surface waters (Fig. 5.7).

Attributing the 100-500m difference solely to changes in particle composition or surface chemistry would presume the validity of several assumptions: (1) equilibrium dissolved/particulate exchange (see Chapter 4), (2) constant surface area to mass ratio with depth, and (3) metal uptake control by surface processes rather than, for example, active biological uptake. Because the increase in Kd (for Zn, Ni, Co, Cu, and Pb) was less than or equal to the increase in Mn content (factor of 10), other phases must act as carriers for these metals in addition to Mn oxides (especially for the nutrient-type metals Ni and Zn). This is supported by the observation that metal/Mn ratios in suspended particles (Fig. 3.6) are approximately an order of magnitude higher than ratios in ferromanganese nodules for Zn, Cu and Pb, although roughly similar for Ni and Co [78](Fig. 3.7). The degree of association of various metals with Mn oxide phases could be explored by a partial leaching procedure (e.g. 25% acetate), with adequate control for readsorption on residual solid phases. Overall, although the above assumptions are not likely to be rigorously satisfied, the increase of K_d with Mn content for all the metals studied (except Cd) suggests an important role of authigenic Mn phases in metal scavenging under natural oceanic conditions.
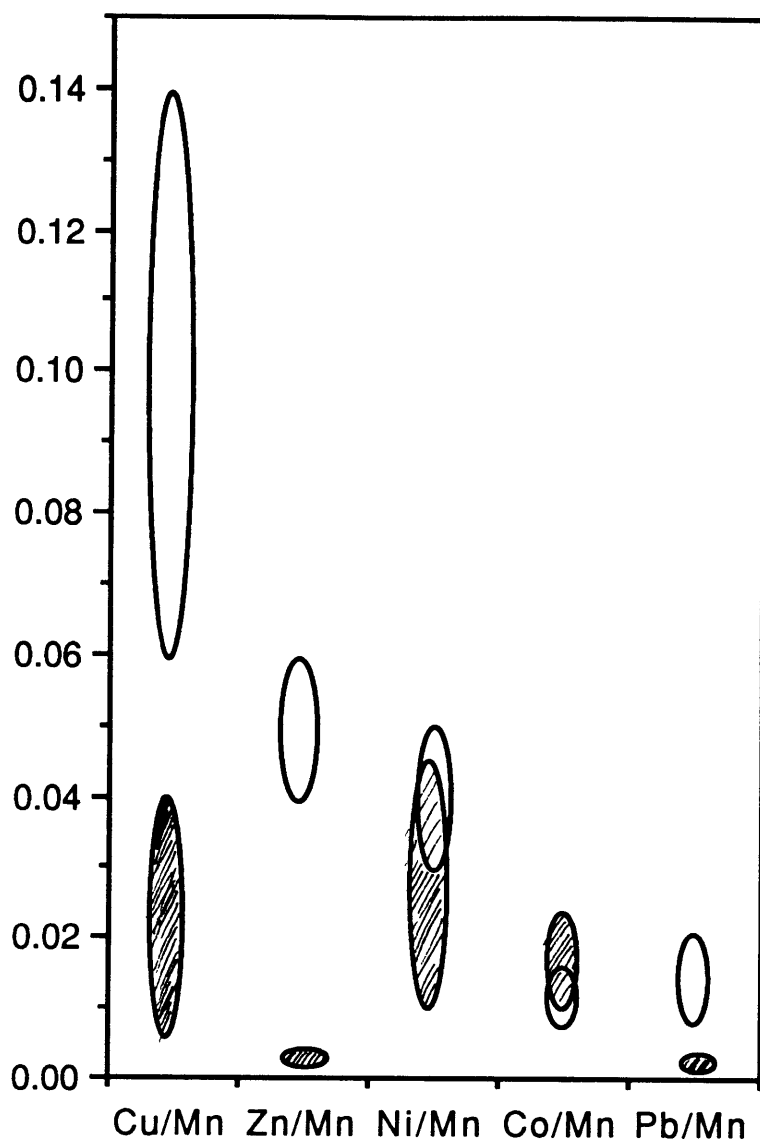
Fig. 3.7. Molar ratios of metal/Mn in Pacific ferromanganese nodules
(shaded, data from Calvert and Price, 1977 [78]) and in suspended
particles at Bermuda (unshaded, samples >200m).

Particulate Cd, which is strongly enriched in surface waters, stands out as an exception throughout this discussion. Its distribution mirrors that of dissolved Cd, and suggests that Cd is dominated by association with organic matter in surface waters, is recycled almost entirely within the upper water column [11,69], and has very low particle affinity in deep waters. The relationship of Cd to P in in particulate and dissolved forms is discussed further in Chapter 5.

3.5. THE ROLE OF SUSPENDED PARTICLES IN DETERMINING METAL FLUX THROUGH THE DEEP OCEAN

Fast-sinking particles produced by biological activity in surface waters interact with slowly-sinking suspended particles in the deep ocean, increasing the removal rate of the smaller particles over that predicted by passive settling [70]. Although details of this interaction are not well understood, removal can be considered as the sum of two processes: (1) incorporation into particles in surface waters forming large aggregates which sink rapidly to the deep ocean, and (2) association with deep suspended particles which are removed by incorporation into the surface-derived flux. Although measurements of total fluxes of trace metals have been made in a few locations [71]), resolution of the relative magnitude of surface-derived versus deep removal of trace metals has not been possible without accurate suspended metal distributions for the same locations. Using the new suspended particulate metal data, we can now estimate the relative contribution of the removal of these particles to the total deep ocean flux for these metals.

To perform this calculation, I adopt a simple steady-state two-box flux model for the Sargasso Sea (Fig. 3.8). Metal scavenging and particle interactions are represented by a model which recognizes two classes of particles into which the natural spectrum of particulate matter is divided [73,73]. Large, fast-sinking particles, which dominate the flux but contribute negligibly to the suspended mass, are assumed to be produced by biological activity in the surface box or by aggregation of deep suspended particles. Small suspended particles, which comprise the bulk of the suspended mass, are assumed to sink only by association with large particles. The large particle flux thus regulates the removal of suspended particles, but only suspended particles, by virtue of their greater concentration, surface area, and residence time, exchange metals with the dissolved pool.

The flux associated with removal of suspended particulate metals, the "repackaging" flux (F_R, nmol/cm^2-yr), is calculated from:

$$F_R = (Me_p * D)/t_p$$

where Me_p is the average deep ocean (500-3000m) suspended metal concentration (pmol/l), D is the depth of the deep box (m), and t_p is the estimated suspended particle residence time (yr). Total metal flux (F_T, nmol/cm^2-yr) is assumed equal to means determined from eleven two-month deployments of a sediment trap at 3200m near Bermuda [6]. The repackaging and total flux of several trace metals, as well as ^{230}Th and ^{228}Th, are compared in Table 3.7. Each of the parameters in the above equation has an associated uncertainty which contributes to the uncertainty in the estimate for F_R. The uncertainty in Me_p is generally
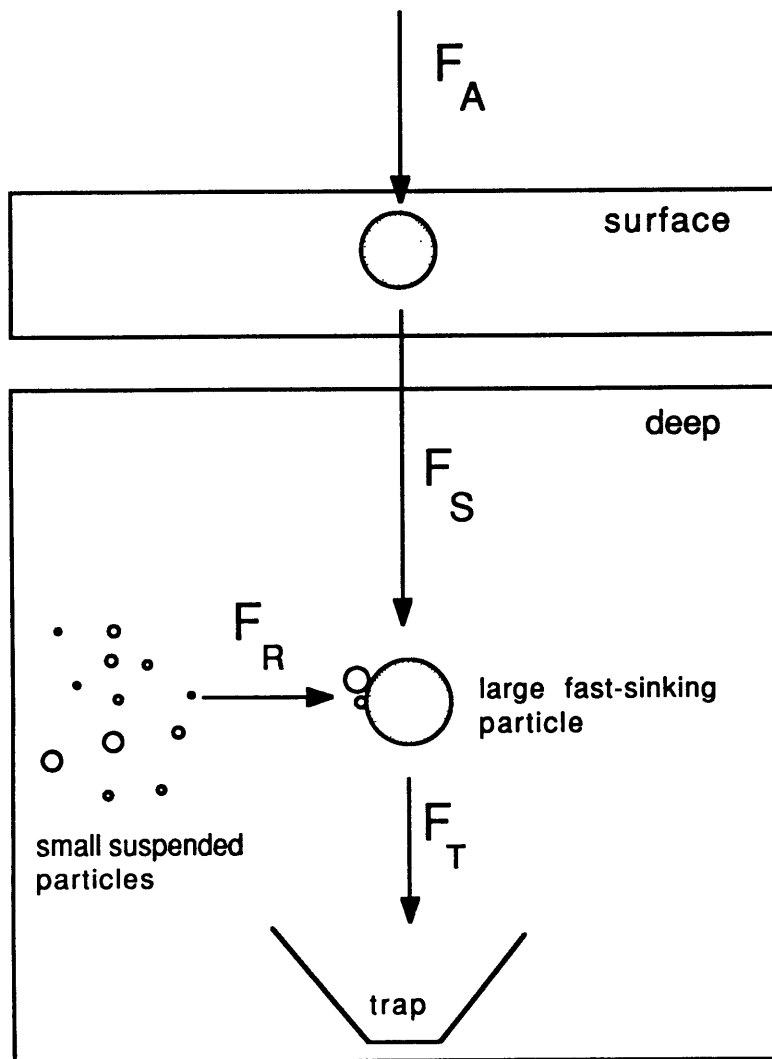
Fig. 3.8. Steady-state two-box metal flux model. See text for explanation of terms.

Table 3.7. Sargasso Sea two-box model flux calculation. Relative
standard deviations (see text) of each measurement in
parentheses.

Element	Mean deep conc.[a] (Me$_p$)	"Repackaging" flux[b,c] (F$_R$)	Total flux[b] (F$_T$)	Atmos. flux[d] (F$_A$)	$\dfrac{F_R}{F_T}$	$\dfrac{F_A}{F_T}$	$\dfrac{F_A + F_R}{F_T}$
Al	3600 (14%)	195	840 (10%)	204	0.23 (65%)	0.24	0.47
Fe	1210 (14%)	65	220 (10%)	57	0.30 (65%)	0.26	0.56
Mn	146 (20%)	7.9	25 (10%)	2.4	0.32 (67%)	0.10	0.40
Ni	5.9 (23%)	0.32	1.0 (12%)	0.73	0.32 (68%)	0.73	1.00
Cu	15 (14%)	0.83	2.0 (10%)	0.91	0.42 (65%)	0.46	0.87
Zn	7.4 (21%)	0.40	3.8 (23%)	5.20	0.11 (70%)	1.37	1.48
Cd	0.06 (48%)	0.003	0.004 (10%)	0.12	0.75 (80%)	30	30.5
Pb[e]	2.1 (17%)	0.12	0.42 (17%)	0.73	0.29 (67%)	1.7	1.94
^{230}Th[f]	0.10 (63%)	55	54 (26%)	0	1.02	0	1.04
^{228}Th[f]	0.34 (10%)	183	430 (15%)	0	0.42 (66%)	0	0.56

(a) concentration units: dpm/m^3 for ^{230}Th and ^{228}Th, pmol/l for other
elements.

(b) flux units: dpm/m^{2}-yr for ^{230}Th and ^{228}Th, nmol/cm^2-yr for other
elements.

(c) "repackaging flux" calculated assuming particle residence time
= 5.5 yr, 3000m deep box, see text.

(d) atmospheric flux assumed equal to total 1983 deposition [67].

(e) Pb fluxes calculated for ~1981, assuming deep suspended Pb is
~constant from 1981-1988.

(f) Th data from Bacon, 1985 [79], and unpublished data, see text.

$\leq$20% (except for Cd and ^{230}Th, see Table 3.7) and D is taken as a model

assumption which therefore has no uncertainty. The uncertainty in F_T is

taken as the range of the means for each integrated year of trap

deployment, divided by the mean for the entire 2-year period [6], or the

reported analytical uncertainty, whichever is larger. The resultant

uncertainty is $\leq$12% for all elements except Zn, Pb, and ^{228}Th. The

largest uncertainty by far is in the estimate of t_p. This is calculated

from suspended particulate ^{230}Th (single profile in March, 1985) and

trapped flux measurements of ^{230}Th (10 observations of ~2 months'

duration from May, 1984 to June, 1986) near Bermuda, assuming that the

flux of ^{230}Th, which has no independent surface source, is totally

determined by removal of suspended particles (M. Bacon, personal

communication). The estimate obtained is 5.5$\pm$3.5 years, within the range

of estimates based on similar modeling of Th distributions in other ocean

basins [74]. This 63% uncertainty in the suspended particle residence

time accounts for almost all of the propagated uncertainty in the

estimate of F_R.

The flux calculations demonstrate that for all trace metals

examined, the repackaging flux provides less than half of the total flux

in the deep ocean (Table 3.7). The fraction (F_R/F_T) is 30$\pm$20% or less

for all metals except Cu (42$\pm$27%), Cd (75$\pm$60%), and ^{228}Th (42$\pm$28%). In

contrast to ^{230}Th, the total flux of most trace metals appears to be

controlled largely by processes occurring in the surface ocean. This

conclusion rests on the assumption that published measurements of trapped

metals are accurate. Because the traps were unpoisoned, some loss of

metals by dissolution may have occurred during the 2-month deployments.

However, this would tend to strengthen the argument by further reducing F_R/F_T for these metals. The consistency of the F_R/F_T values for Al, Fe, Mn, Ni, Cu, and Cd suggests that a common particle interaction process controls surface-derived versus deep scavenged flux components for all of these metals. Zinc appears to be an exception, with the repackaging flux contributing only $11\pm8\%$ of the total flux (note, however that Zn is very subject to contamination and that while the sample-to-sample variability in the trap measurements was not much larger than for the other elements, at least one of the 11 samples was obviously contaminated).

Calculated repackaging fractions reflect the net effect of several processes with different intensities for each element: (1) magnitude of surface ocean sources relative to deep sources, (2) affinity for surface particles, (3) depth and extent of remineralization from sinking particles, and (4) scavenging from the dissolved phase in the deep ocean. While it is difficult to ascertain the relative contributions of each process for each element, and thereby formulate a quantitative justification for the results, the general conclusion of the flux calculation is clear: the vertical transport of deep ocean suspended particles and their associated metals is a relatively minor component of total metal removal in the Sargasso Sea. If this result can be extrapolated to central gyre conditions in general, it suggests that although dissolved/particulate interactions influence metal distributions throughout the deep ocean, deep particle removal in the open ocean cannot be the primary determinant of metal removal from the oceanic system. This control must exist at the oceans boundaries.

3.6. SOURCES OF PARTICULATE TRACE METALS IN THE DEEP OCEAN

The model result is simply a comparison of fluxes which does not rest on an assumption of how the standing stock of deep suspended particles is maintained, or how these particles acquire trace metals. In one hypothetical extreme, particles might acquire all of their metals by in situ scavenging from the dissolved pool, implying a source of metal-free particles transported from elsewhere or created de novo. In the other extreme, suspended particles might be delivered to the deep ocean with a "pre-formed" metal content and undergo no subsequent exchange with the dissolved phase. The balance between these two extremes is difficult to determine from steady-state distributions. Some progress can be made, however, by examining other lines of evidence in the context of the present model. The following sections discuss the roles of (1) scavenging of dissolved metals in the deep ocean, (2) disaggregation from sinking particles, and (3) horizontal particle advection.

3.6.1. Internal scavenging of dissolved metals

If we adopt the first extreme hypothesis, we can calculate deep ocean scavenging residence times by dividing the deep ocean dissolved metal inventory by the "repackaging" flux. For Mn, Cu and Pb, the results (Table 3.8) are in very good agreement with residence times calculated on the basis of advection/diffusion modeling of dissolved profiles (Mn, Cu) or radioactive disequilibrium (Pb). Longer residence times calculated for the other elements (except Co) suggest that other

sources ("pre-formed" particulate metals) may be important, but no independent estimates of deep scavenging rates exist for comparison.

Although this analysis must be considered a first approximation, it appears that _in situ_ scavenging of dissolved trace metals in the deep water column could explain the entire suspended particulate content of reactive metals (Mn, Cu, Pb) except those with significant refractory particulate components (Al, Fe, and perhaps Co).

3.6.2. Disaggregation of sinking particles

An alternative source is the disaggregation of sinking particles. Previous authors have suggested that a quasi-continuous exchange between sinking and suspended particles maintains the suspended pool at a constant concentration [2,72]. If no other mechanisms influenced the composition of suspended particles, we would expect their metal composition to resemble that of sinking particles. Because as we have seen, the fraction of repackaging flux is not constant (Table 3.7), we know that the inter-element ratios differ between the two classes of particles. The absolute composition (mol/g dry weight) is rather similar, however (Table 3.9).

Suspended particles are enriched by 10-90±25% in Fe, Mn, Cu and perhaps Pb relative to sinking particles (Table 3.9). These enrichments suggest that some degree of deep water scavenging contributes to the suspended concentrations for these elements [5], and that exchange between the two particle classes is not complete. Thus total disaggregation and re-aggregation of the surface-derived particles does not occur in the deep ocean. If it did, we would expect the repackaging

Table 3.8. Deep ocean scavenging residence times for several trace metals

Element	Model-derived[a] (this work)	Previous Estimates	Reference
Mn	20	50±25	[13,73]
Pb	150	130±70	[49]
Co	110		
Cu	550	1100	[5]
Zn	1100		
Ni	6000		
Cd	41000		

(a) Calculated from total mean particulate metal concentration for deep water column and mean deep Sargasso Sea dissolved metal concentrations [49,60,63]. Assumes particle residence time = 5.5 yr, and that particulate metals are derived only from deep dissolved reservoir.

Table 3.9. Bulk composition of deep sinking, deep suspended, and surface suspended particles, Sargasso Sea.[a]

Constituent	surface suspended[c]	deep trapped[b]	deep suspended[c]	deep sus. / deep tr.
% $CaCO_3$	30	62	45	0.7
% aluminosilicate	2	27	25	0.9
% opal	5	5.5	7	1.3
% organic carbon	30	5.0	7	1.4
Al	50	690	800	1.2
Fe	10	165	230	1.4
Mn	1.5	20	25	1.3
Co	0.05	--	0.25	--
Zn	0.2	2.9	1.5	0.5
Cu	0.2	1.6	3.0	1.9
Ni	0.2	0.78	0.9	1.2
Cd	0.010	0.008	0.006	0.8
Pb	0.05	0.33	0.35	1.1

(a)   All metal concentrations in $\mu mol/g$ dry weight.
(b)   Bermuda, 3200m, Jickells et al., 1984 [6] and Deuser et al.,1981 [76], except %opal, Sohm Abyssal Plain, Honjo et al., 1982 [35].
(c)   Mean values, this work.

flux to equal the total flux. Since this is not observed, this scenario suggests that a minor portion of the large particle flux is involved in "sweeping out" and then restocking suspended particles through aggregation/disaggregation processes, and the major portion sinks rapidly with little alteration. It should be noted, however, that trapped particles are significantly different in composition from surface particles (Table 3.9), so the large particles have been substantially modified at some point during their descent. The flux comparison indicates that this does not happen in the deep ocean, but occurs during particle transformations in the dynamic and poorly understood upper thermocline (0-500m).

The rate of exchange with suspended particles might depend on the seasonally variable large particle flux [72]. If so, the composition of sinking and suspended particles would be more similar during some periods than others. Apparently, however, sinking particle composition is more constant than the flux: relative standard deviations of mean metal contents were generally less than 25% compared to 55% for total mass flux over the same period [6]. The conclusion is that the trace metal composition of sinking and suspended particles appear to be linked through particle interactions over a large range of flux conditions.

3.6.3. Horizontal advection of particles

A third possible source for deep suspended metals is horizontal particulate transport from other regions. This source may be important for metals with longer scavenging residence times or a significant detrital component. Jickells et al. (1987) [75] argued that the flux due

to vertical removal of particulate Al which is transported horizontally from outside the region could be estimated as the difference, F_T - F_A, between the deep flux and total atmospheric input (wet plus dry deposition) (Table 3.7). If this is true, horizontal advection supplies about 70% of total deep Al flux. Observations of increasing sediment trap Al fluxes in the Sargasso Sea [7,9] led other workers to similar conclusions. However, the model results (Table 3.7) indicate that removal of deep suspended Al, including suspended Al horizontally transported from other regions, can only supply 30% of F_T - F_A.

This is a significant discrepancy which is unlikely to be caused by uncertainties in the flux measurements or model assumptions. For example, deep flux measurements for 1980-82 are within 20% of mean fluxes for the period 1978-84, based on the correlation between fluxes of Al and organic carbon, and average organic carbon fluxes for this period [6,76]. Calculated repackaging flux, which depends on assumed particle residence time, cannot be more than 60% off without unreasonably violating the ^{230}Th constraint. Although the atmospheric input is based on total annual deposition only for the year 1983, the value lies within 30% of previous estimates of atmospheric Al flux at Bermuda or the North Atlantic as a whole [40,77]. These uncertainties are unlikely to cause the factor of three discrepancy between our results and the previous conclusion. The model results suggest that the atmospheric and repackaging fluxes are of similar magnitude, and that horizontal advection is not the major contributor to total Al flux.

The horizontally advected component of the total flux for other metals is also probably small. It is clear that the discrepancy for Al

does not exist for Ni, Cu, Zn, Cd and Pb, for which $(F_A+F_R)/F_T \geq 1.0$. For these elements, the atmospheric input is more than enough to provide the difference between F_T and F_R, indicating that some fraction of the atmospheric input is removed outside the study area. (It is important to remember, however, that the atmospheric flux is based on measurements for a single year, and is uncertain due to probable interanual variability in wet and dry deposition.) In addition, transect data indicate that deep water gradients of particulate Zn, Cu, and Cd between the Gulf Stream and Bermuda are small (see Chapter 6), although sample coverage is inadequate for a rigorous comparison of concentrations along isopycnal surfaces. Values suggested by Jickells et al. [75], calculated by multiplying F_T - F_A for aluminum by the metal/Al ratio in pelagic clays, are certainly overestimates, since they exceed the total repackaging flux calculated here (except for Cd).

In summary, the evidence is consistent with a significant deep scavenging source for particulate Mn, Cu, and Pb, and with sinking particle disaggregation being a generally dominant control on suspended particle trace metal composition. Horizontal particle advection is probably not the major contributor to suspended particulate metal distributions, and is certainly a minor component of the total deep metal flux.

3.7. Conclusions

The measurements presented here constitute the first accurate open-ocean profiles of suspended particulate concentrations for several

trace elements. This has enabled a better understanding of the factors which might control particulate metal contents in the sub-surface ocean. In particular, vertical variations in the dissolved/particulate partitioning for many of these elements appear to be related to the distribution of particulate Mn, and are anti-correlated with other major components (organic carbon, calcium carbonate, opal, aluminosilicates). Reasonable estimates for the residence time of suspended particles in the deep water column imply metal fluxes due to their removal which are less than half the fluxes actually measured in the deep ocean. This indicates that processes occurring in the surface ocean are more important determinants of metal removal from the open ocean environment than uptake on small particles in the deep ocean. This result is consistent with large particle disaggregation as a source which maintains the suspended particle reservoir, but suggests that the extent of this process exerts a minor control on the total metal flux.

REFERENCES

1. E.D. Goldberg, Marine geochemistry 1. Chemical scavengers of the
    sea, J. Geol. 62, 249-265, 1954.

2. D. Lal, The oceanic microcosm of particles, 198, 997-1009, 1977.

3. K.K. Turekian, The fate of metals in the ocean, Geochim. Cosmochim.
    Acta 41, 1139-1144, 1977.

4. M. Whitfield, and D.R. Turner, The role of particles in regulating
    the composition of seawater, in Aquatic Surface Chemistry, W. Stumm,
    ed., Wiley Interscience, pp. 457-493, 1987.

5. K.W. Bruland, Trace elements in sea-water, in Chemical Oceanography
    Vol. 8, J.P. Riley, R. Chester, eds., Academic Press, pp.158-220,
    1983.

6. T.D. Jickells, W.G. Deuser and A.H. Knap, The sedimentation rates of
    trace elements in the Sargasso Sea measured by sediment trap,
    Deep-Sea Res. 31, 1169-1178, 1984.

7. J. Dymond and R. Collier, Nares Abyssal Plain sediment flux studies,
    in: Subseabed disposal project annual report, physical oceanography
    and water column studies, S.L. Kupferman, ed., pp. B1-B24, Sandia
    National Laboratories, Livermore CA, 1987.

8. D.W. Spencer, P.G. Brewer, A. Fleer, S. Honjo, S. Krishnaswami and
    Y. Nozaki, Chemical fluxes from a sediment trap experiment in the
    deep Sargasso Sea, J. Marine Res. 36, 493-523, 1978.

9. P.G. Brewer, Y. Nozaki, D.W. Spencer and A.P. Fleer, Sediment trap
    experiments in the deep North Atlantic: isotopic and elemental
    fluxes, J. Mar. Res. 38, 703-728, 1980.

10. J.H. Martin, G.A. Knauer and W.W. Broenkow, VERTEX: the lateral
    transport of manganese in the northeast Pacific, Deep-Sea Res. 32,
    1405-1427, 1985.

11. K.W. Bruland, R.P. Franks, W.M. Landing and A. Soutar, Southern
    California inner basin sediment trap calibration, Earth Planet. Sci.
    Lett. 53, 400-408, 1981.

12. J.K.B. Bishop, and M.Q. Fleisher, Particulate manganese dynamics in
    gulf stream warm-core rings and surrounding waters of the N.W.
    Atlantic, Geochim. Cosmochim. Acta 51, 2807-2827, 1987.

13. W.M. Landing and K.W. Bruland, The contrasting biogeochemistry of
    iron and manganese in the Pacific Ocean, Geochim. Cosmochim. Acta,
    51, 29-43, 1987.

14. D.K. Spencer, Aluminum concentrations and fluxes in the ocean, in: GOFS, Global Ocean Flux Study, Procedings of a Workshop, pp. 206-220, National Academy Press, Washington, D.C., 1984.

15. K.J. Orians and K.W. Bruland, The biogeochemistry of aluminum in the Pacific Ocean, Earth Planet. Sci. lett. 78, 397-410, 1986.

16. R. Collier and J. Edmond, The trace element geochemistry of marine biogenic particulate matter, Prog. Oceanog. 13, 113-199, 1984.

17. S. Krishnaswami and M.M. Sarin, Atlantic surface particulates: Composition, settling rates and dissolution in the deep sea, Earth Planet. Sci. Lett. 32, 430-440, 1976.

18. G.T. Wallace, G.L. Hoffman and R.A. Duce, The influence of organic matter and atmospheric deposition on the particulate trace metal concentrations of northwest Atlantic surface seawater, Marine Chem. 5, 143-170, 1977.

19. J.H. Martin and G.A. Knauer, The elemental composition of plankton, Geochim. Cosmochim. Acta, 37, 1639-1653, 1973.

20. P. Buat-Menard and R. Chesselet, Variable influence of the atmospheric flux on the trace metal chemistry of oceanic suspended matter, Earth Planet. Sci. Lett. 42, 399-411, 1979

21. W.D. Gardner, Incomplete extraction of rapidly settling particles from water samples, Limnol. Oceanogr. 22, 764-768, 1977.

22. S.E. Calvert and M.J. McCarthy, The effect of incomplete recovery of large particles on the chemical composition of oceanic particulate matter, Limnol. Oceanogr. 24, 532-536, 1979.

23. J.D.H. Strickland and T.R. Parsons, A Practical Manual of Seawater Analysis, Fisheries Research Board of Canada, Ottawa, 1968.

24. D.W. Eggimann, F.T. Manheim and P.R. Betzer, Dissolution and analysis of amorphous silica in marine sediments, J. Sediment. Petrol. 50, 215-225, 1980.

25. P.G. Brewer, D.W. Spencer, P.E. Biscaye, A. Hanley, P.L. Sachs, C.L. Smith, S. Kadar and J. Fredericks, The distribution of particulate matter in the Atlantic Ocean, Earth Planet. Sci. Lett. 32, 393-402, 1976.

26. Station S Hydographic data, Bermuda Biological Station, 1988.

27. T. D. Jickells, W.G. Deuser, and R.A. Belastock, Temporal variations in the concentrations of some particulate elements in the surface waters of the Sargasso Sea and their relationship to deep sea fluxes, Marine Chem., in press, 1989.

28. D.W. Menzel and J.H. Ryther, The annual cycle of primary production in the Sargasso Sea off Bermuda, Deep-Sea Res. 6, 351-367, 1960.

29. J.K.B. Bishop, J.M. Edmond, D.R. Ketten, M.P. Bacon and W.B. Silker, The chemistry, biology, and vertical flux of particulate matter from the upper 400 m of the equatorial Atlantic Ocean, Deep-Sea Res. 24, 511-548, 1977.

30. P.G. Brewer, GEOSECS Atlantic particle analyses, unpublished data, 1988.

31. J.K.B. Bishop, R.W. Collier, D.R. Ketten and J.M. Edmond, The chemistry, biology, and vertical flux of particulate matter from the upper 1500 m of the Panama Basin, Deep-Sea Res. 27A, 615-640, 1980.

32. S.R. Taylor, Abundance of chemical elements in the continental crust: a new table, Geochim. Cosmochim. Acta 28, 1273-1285, 1964.

33. D.M. Nelson and J.J. Goering, Near-surface silica dissolution in the upwelling region off northwest Africa, Deep-Sea Res. 24, 65-74, 1977.

34. D.M. Nelson and L.I. Gordon, Production and pelagic dissolution of biogenic silica in the Southern Ocean, Geochim. Cosmochim. Acta, 46, 491-501, 1982.

35. S. Honjo, S.J. Manganini and J.J. Cole, Sedimentation of biogenic matter in the deep ocean, Deep-Sea Res. 5A, 609-625, 1982.

36. C. Copin-Montegut and G. Copin-Montegut, Stoichiometry of carbon, nitrogen, and phosphorous in marine particulate matter, Deep-Sea Res. 30, 31-46, 1983.

37. A.C. Redfield, B.H. Ketchum and F.A. Richards, The influence of organisms on the composition of sea water. In: The Sea: Vol. 2, M.N. Hill, ed., Wiley, 1963.

38. P.E. Biscaye and S.L. Eittreim, Suspended particulate loads and transports in the nepheloid layer of the abyssal Atlantic Ocean, Marine Geol. 23, 155-172, 1977.

39. C.E. Lambert, J.K.B. Bishop, P.E. Biscaye and R. Chesselet, Particulate aluminum, iron and manganese chemistry at the deep Atlantic boundary layer, Earth Planet. Sci. Lett. 70, 237-248, 1984.

40. R.A. Duce, B.J. Ray, G.L. Hoffman and P.R. Walsh, Trace metal concentration as a function of particle size in marine aerosols from Bermuda, Geophys. Res. Lett. 3, 339-342, 1976.

41. R. Chester, The marine mineral aerosol, in: The Role of Air-Sea Exchange in Geochemical Cycling, P. Buat-Menard, ed., pp 443-476, NATO ASI Series, Reidel, Holland, 1986.

42. R.M. Gordon, J.H. Martin and G.A. Knauer, Iron in north-east Pacific waters, Nature 299, 611-612, 1982.

43. J.K.B. Bishop and P.E. Biscaye, Chemical characterization of individual particles from the nepheloid layer in the Atlantic ocean, Earth and Planet. Sci. Lett. 58, 265-275, 1982.

44. M.M. Benjamin and J.O. Leckie, Multiple-site adsorption of Cd, Cu, Zn, and Pb on amorphous iron oxyhydroxide, J. Coll. Interf. Sci. 79, 209-221, 1981.

45. K.K. Turekian, A. Katz and L. Chan, Trace element trapping in pteropod tests. Limnol. Oceanogr. 18, 240-249, 1973.

46. T.C. Moore, Radiolaria: change in skeletal weight and resistance to solution, Geol. Soc. Am. Bull. 80, 2103-2108, 1969.

47. K.W. Bruland, R.P. Franks, G.A. Knauer and J.H. Martin, Sampling and analytical methods for the determination of copper, cadmium, zinc, and nickel at the nanogram per liter level in sea water, Anal. Chim. Acta 105, 233-245, 1979.

48. B.K. Schaule and C.C. Patterson, Lead concentrations in the Northeast Pacific: evidence for global anthropogenic perturbations, Earth Planet. Sci. Lett. 54, 97-116, 1981.

49. E.A. Boyle, S.D. Chapnick and G.T. Shen, Temporal variability of lead in the western North Atlantic, J. Geophys. Res. 91:8573-8593, 1986.

50. K.B. Krauskopf, Factors controlling the concentration of thirteen rare metals in sea water, Geochim. Cosmochim. Acta 9, 1-32, 1956.

51. P.W. Schindler, Removal of trace metals from the oceans: a zero order model, Thalassia jugoslavica 11, 101-111, 1975.

52. P.G. Brewer and W.M. Hao, Oceanic Elemental Scavenging, in: Chemical Modeling in Aqueous Systems, E.A. Jenne, ed., ACS Symposium Series No. 93, pp. 261-274, Am. Chem. Soc., 1979.

53. B.D. Honeyman and P.H. Santschi, Metals in aquatic systems, Enviro. Sci. Tech. 22,862-871, 1988.

54. L. Balistrieri, P.G. Brewer and J.W. Murray, Scavenging residence times of trace metals and surface chemistry of sinking particles in the deep ocean, Deep-Sea Res. 28A, 101-121, 1981.

55. N. Takematsu, Ultimate removal of trace elements from seawater and adsorption, J. Earth Sci. 35, 227-248, 1987.

56. J.W. Murray, The interaction of metal ions at the manganese dioxide-solution interface, Geochim. Cosmochim. Acta 39, 505-519, 1975.

57. U.P. Nyffeler, Y.H. Li and P.H. Santschi, A kinetic approach to desribe trace-element distribution between particles and solution in natural aquatic systems, Geochim. Cosmochim. Acta 48, 1513-1522, 1984.

58. J.H. Martin and G.A. Knauer, VERTEX: Manganese transport with $CaCO_3$, Deep-Sea Res. 30, 411-425, 1983.

59. J.P. Cowen and K.W. Bruland, Metal deposits associated with bacteria: implications for Fe and Mn marine biogeochemistry, Deep-Sea Res. 32, 253-272, 1985.

60. K.W. Bruland and R.P. Franks, Mn, Ni, Cu, Zn, and Cd in the western North Atlantic, in Trace Metals in Sea Water, C.S. Wong, E.Boyle, K.W. Bruland , T.D. Burton, E.D. Goldberg, eds., Nato Conf. Series, Plenum Press, pp. 395-414, 1983.

61. P.A. Yeats and J.M. Bewers, Manganese in the western North Atlantic Ocean, Marine Chem. 17, 255-263, 1985.

62. P.J. Statham and J.D. Burton, Dissolved manganese in the North Atlantic Ocean, 0-35 N, Earth Planet. Sci. Lett. 79, 55-65, 1986.

63. T.D. Jickells and J.D. Burton, Cobalt, copper, manganese and nickel in the sargasso sea, Marine Chem. 23, 131-144, 1988.

64. M.S. McCartney, The subtropical circulation of mode waters, J. Mar. Res. 40 (Suppl.), 427-464, 1982.

65. W.J. Jenkins, Tritium and He-3 in the Sargasso Sea, J. Mar. Res. 38, 533-569, 1980.

66. R.F. Weiss, Hydrothermal manganese in the deep sea: scavenging residence time and Mn/H-3 relationships, Earth Planet. Sci. Lett. 37, 257-262, 1977.

67. T.D. Jickells and A.H. Knap, Trace metals in Bermuda rainwater, J. Geophys. Res. 89, 1423-1428, 1984.

68. W.G. Sunda and S.A. Huntsman, Effect of sunlight on redox cycles of manganese in the southwestern Sargasso Sea, Deep-Sea Res. 35, 1297-1317, 1988.

69. G.A. Knauer and J.H. Martin, Phosphorus-cadmium cycling in northeast Pacific waters, J. Mar. Res. 39, 65-78, 1981.

70. I.N. McCave, Vertical flux of particles in the ocean, Deep-Sea Res. 22, 491-502, 1975.

71. J.H. Martin and G.A. Knauer, VERTEX I trap studies, unpublished manuscript.

72. M.P. Bacon, C.-A. Huh, A.P. Fleer and W.G. Deuser, Seasonality in the flux of natural radionuclides and plutonium in the deep Sargasso Sea, Deep-Sea Res. 32, 273-286, 1985.

73. Y. Nozaki, H.-S. Yang and M. Yamada, Scavenging of thorium in the ocean, J. Geophys. Res. 92, 772-228, 1987.

74. M.P. Bacon, Radionuclide fluxes in the ocean interior, in: GOFS, Global Ocean Flux Study, Procedings of a Workshop, pp. 180-205, National Academy Press, Washington, D.C., 1984.

75. T.D. Jickells, T.M. Church and W.G. Deuser, A comparison of atmospheric inputs and deep-ocean particle fluxes for the Sargasso Sea, Global Biogeochem. Cycles 1, 117-130, 1987.

76. W.G. Deuser, E.H. Ross and R.F. Anderson, Seasonality in the supply of sediment to the deep Sargasso Sea and implications for the rapid transfer of matter to the deep ocean, Deep-Sea Res. 28, 495-505, 1981.

77. J.M. Prospero, Eolian transport to the world ocean, in The Sea, Vol. 7, The Oceanic Lithosphere, C. Emiliani, ed., Wiley-Interscience, New York, 1981.

78. S.E. Calvert and N.B. Price, Geochmical variation in ferromanganese nodules and associated sediments from the Pacific Ocean, Marine Chem. 5, 43-74, 1977.

79. K.K. Turekian and K.H. Wedepohl, Distribution of the elements in some major units of the earth's crust, Geol. Soc. Am. Bull. 72, 175-192, 1961.

CHAPTER 4

ISOTOPIC EQUILIBRATION BETWEEN DISSOLVED AND SUSPENDED PARTICULATE LEAD

IN THE ATLANTIC OCEAN

4.1. INTRODUCTION

Suspended particles in the Sargasso Sea near Bermuda have been analyzed for total Pb, ^{210}Pb and stable lead isotopic composition to determine whether particles exhibit similar depth variations to those observed for Pb dissolved in seawater. This constitutes a test of a central question in oceanic trace metal scavenging: how rapidly do metals exchange between solution and suspended particles? The distribution of ^{230}Th and ^{234}Th, highly particle-reactive radionuclides with a uniform source throughout the ocean, has been shown to be consistent with a reversible uptake mechanism with exchange times which are rapid (months) relative to the residence time of suspended particles (years)[1,2]. The implied state of approximate exchange equilibrium has not been demonstrated for less reactive trace metals, which are introduced at the ocean's boundaries rather than in its interior. Lead, in particular, is somewhat less reactive than Th and has a deep ocean scavenging residence time of a century or two[3-6], as compared with a few decades for Th[8,9].

Anthropogenic input during the last century has completely altered the natural distribution of lead in the Sargasso Sea. Downwind from North American industrial and automotive sources, the Pb distribution in this region is no longer in steady-state. Since 1970, when the use of alkyl leaded gasolines began to be curtailed in the U.S., atmospheric

input of lead to the Sargasso Sea has been decreasing. The concentration of lead in the upper ocean near Bermuda, recorded in the skeletons of corals, has been decreasing since the early 1970's[10]. Gasoline additive lead was mined from unusually radiogenic ores during approximately 1965-1975, and from less radiogenic sources since then. Thus the concentration decrease has been accompanied by a decrease in $^{206}Pb/^{207}Pb$ to near the pre-alkyl lead ratio by 1985[11].

^{210}Pb is produced in the atmosphere by a constant decay of continentally-derived Rn-222. It enters the surface of the western North Atlantic via atmospheric pathways similar to those followed by anthropogenic Pb[12]. ^{210}Pb is also generated in the ocean interior by decay of dissolved Ra-226. The oceanic distribution of ^{210}Pb, in contrast to that of stable Pb, is in approximate steady-state[3-6]. As a result, both the $^{206}Pb/^{207}Pb$ ratio and the total $Pb/^{210}Pb$ ratio show substantial changes in the upper ocean over the last decade[11,13]. The $^{206}Pb/^{207}Pb$ ratio of Bermuda surface water decreased from about 1.203 in 1980-84[11] to 1.192 in 1987[14], and the $Pb/^{210}Pb$ ratio fell from 1250 pmol/dpm in 1979 to 690 pmol/dpm in 1984[13] and to ~300 pmol/dpm by 1987 (Boyle, pers. comm.). The vertical propagation of these changing surface signals into the ocean interior has produced isotopic depth distributions which are evolving on a yearly to decadal time scale[11].

4.2. SAMPLING AND ANALYSIS

Suspended particulate matter was filtered *in situ* from 200-1200 liters of seawater on five separate occasions from September, 1986 to April, 1988, ~50 km southwest of Bermuda (32°00'N, 64°10'W). Sample

contamination is an acute concern in obtaining accurate Pb concentrations in natural waters[16], so specially designed battery-powered pumps were used to collect the samples _in situ_. Details of the sampling and analytical procedures will be presented elsewhere. Briefly, 4-11 mg of suspended matter was collected on 1.0 μm pore size Nuclepore polycarbonate filters from depths of 10 to 4000m (4200m bottom depth). In an effort to obtain samples more representative of small suspended particles which are expected to dominate exchange with dissolved Pb, a 53 μm polyester prefilter was used on some deployments to exclude larger, fast-sinking particles. The >53 μm fraction comprised 6-25% of the total mass. No compositional differences between the <53 μm samples and total particulate matter samples could be discerned in any property examined here. Samples were rinsed with distilled water (adjusted to pH 8.3 with NaOH), dried, weighed, and subsampled.

Subsamples of the filters were completely dissolved in 3-x Vycor-distilled concentrated HNO_3 and sub-boiling distilled HF. Resulting solutions were analyzed for total Pb by graphite furnace atomic absorption spectroscopy, and for ^{210}Pb (9/87 and 3/88 samples only) by alpha spectrometric determination of the activity of ingrown daughter Po-210[17]. Separate subsamples (3/87 and 3/88 samples only) were dissolved in 0.5M HBr and analyzed for Pb content stable Pb isotope ratios using thermal ionization mass spectrometry with Faraday cup and Daly detection (these analyses carried out by Bruno Hamelin, Lamont-Doherty Geological Observatory). Reported ratios are for the Faraday cup; Daly detector results were equivalent within counting error. The particulate Pb contents determined by the mass spectrometric method

were equivalent to the atomic absorption analyses, within subsampling uncertainty (m.s./a.a. = 0.87 ± 0.17 [1σ] for 14 samples). It is therefore reasonable to conclude that both leaching procedures dissolved essentially all of the particulate Pb, and that the isotopic ratios are representative of total particulate Pb.

4.3. RESULTS

Suspended particulate Pb concentrations resemble but do not exactly parallel dissolved Pb profiles (Figure 4.1). Concentrations increase from about 1 pmol/kg in near-surface waters to a maximum of almost 3 pmol/kg at about 500m, then decrease to approximately constant deep water values of 1.6 pmol/kg. The results indicate that particulate Pb varies from 1% (surface) to 4% (deep water) of total Pb. I believe this is the first accurate measurement of suspended particulate Pb in the open ocean. Previous investigators analyzed particulate Pb filtered from Niskin bottles (0.4 μm filter), and obtained an average deep water concentration of 42 pmol/kg for the North Atlantic in 1974-75[18]. Because dissolved Pb in surface waters has changed by only a factor of ~4 during 1979-1987[15], and deeper waters by much less, such a high value is unlikely to be the result of historical input variations and is more likely due to sample contamination. Based on average crustal Pb/Al[19], less than 5% of particulate Pb is associated with refractory alumino-silicate particles. Most of the particulate Pb must therefore be acquired from solution, consistent with the observation that almost all atmospheric Pb is introduced dissolved in rain[20].

Figure 4.1. Vertical profiles of dissolved and particulate Pb and ^{210}Pb
near Bermuda. (A) Total dissolvable Pb for three station occupations in
1984: April (crosses), June (open circles) and September (filled
circles)[13]. (B) Total dissolvable ^{210}Pb for six station occupations in
1983-84[13]. (C) Suspended particulate Pb for five station occupations
1986-88 (see Chapter 3). Replicate symbols at a single depth represent
replicate subsamples of the same filter. (D) Suspended particulate ^{210}Pb
for September, 1987 (750m point only) and March, 1988 (all other points).
Depths in meters.

Total Pb (pmol/kg)

(A) 1984

Total Pb-210 (dpm/100kg)

(B) 1983-84

Particulate Pb (pmol/l)

(C) 1986-88

Particulate Pb-210 (dpm/100kg)

(D) 1987-88
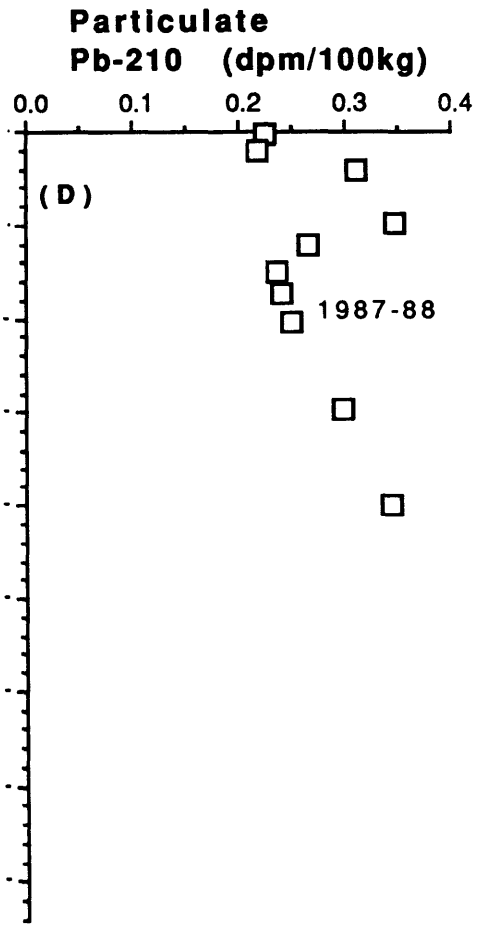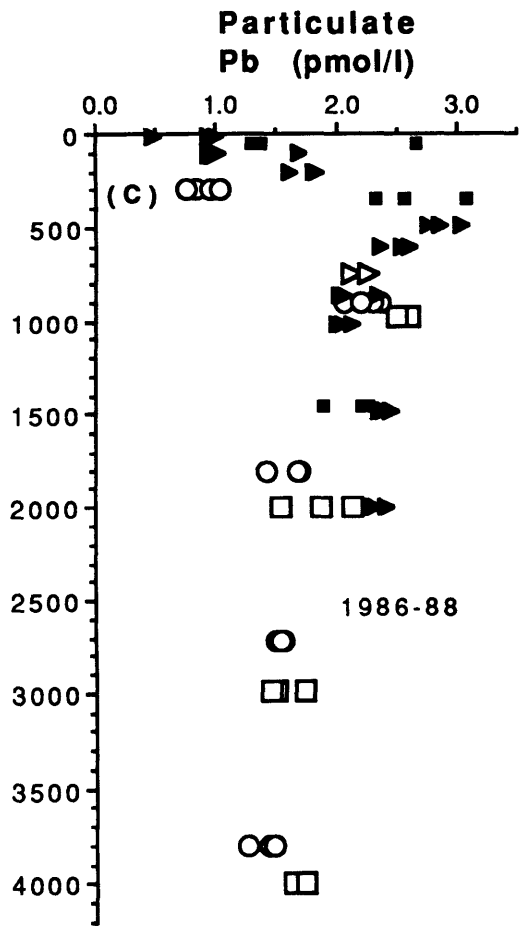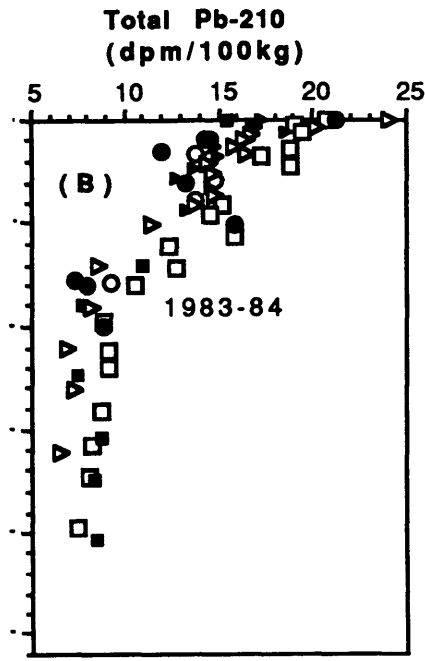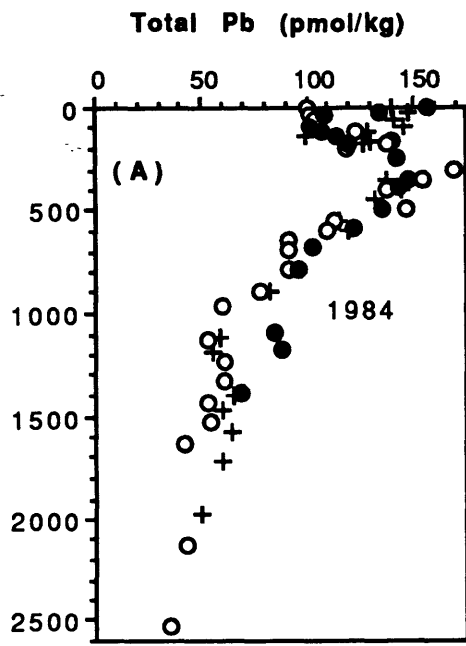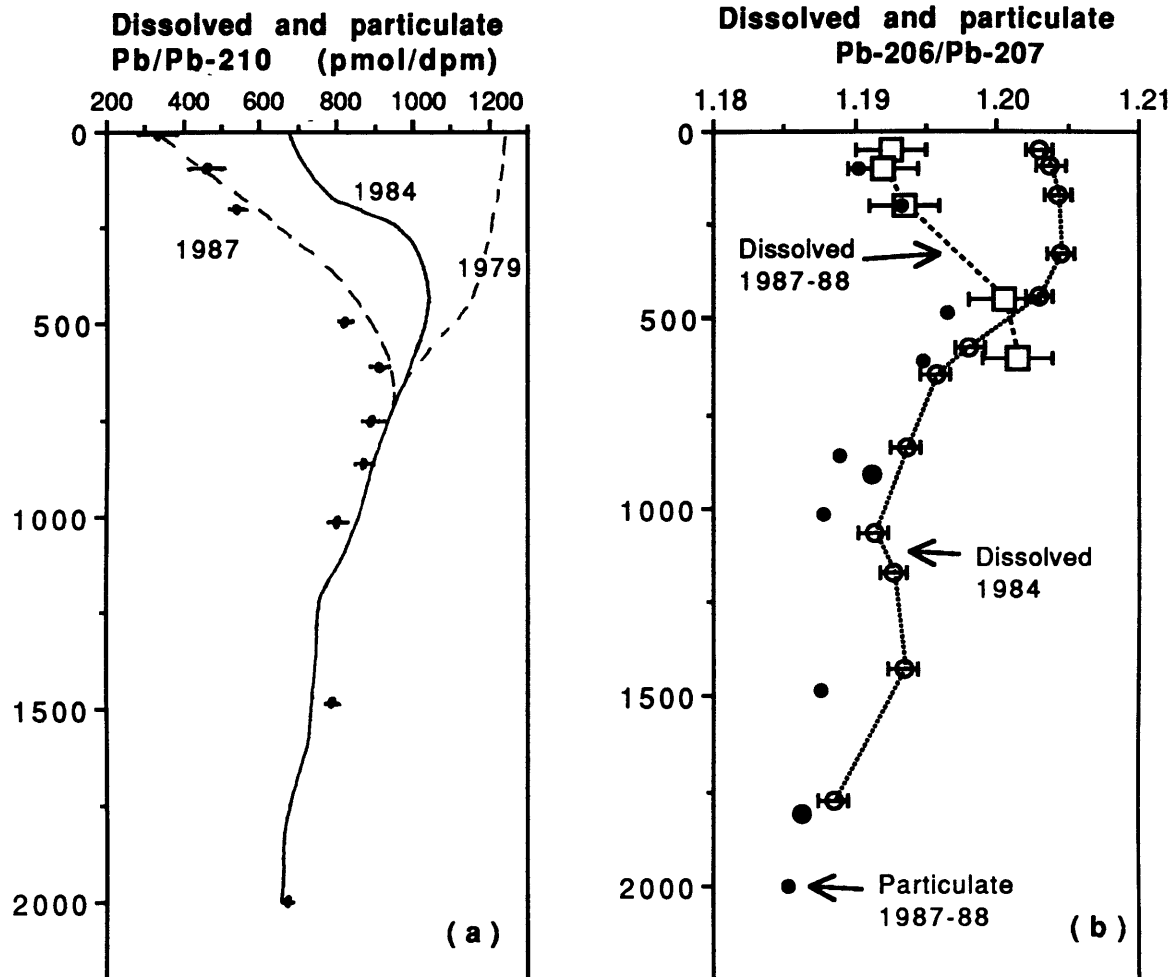
Figure 4.2. (a) Dissolved and particulate $Pb/^{210}Pb$ ratio. Dissolved profile for 1984 (solid line) calculated from mean ratios determined on three separate station occupations in 1984. Dissolved profiles for 1979 and 1987 (dashed lines) based on surface data[13] and thermocline ventilation model projections (Shen and Boyle, 1988)[11]. Suspended particulate data represented by solid symbols with error bars.
(b) Dissolved and particulate $^{206}Pb/^{207}Pb$ ratio. Dissolved profile for 1984 from Shen and Boyle, 1988 (open circles)[11], for 1987 from Hamelin, unpublished data (open squares). Suspended particulate data from March 1987 (large filled circles) and March, 1988 (small filled circles).

An upper thermocline maximum is also observed for suspended particulate ^{210}Pb, although no sub-surface maximum is seen in the dissolved ^{210}Pb profile (Figure 4.1). Between 800m and 2000m, particulate ^{210}Pb concentration increases by ~40% while particulate Pb appears to decrease slightly.

Profiles of lead isotopic composition (^{206}Pb/^{207}Pb values reported here) and Pb/^{210}Pb in the suspended particles were very similar to contemporaneous seawater profiles throughout the upper 2000m (Figure 4.2). In the upper 500m, particulate and dissolved ratios in 1987-88 were distinctly lower than dissolved ratios in both 1984 and 1979, consistent with the relatively rapid renewal of Pb in the upper thermocline[13]. Below this depth, 1987-88 values for both ratios converge with the 1984 dissolved profiles, indicating a relatively longer Pb residence time in deeper waters.

In surface waters, living or recently living forms dominate the suspended load; exogenous particles are a relatively minor fraction of the total mass (see Chapter 3). Because these particles are created de novo, they must have acquired their Pb directly from surface waters. Therefore, a good match between particulate and dissolved Pb composition is not surprising in the euphotic zone (upper 100m). Deeper in the water column, particle sources are more complex; some may be formed in situ, but most are likely to have settled vertically or been horizontally transported to their sampling location. Particles thus transported from other water masses with distinct Pb isotopic composition must exchange Pb with ambient seawater to acquire a matching isotopic signature. The agreement between the particulate and dissolved profiles suggests that

suspended particles undergo complete isotopic exchange of Pb with the surrounding seawater before they are removed from the water column. If, however, suspended particles at all depths are supplied by the disaggregation of surface-derived aggregates, then an alternative scenario is possible. Since surface particles have low Pb contents (per gram particles), suspended particles of recent surface origin would approach isotopic equilibrium with ambient seawater by an essentially unidirectional uptake. A better understanding of particle size-class interactions and the origin of suspended particles is necessary to discriminate the complete exchange versus one-way uptake scenarios.

The result is strengthened by the combined use of $^{206}Pb/^{207}Pb$ and $Pb/^{210}Pb$ ratios. The $Pb/^{210}Pb$ ratio displays a larger surface/deep signal, relative to measurement precision, than the $^{206}Pb/^{207}Pb$. On the basis of the $^{206}Pb/^{207}Pb$ ratio alone, it would not be possible to prove that particles at 1000m were isotopically distinct from surface particles. In addition, while the $^{206}Pb/^{207}Pb$ values observed in the water column are very similar to the "background" pre-anthropogenic values observed in bottom sediments[14], the water column $Pb/^{210}Pb$ ratios are indicative of Pb which was introduced to the surface ocean within the last few decades[11]. Because surface $^{206}Pb/^{207}Pb$ is unlikely to fall below the pre-gasoline Pb value of ~1.185, while $Pb/^{210}Pb$ may continue to decrease, this utility of the combined tracers for investigating water column exchange processes is likely to continue for at least the next few years.

4.4. <u>DISCUSSION</u>

Observations of recent anthropogenic Pb in surface sediments of the deep ocean have demonstrated that Pb can be transported rapidly from surface sources to the bottom[21,22], probably in the form of large, rapidly-sinking aggregates[23]. This result suggests that large-particulate Pb does not equilibrate with dissolved Pb during its descent. Using the present data and a simple model of particle interactions in the water column, it is possible to predict the composition of rapidly sinking Pb in the present and in the near future.

I adopt a model of particle interactions which arbitrarily divides the particle size continuum into two size classes: small particles with negligible sinking rates which dominate exchange with the dissolved pool by virtue of their abundance and surface area, and large rapidly-sinking aggregates originating in surface water which remove and regenerate the small particle population through aggregation/disaggregation processes occurring at all depths[2,24] (see Chapter 3). The degree to which the Pb isotopic composition of rapidly-sinking particles is modified from the surface value depends on the rate of small particle removal and the magnitude of the surface-derived Pb flux. Knowing the Pb content of small suspended particles, it is possible to calculate the contribution of their removal (the "repackaging flux") to the total Pb flux by assuming a reasonable residence time for these particles, and comparing the resultant calculated flux with the actual total flux measured with deep ocean sediment traps.

The results of such a calculation for Pb and for ^{210}Pb are presented in Table 4.1. Small particle residence time is calculated using

Table 4.1. Model-calculated small particle flux versus measured total fluxes of trace metals, Sargasso Sea.

Element	"Repackaging" flux[a] F_R	Total flux[b] F_T	$\dfrac{F_R}{F_T}$
Pb[c] 1979	[1.3] μmol m^{-2} yr^{-1}	[6.3] μmol m^{-2} yr^{-1}	0.21
1981	[1.2]	4.2	0.29
1987	1.0	[1.6]	0.63
^{210}Pb[d]	1640 dpm m^{-2} yr^{-1}	4180 dpm m^{-2} yr^{-1} ($\pm$39%)	0.39$\pm$0.30 ($\pm$76%)
^{230}Th[e]	55 dpm m^{-2} yr^{-1}	54 dpm m^{-2} yr^{-1}	1.02

(a) Calculated using mean deep water suspended particulate concentration data, assuming suspended particle residence time = 5.5y, 3000m water deep box.

(b) After Jickells et al.[26]. Mean fluxes of two-year time series sediment trap deployment (1980-1982) at 3200m.

(c) Brackets indicate model-projected values, see text.

(d) ^{210}Pb data from this study, and Bacon, unpublished data[24]. $F_T(^{210}$Pb) is mean of 1980-1986 deployments at 3200m ($\pm$1σ).

(e) Th data from Bacon (1988) unpublished data[24].

suspended and trapped ^{230}Th data for the same region. It is assumed that the flux of ^{230}Th, which has no independent surface source, is totally controlled by removal of the suspended particles. Results indicate that small particle "repackaging" processes which account for 100% of ^{230}Th removal only contribute 30±20% of the Pb (in 1981) and 39±34% of the ^{210}Pb sinking through the deep water. Thus most of the Pb and ^{210}Pb in rapidly-sinking particles must originate at the surface, and the isotopic composition of this material cannot be greatly shifted from the surface value; certainly it cannot equal the deep suspended particulate value. The history of Pb inputs to Bermuda waters suggests that sinking particulate Pb isotopic composition has been cominated by surface input ratios for at least the last 30 years[10].

Because of the continuing reduction in anthropogenic Pb input since the trap measurements were made, surface-derived Pb may cease to dominate the deep ocean Pb flux in the near future. If yearly average surface-derived Pb flux is dependent on the dissolved Pb concentration in surface waters (normalized to ^{210}Pb to eliminate short-term source strength variability), then we expect a decrease of 50% from 1979 to 1984[13], and half again by 1987[15]. The repackaging flux has probably been much less variable; if it is proportional to the total sub-surface Pb inventory, then this component of the total flux has probably decreased by <30% over the same period[13]. Thus the ratio of surface- versus deep-derived Pb flux ($[F_T - F_R]/F_R$) may have diminished from ~4 in 1979 to 0.6 in 1987 (Table 4.1). If surface concentrations continue to decrease as use of leaded gasoline ceases in the U.S., Pb derived from surface waters may become a minor portion of total deep ocean flux until the deep

water Pb inventory has diminished to a new steady-state. During this period, lead isotopic composition of sinking particles would be expected to resemble values observed in deep water suspended (and dissolved) Pb.

Recently obtained ^{210}Pb flux data from deep waters near Bermuda display substantial variability on sub-annual and interannual time scales, but are in reasonable agreement with the model overall. Time-series sediment trap measurements in mid- and deep-water (trap deployments by W. Deuser, ^{210}Pb analyses by M. Bacon) indicate that ^{210}Pb flux at 1500m averaged $63\pm18\%(1\sigma)$ of 3200m flux over the period May, 1984 to July, 1986 (n=9, two anomalously high ratios rejected), even though average mass flux was equal at the two depths[25]. Assuming this gradient to be constant with depth, and extrapolating the flux difference to a 3000m-deep water column, suggests that the flux increase due to deep ocean scavenging processes accounts for 65% ([100%-63%] x [3000m/1700m]) of the total ^{210}Pb flux at 3200m. This is in the upper range of (F_R/F_T) predicted by the model. In light of the large variability in 3200m ^{210}Pb flux from 1980-1986 (RSD of yearly means of F_T = 39%, Table 4.1), it is unclear whether the 1984-1986 1500m/3200m flux ratio can be considered a long-term mean for the Bermuda station.

The variability of sinking particle composition is further illustrated by combined Pb and ^{210}Pb measurements. The Pb/^{210}Pb ratio in trapped particles at 3200m varied between values higher than 1979 surface water and lower than 1984 deep water (2000m) over the period 1980-82, with no apparent dependence on mass flux (mean=970$\pm$560 [1σ] pmol/dpm[24,25,26]). The degree of interaction of the large-particle flux with the standing stock of suspended particles may thus be highly

variable on seasonal or shorter time scales. This result indicates that long-term observations of sinking particle composition might be required to significantly test the model prediction that sinking particle Pb isotopic composition should approch deep suspended composition over the next few years to decades.

REFERENCES

1. Bacon, M.P. & Anderson, R.F. J. Geophys. Res. 87, 2045-2056 (1982).

2. Nozaki, Y., Yang, H.S. & Yamada, M. J. Geophys. Res. 92, 772-778 (1987).

3. Rama, Koide, M. and Goldberg, E.D. Science 134, 98 (1961).

4. Craig, H., Krishnaswami, S. and Somayajulu, B.L.K. Earth Planet . Sci. Lett. 17, 295-305 (1973).

5. Bacon, M.P., Spencer, D.W. & Brewer, P.G. Earth Planet. Sci. Lett. 32, 277-296 (1976).

6. Nozaki, Y., Thomson, J. & Turekian, K.K. Earth Planet. Sci. Lett. 32, 304-312 (1976).

7. Nozaki, Y., Turekian, K.K. & von Damm, K. Earth Planet. Sci. Lett. 49, 393-400 (1980).

8. Moore, W.S. & Sackett, W.M. J. Geophys. Res. 69, 5401-5405 (1964).

9. Anderson, R.F., Bacon, M.P. & Brewer, P.G. Earth Planet. Sci. Lett. 62, 7-23 (1983).

10. Shen, G.T. & Boyle, E.A. Earth Planet Sci. Lett. 82, 289-304 (1987).

11. Shen, G.T. & Boyle, E.A. J. Geophys. Res. 93, 15, 715-15,732 (1988).

12. Settle, D.M., & Patterson, C.C. J. Geophys. Res. 87, 8857-8869 (1982).

13. Boyle, E.A., Chapnick, S.D. & Shen, G.T. J. Geophys. Res. 91, 8573-8593, (1986).

14. Hamelin, B., Grousset, F. & Sholkovitz, E.R., Geochim. Cosmochim. Acta, submitted (1989).

15. Boyle, E.A. Unpublished data (1989).

16. Schaule, B.K. and Patterson, C.C. Earth Planet. Sci. Lett. 54, 97-116 (1981).

17. Fleer, A.P. & Bacon, M.P. Nuclear Instr. Meth. Phys. Res. 223, 243-249 (1984).

18. Buat-Menard, P. & Chesselet, R. Earth Planet Sci. Lett. 42, 399-411 (1979).

19. Taylor, S.R. Geochim. Cosmochim. Acta 28, 1273-1285 (1964).

20. Jickells, T.D., Church, T.M. & Deuser, W.G. Global Biogeochem. Cycles 1, 117-130 (1987).

21. Hamlin, B., Shen, G.T. & Sholkovitz, E.R. EOS, 68, 1319 (1987).

22. Veron, A., Lambert, C.E., Isley, A. Linet, P. & Grousset, F. Nature 326, 278-280 (1987).

23. Fowler, S.W. & Knauer, G.A. Prog. Oceanog. 16, 147-194, (1986).

23. Bacon, M.P., Huh, C.A., Fleer, A.P. & Deuser, W.G. Deep-Sea Res. 32, 273-286 (1985).

25. Bacon, M.P. & Deuser, W.G. person. comm. (1989).

26. Jickells, T.D. Deuser, W.G. & Knap, A.H. Deep-Sea Res. 31, 1169-1178, (1984).

CHAPTER 5

PARTITIONING OF TRACE METALS ON OCEANIC SUSPENDED MATTER: EVIDENCE FROM

THE SARGASSO SEA AND THE NORTHEAST PACIFIC

5.1. <u>INTRODUCTION</u>

Oceanic scavenging of trace metals depends on two fundamental
variables: partitioning of metals between particles and solution, and the
removal rate of the particles. Neither of these processes is easily
quantified in the open ocean water column. Sediment traps can be used to
estimate the vertical flux of material at any depth, but the origin of
this material is difficult to determine. Near-bottom particle fluxes may
be more closely related to variable productivity in surface waters than
to the removal rate of suspended particles in the sub-surface water
column (Deuser et al., 1981; Deuser, 1986; Billet, et al., 1983).
Partitioning of metals between dissolved and suspended phases is also
difficult to determine: particulate metal concentrations in the open
ocean are low, making sample collection difficult and
contamination-prone. Determining the controls on the magnitude of these
two processes is central to understanding how particles influence metal
concentration and distribution in the ocean. The purpose of this study
was to investigate the latter problem, the magnitude and variability of
seawater/particle partitioning of metals in the open ocean. Here I
present vertical profiles of suspended particulate trace metals at two
oceanographically distinct locations, the northeast Pacific and the
Sargasso Sea.

Many investigators have suggested that the major process by which metals become associated with oceanic particles is by adsorption on particle surfaces (Goldberg, 1954; Craig, 1974; Lal, 1977; Turekian, 1977; Whitfield and Turner, 1987). Aquatic surface chemists have endeavored to attain a predictive understanding of metal partitioning based on the fundamental chemical properties of each individual element and on a knowledge of the important functional groups on the particle surface. To this end, scavenging behavior is modeled as a surface complexation process, and correlations are sought between observed partition coefficients and an intrinsic chemical property, such as the first hydrolysis constant of the free cation (Schindler, 1975; Balistrieri et al., 1981). The partition coefficients used in these studies have, in most cases, been determined in laboratory uptake experiments on simple pure phase surfaces, mostly mineral oxides (Murray, 1975; Benjamin and Leckie, 1980). The relationship between the partition coefficient and the intrinsic chemical property can be compared to observations in natural systems to characterize the surfaces of natural particles with respect to their metal affinity. On this basis, several authors have suggested that ubiquitous organic coatings may dominate the surface chemistry of suspended particles, and that mineral oxides, for example, are less important adsorbers (Balistrieri et al., 1981; Hunter, 1983). In general, however, the use of surface complexation models and data from pure phase adsorption experiments to distinguish between possible surfaces responsible for oceanic scavenging has produced equivocal results (Whitfield and Turner, 1987).

Recently, marine geochemists have studied metal uptake by measuring uptake of radiotracers onto several natural particle types, in an effort to relate adsorption behavior on heterogeneous particles to that observed on well-defined surfaces (Li et al., 1984; Nyffeler et al., 1984). These experiments allow "equilibrium" distribution coefficients to be determined for the sediment types investigated, and enable the kinetics of adsorption and desorption to be modeled. The validity of extrapolating the magnitude and mechanism of uptake measured in the laboratory to real oceanic environments remains open to question, however. Among the reasons for this are (1) the particle types used, usually sediment trap or bottom sediments (Li et al., 1984; Nyffeler et al., 1984), may not be the particles responsible for exchange with dissolved metals in the real system, (2) the particle concentrations used are frequently several orders of magnitude higher than exist in the deep ocean, and (3) time scales of reaction are shorter in laboratory experiments than those in the open ocean. Some of these concerns are now beginning to be addressed (Jannasch et al., 1988).

In order to understand metal scavenging in natural systems, it is necessary to determine whether processes which appear to control metal partitioning under artificial conditions could explain the magnitude and variability of partition coefficients observed in the field.

The link between experiment, theory, and observation would be strengthened by a greater understanding of metal association with oceanic suspended matter. This material, in contrast to the rapidly-sinking material collected in a sediment trap, comprises the bulk of the standing stock of mass and surface area, and is therefore most likely to dominate

interaction with dissolved metals. While some information exists on the dissolved/particulate partitioning of Th isotopes (Bacon and Anderson, 1982), Pu, (Cochran et al., 1987), and relatively major constituent metals in marine particles (e.g. Fe, Mn; Landing and Bruland, 1987, Bishop and Fleisher, 1987; Ba, Collier and Edmond, 1984), current knowledge of trace metal distribution coefficients in the oceanic water column is limited. Measurements of filtered and unfiltered water samples provide estimates of dissolved versus "total dissolvable" metals, and indicate that suspended particulate metals (0.4 μm filter) generally comprise <10% of dissolved metal. However, a much more accurate measurement of both particulate metal concentration and particle mass concentration is necessary for accurate determination of partition coefficients. Little is known, therefore, of how dissolved/particulate partitioning varies with depth, particle concentration, bulk particle composition, dissolved metal concentration, or oceanographic regime. Moreover, the importance of processes other than adsorption (e.g ion exchange, (co-)precipitation, incorporation in refractory mineral phases, or active biological uptake) in determining observed distribution coefficients is not well understood.

To begin to address this problem, I present a depth profile of suspended particulate Mn, Co, Cu, Zn, Ni, Cd and Pb in the northeast Pacific, and compare these results with particulate metal distributions observed previously in the Sargasso Sea (Chapter 3). The particulate metal concentrations are of similar magnitude at the two stations, and the relative partitioning of these metals onto marine particles is consistent in a broad sense with the results of laboratory sorption

experiments and surface chemical scavenging models. However, the absolute magnitude of the particulate metal concentrations, and the differences (< 1 order of magnitude) in partitioning between the two stations are difficult to reconcile with simple surface chemical models. The results suggest that bulk particle composition and/or biological activity may be important in determining metal partitioning both in surface and sub-surface waters.

5.2. SAMPLING AND ANALYSIS

Samples were collected in the Sargasso Sea near Bermuda, and in the northeast Pacific. Collection and analysis of the Sargasso Sea samples, obtained during five station occupations from September, 1986 to April, 1988, has been described previously (Chapter 3). The northeast Pacific samples were collected by in situ pumping over the period June 4-12, 1988 at 41°00'N, 127°30'W, on Atlantis II/ALVIN cruise 118/35. The station is located over the southern Escanaba Trough, a portion of the Gorda Ridge system, about 300km off the northern California coast (Fig. 5.1).

Samples of <53μm suspended particulate matter were collected and analyzed for Al, Fe, Mn, Co, Cu, Zn, Ni, Cd, Pb and P by techniques described previously (Chapters 2 and 3). Profiles of in situ temperature were determined using reversing thermometers, and salinity, phosphate, silicate and dissolved oxygen were determined by standard techniques.
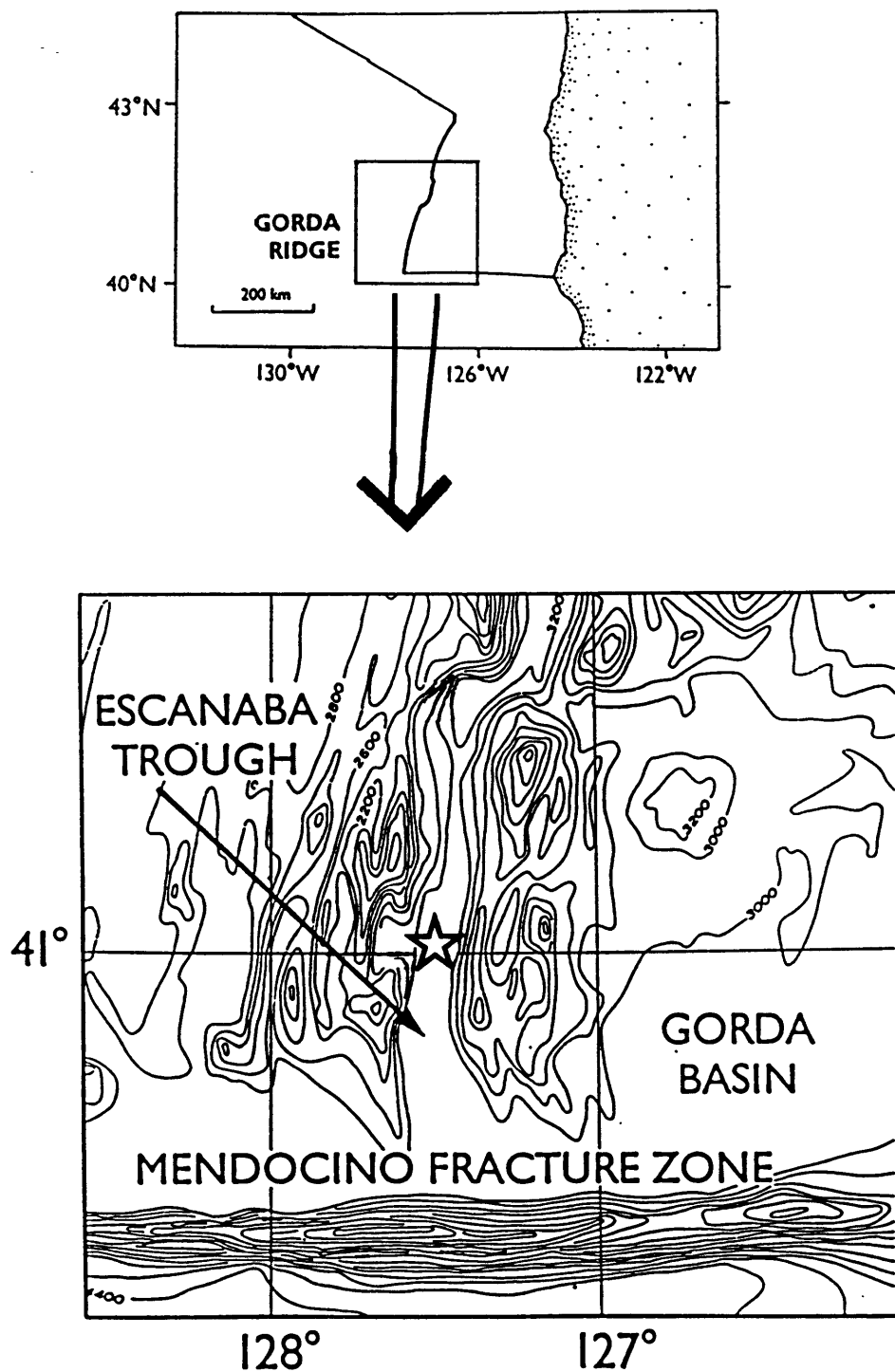
Fig. 5.1. Bathymetric chart showing location of northeast Pacific station in southern Escanaba Trough.
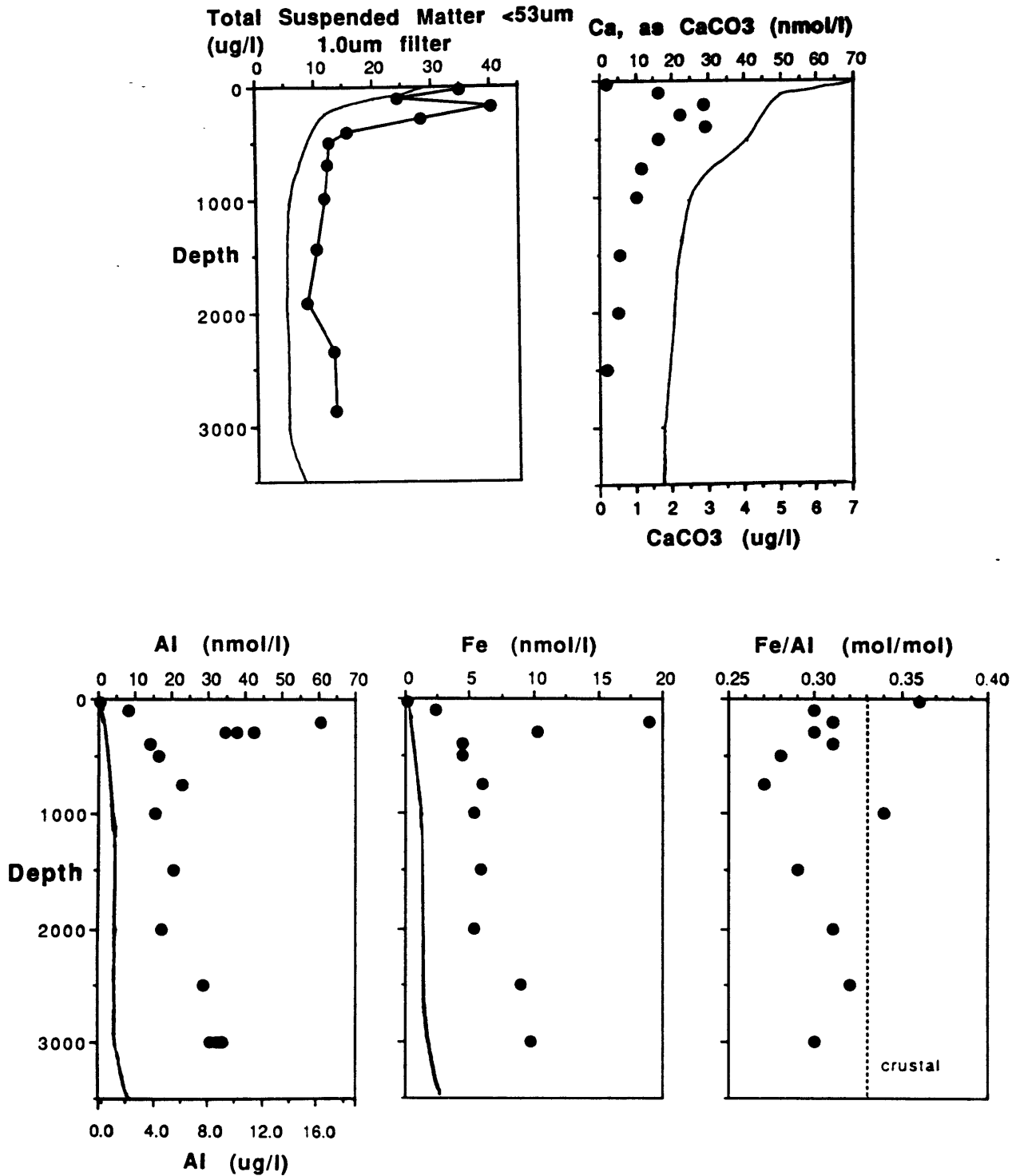
Fig. 5.2. Profiles of total suspended mass concentration and major particulate constituent elements. Sargasso Sea profile shown in solid line for comparison. Note Fe/Al ratio approximately equal to average crustal ratio (Taylor, 1964) throughout water column.

5.3. RESULTS

The particulate metal data for the Sargasso Sea station has been presented previously (Chapter 3). To summarize, concentrations of Fe, Co, Zn, Cu, Cd, Ni, and Pb on suspended particles were seen to be lower than previously measured values by factors of 3 to 50. Al and Mn concentrations, on the other hand, were similar to previous estimates. Principal features of the profiles were similar for all the trace metals analyzed except Cd. In general, surface concentrations of particulate metals were low and variable, a metal concentration maximum was found at ~500m, and deep water concentrations (per liter seawater) were constant or slightly decreasing from 1000-3000m. Particulate Cd concentrations, on the other hand, were highest in surface water, decreasing to very low and constant values in deep water. Mean deep water particle concentration was about 6 ± 1 μg/l, increasing to 11 μg/l in two near-bottom nepheloid layer samples.

Suspended particulate mass and major constituent composition for the Pacific station are presented in Fig. 5.2. The particle distribution and composition at this site reflect proximity to continental particle sources and higher surface productivity compared with the Sargasso Sea station (California Current average primary productivity ~3-6 times greater than Sargasso Sea productivity, estimated on the basis of the compilations of Berger et al., 1987). The particle mass concentration is similar to Sargasso Sea values in surface water (although >53μm fraction was not analyzed for Pacific samples, and may contribute significantly to total mass in near-surface waters), but is about two times higher in intermediate and deep waters (Fig. 5.2). This can be

Bulk Composition (Wt. %)
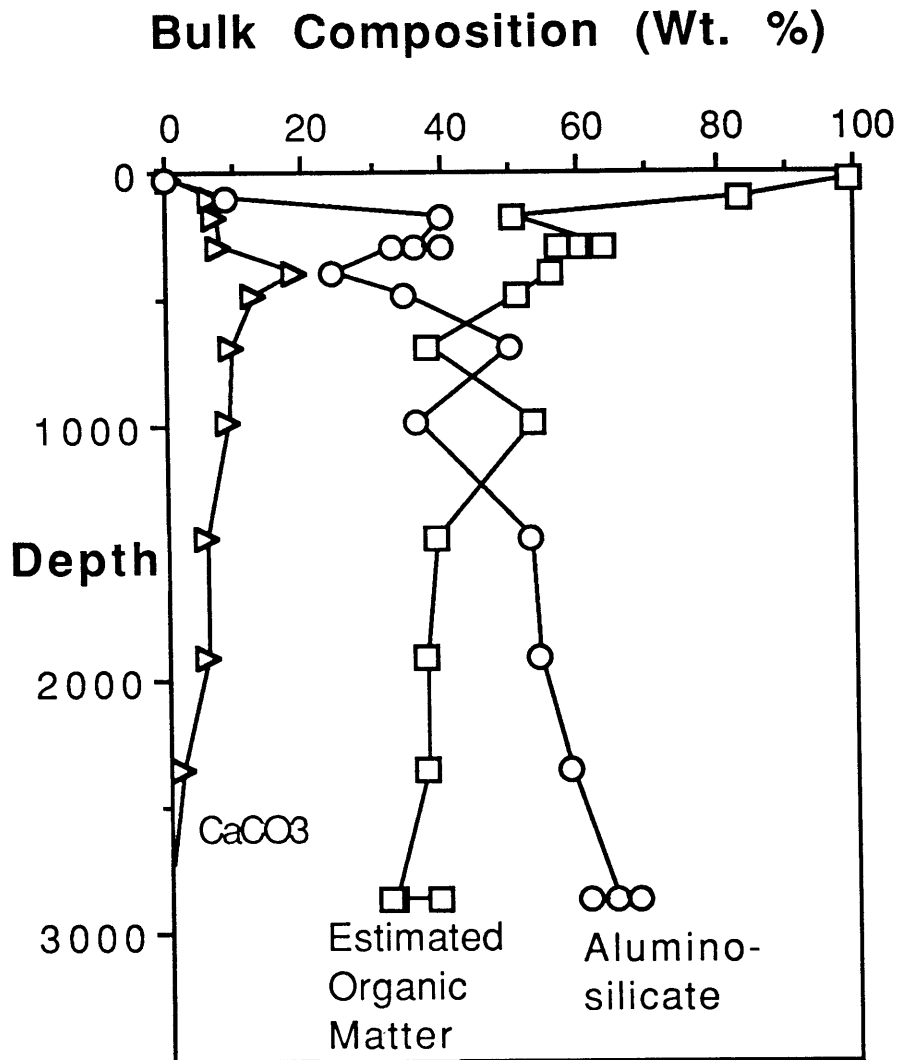
Fig. 5.3. Relative bulk composition of suspended particulate matter, Pacific station. Organic matter is an upper limit estimate.

attributed largely to the presence of aluminosilicates, which contribute about half the suspended mass in sub-surface waters (Fig. 5.3). This terrigenous material is most likely derived from major rivers draining the northwest U.S., of which the Columbia River is dominant. Southward flowing sediment-laden bottom waters are apparently diverted by the Mendocino Fracture Zone and flow northward into the Escanaba Trough; a core at DSDP Site 35 in the Escanba Trough revealed 390m of turbidites in the axial valley (DSDP, 1970). Comparable particulate Al and Fe values were found at Vertex-I and CEROP-I by Landing and Bruland (1987) several hundred kilometers south in the California Current.

Particulate Ca is lower throughout the water column than near Bermuda, suggesting that $CaCO_3$ is not the major biogenic mineral produced in surface waters at the Pacific station (Fig. 5.2 and 5.3). While particulate C and P are both higher at the Pacific station, the C/P ratio is apparently 2-3 times the Redfield value (106-140 mol/mol, Redfield et al., 1963;, Takahashi, 1985; Peng and Broecker, 1987) and approximately constant with depth (Fig. 5.4). It should be noted that the C/P estimate at the Pacific station is an upper limit, since the opal fraction was not measured. This is likely to lead to substantial overestimates of organic carbon (and therefore C/P), especially in the upper water column.

Superimposed on these general trends are two features unique to the Pacific station. First, a sub-surface particle maximum is observed at ~200m, where suspended mass concentration increases to about twice the values above and below the maximum (Fig. 5.2). Second, in the lower water column, resuspended material, probably of hydrothermal and
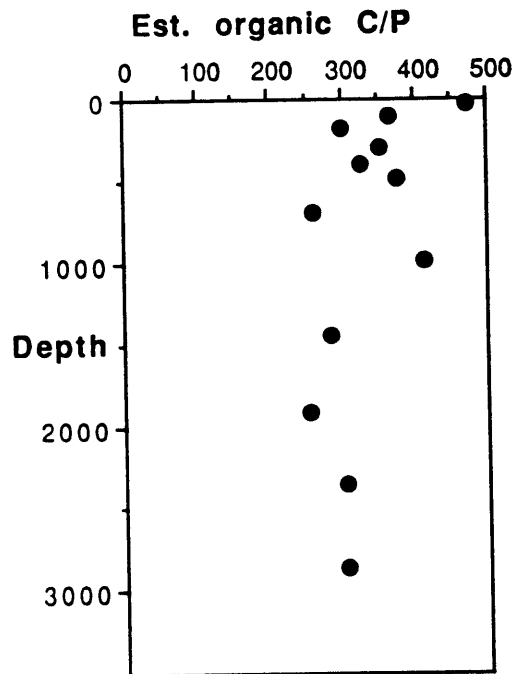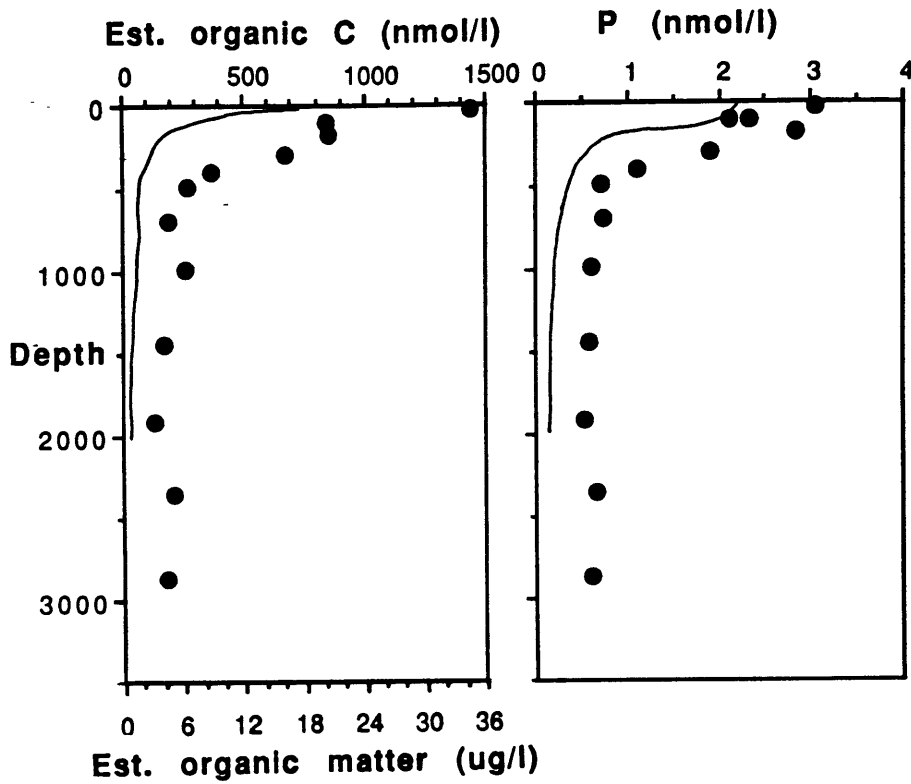
Fig. 5.4. Particulate organic carbon (estimated), phosphorus (measured), and organic C/P ratio (upper limit estimate).

Fig. 5.5. Profiles of suspended particulate trace metals (<53 μm) at
Pacific station. Filled circles represent total particulate metal, open
circles represent "excess" particulate metal (estimated aluminosilicate
fraction subtracted). Replicate symbols at a single depth represent
analyses of replicate subsamples. Solid lines represent Sargasso Sea
total particulate metal profiles (uncorrected for the generally minor
aluminosilicate fraction), for comparison. Note scale change in Mn plot.

Mn (pmol/l)

Co (pmol/l)

Pb (pmol/l)

Zn (pmol/l)

Cu (pmol/l)

Ni (pmol/l)

Cd (pmol/l)
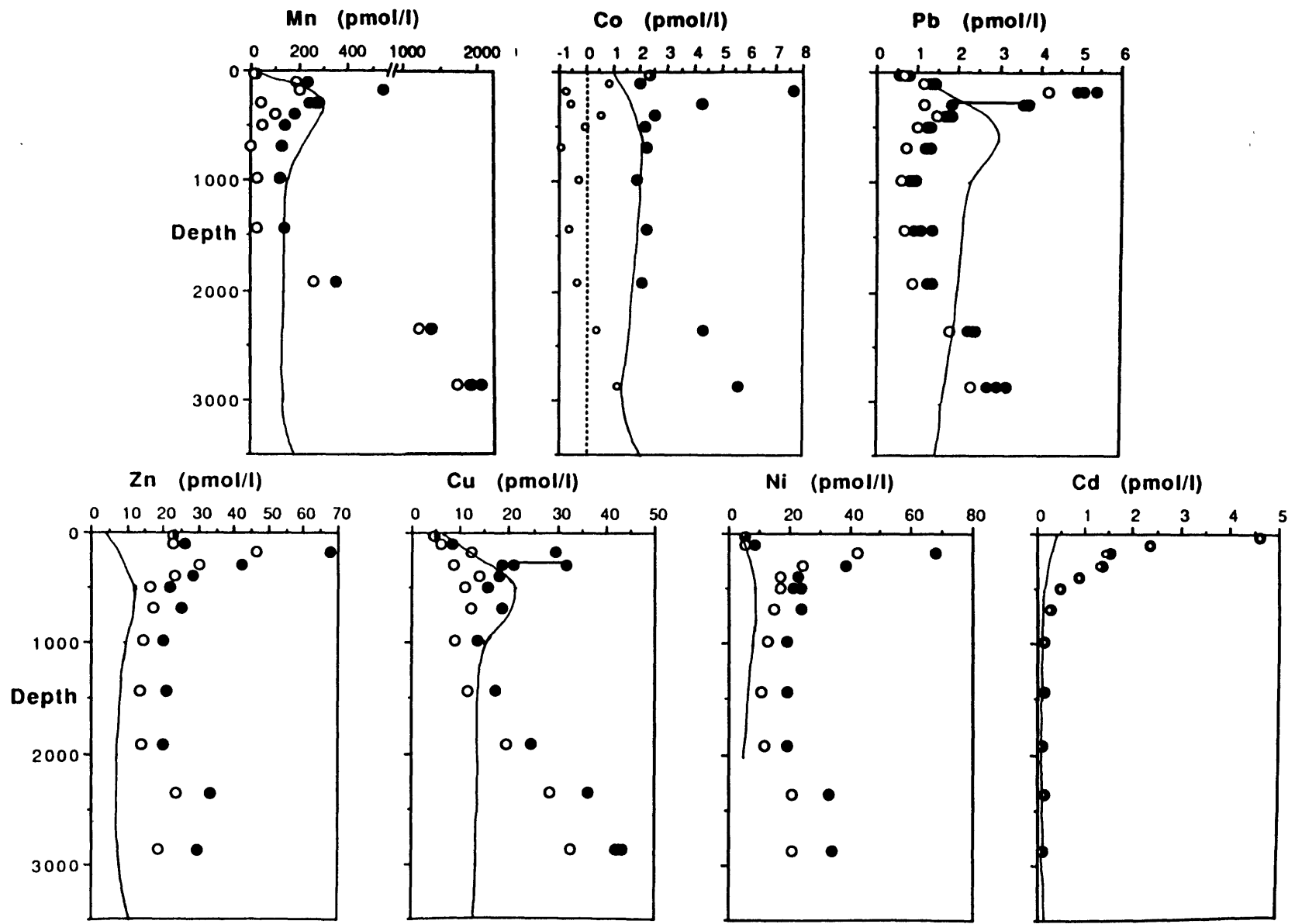
continental origin, influences particulate metal distributions below 1500m.

Depth profiles for particulate Mn, Co, Cu, Zn, Ni, Cd and Pb are shown in Fig. 5.5, with Sargasso Sea profiles represented by solid lines for comparison. In general, concentrations are similar at the two stations. Intermediate water values (1500m) generally differ by a factor of two or less, the total particulate metal concentration being higher in the Pacific station for Cu, Zn, and Ni, about the same for Cd and Co, and lower for Mn and Pb. Surface waters at the two stations have similar suspended mass concentrations, and similar concentrations of particulate Mn, Cu, Ni and Pb. Surface concentrations of particulate Zn and Cd are higher at the Pacific site by factors of 5 and 10, respectively.

In the following discussion, I will briefly address the possible sources of the sub-surface particle maximum and the lower water column increases in metal concentration observed at the Pacific station. Next, I will focus on particulate metal concentrations in intermediate waters at the Atlantic and Pacific stations and their relation to dissolved metal distributions. Finally, biological control of particulate metal concentrations in surface waters at the two stations will be addressed. The overall conclusion is that metal partitioning in the open ocean varies from one location to another in response to variables which are outside the predictive capability of simple surface chemical models.

5.4. DISCUSSION

5.4.1. Sources of sub-surface and near-bottom particulate metal maxima at the northeast Pacific station.

The sub-surface particle maximum at the Pacific station is evident
in all metal profiles except Cd (Fig. 5.5). Normalizing the metal
concentration to particle mass, however, reveals that for most of these
elements the metal content of particles in the maximum does not fall
significantly off the trend defined by samples above and below the
maximum (Fig. 5.6). Exceptions are the Al and Fe content, which are
about 2 times higher in the maximum than expected from the trend (not
plotted), and Cd, which falls low of the trend defined by the shallowest
samples and the >400m samples bracketing the particle maximum.

These observations do not immediately point to a source for the
particle maximum. Lerman et al. (1974) have suggested a mechanism
whereby particle maxima can be caused by a rapid decrease in average
particle sinking speed as particles disaggregate and dissolve.
Subsequent elimination of particles below the maximum is hypothesized to
occur when particles re-aggregate, possibly through the activities of
zooplankton. Such variations in particle dynamics are difficult to
observe, however, and this hypothesis has not been verified. It is more
likely that the sub-surface particle maximum is the result of horizontal
advection of resuspended matter from the shelf/slope region.
Transmissometer studies have demonstrated the presence of nepheloid
layers created at the shelf/slope break off the coast of Washington,
which are laterally advected as much as 100km offshore (Pak et al.,
1980). These features have not been observed as far from the coast as
our station. However, recent satellite observations of large filaments or
jets of coastal water extending hundreds of kilometers into the
California Current suggest a mechanism by which particles of coastal

Fig. 5.6. Profiles of suspended particulate metals (total, <53 μm), expressed per gram dry weight of suspended material for Pacific station (filled circles) and Sargasso Sea station (open circles).
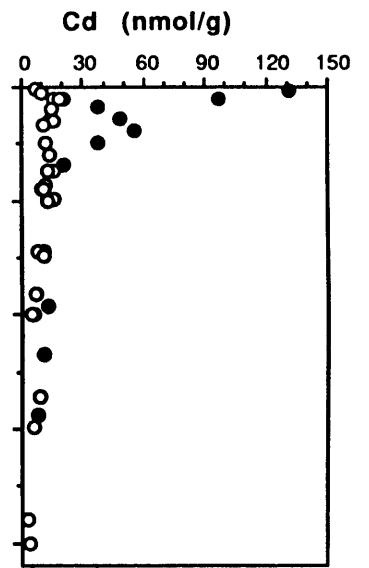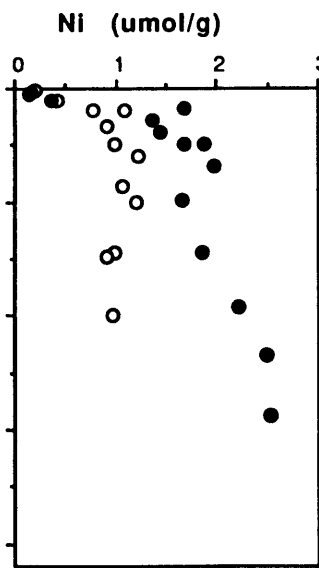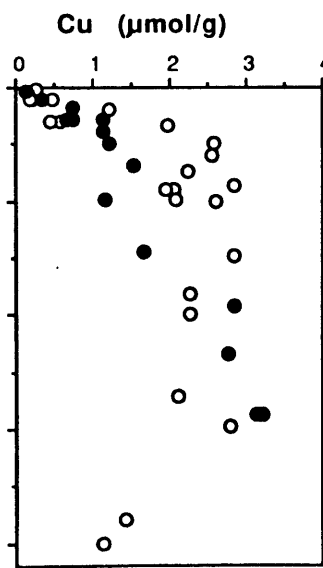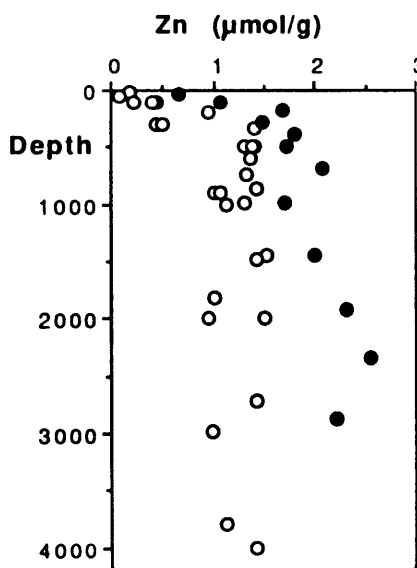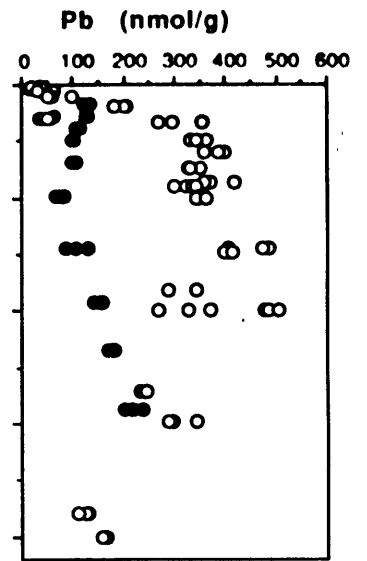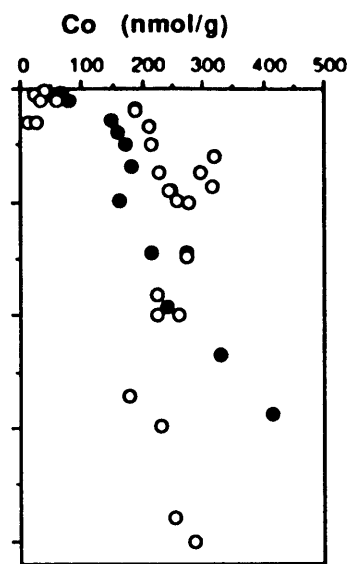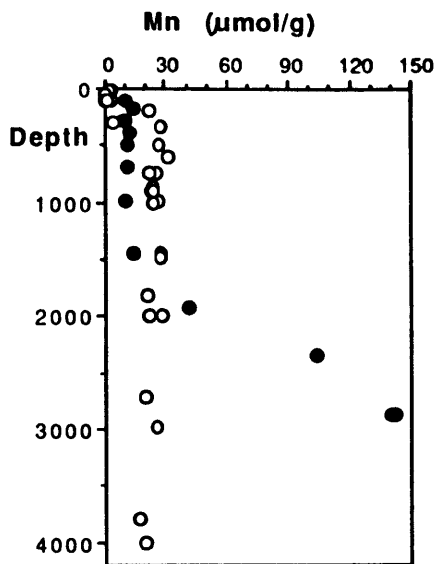
origin could be transported over this distance (Mooers and Robinson, 1984; Flament et al., 1985). The enrichment in detrital minerals (evidenced by increased Al and Fe) at the particle maximum is consistent with this explanation. A transect of stations demonstrating continuity of the feature from the shelf to our station would be necessary to prove this hypothesis.

In the lower water column, concentrations of particulate Mn, Co, Cu and Pb increase with depth, and particulate Zn and Ni increase slightly, while particulate mass increases only ~50% in the bottom two samples (Fig. 5.5). This feature is most evident in the Mn profile, where total Mn content increases by an order of magnitude from 1500m to 3000m, to a maximum of about 0.8 wt.% Mn. Evidence of past and present hydrothermal activity within the axial valley at this location were observed by ALVIN personnel on this cruise (Campbell et al., 1988). The metal enrichments probably do not reflect the presence of hydrothermal plume particles of recent origin because, (1) previously observed hydrothermal plumes (e.g. TAG, Mid-Atlantic Ridge, 26°N, Nelson et al., 1986; Chapter 6) rise to discrete depth zones of neutral buoyancy and spread horizonally; limited vertical mixing confines the plume to a vertical thickness of a few hundred meters within tens of kilometers of the source (Klinkhammer et al., 1986; Trocine and Trefry, 1988), and (2) vent fluids observed in this section of the southern Escanaba Trough were in fact depleted in Mn relative to previously sampled hydrothermal fluids, and no "black smokers" were observed (Campbell et al., 1988). Although this does not rule out active plume sources from elsewhere on the ridge system (Baker et al., 1987) it is more likely that the increase in particulate Mn is

Table 5.1. Comparsion of elemental composition of deepest (2872m)
Escanaba Trough suspended particles with that of surface
sediments from a nearby giant gravity core.

Element	Core 10GC[a]		2872m suspended particles[b]
Al	3.1	(mmol/g)	2.4
Fe	1.1	(mmol/g)	0.72
Mn	180	(μmol/g)	144
Co	[508]	(nmol/g)	416
Zn	2.65	(μmol/g)	2.2
Ni	[2.56]	(μmol/g)	2.53
Cu	1.76	(μmol/g)	3.12
Pb	[575]	(nmol/g)	215

a) Surface sediments from L685NC Core 10GC, 41°00.55'N, 127°27.05'W,
analyzed by XRF (M. Lyle, Lamont-Doherty Geological Observatory,
pers. comm.). Values in brackets have poor precision (high
background).

b) See Appendix B, Table B.2.

caused by resuspension of sediments on the valley floor and on its walls, which rise to a depth of ~2300m about 10 km on either side of the sampling station (Fig. 5.1). This is further demonstrated by a comparison of the elemental composition of the deepest (2872m) suspended particle sample with that of surface sediment from a nearby giant gravity core (Table 5.1). Note that the suspended/surface sediment ratio is 0.75±0.10 for Al, Fe, Mn, Co and Zn. Ni concentrations are also of similar magnitude, although the sediment value is imprecise (high background on XRF). The Cu content of the suspended particles is anomalous (75% higher than surface sediments), suggesting an additional deep-scavenging source.

The degree of metal enrichment in the lower water column most likely reflects the composition of hydrothermal sediments relative to that of ambient deep water suspended particles (although metal contents of surface sediments at this site are not well known) and, below 2000m, the contribution from increased concentrations of aluminosilicate particles (Fig. 5.2 and 5.3). In addition, there may be some contribution from metals which are scavenged from the water column by the high-Mn resuspended material (Trocine and Trefry, 1988).

5.4.2. Controls on metal partitioning in intermediate water in the northeast Pacific and the Sargasso Sea

By comparing suspended particulate metal distributions in intermediate waters at the Sargasso Sea and northeast Pacific stations we can perform a simple test of the hypothesis that metal partitioning in the ocean is controlled by adsorption on a single ubiquitous surface

type. If such a simple model were appropriate, we would expect to find proportionality between the metal contents of particles and the concentration of metals dissolved in the water in which the particles are suspended. If no such relationship were found, other controls on oceanic metal partitioning would be implied. Intermediate waters (500-1500m) are chosen for this comparison because particles in this depth interval are below the surface layer where it is expected that biological processes dominate physio-chemical interactions, and above the influence of resuspended material at the Pacific site.

Profiles of the metal content of suspended particles (expressed as mol/g dry weight of <53 μm particulate matter) at the Pacific and Atlantic stations are plotted in Fig. 5.6. It can be seen that the concentrations of Zn, Ni, and Cd in the 500-1500m depth range are approximately equal or slightly higher at the Pacific station. For each of these metals, about half of the difference is due to the higher concentration of aluminosilicates at the Pacific station. If we subtract this portion (estimated from average crustal ratios [Taylor, 1964]) from the total metal content on the assumption that the refractory mineral fraction is not involved in interactions with the dissolved phase, the Pacific/Atlantic ratios of particulate metal content become: Zn, 1.2; Ni, 1.4; Cd, 1.1. These differences are considerably smaller than the corresponding ratios for dissolved metals: Zn, 5; Ni, 2; Cd, 3 (Bruland, 1980; Bruland and Franks, 1983)(Table 5.2 and Fig. 5.7). Thus the particulate content of these three metals is remarkably constant at two oceanographically distinct locations with large differences in dissolved concentration. This suggests that processes other than surface

Table 5.2. Ratios of North Pacific to North Atlantic dissolved
           and particulate trace metals (500-1500m means).
           See text for explanation.

Element	Pacific/Atlantic	
	Dissolved	Particulate
Mn	1.0	0.5
Co	1.0	0.6
Cu	1.5	0.5
Zn	5	1.2
Ni	2	1.4
Cd	3	1.1
Pb	0.2	0.25
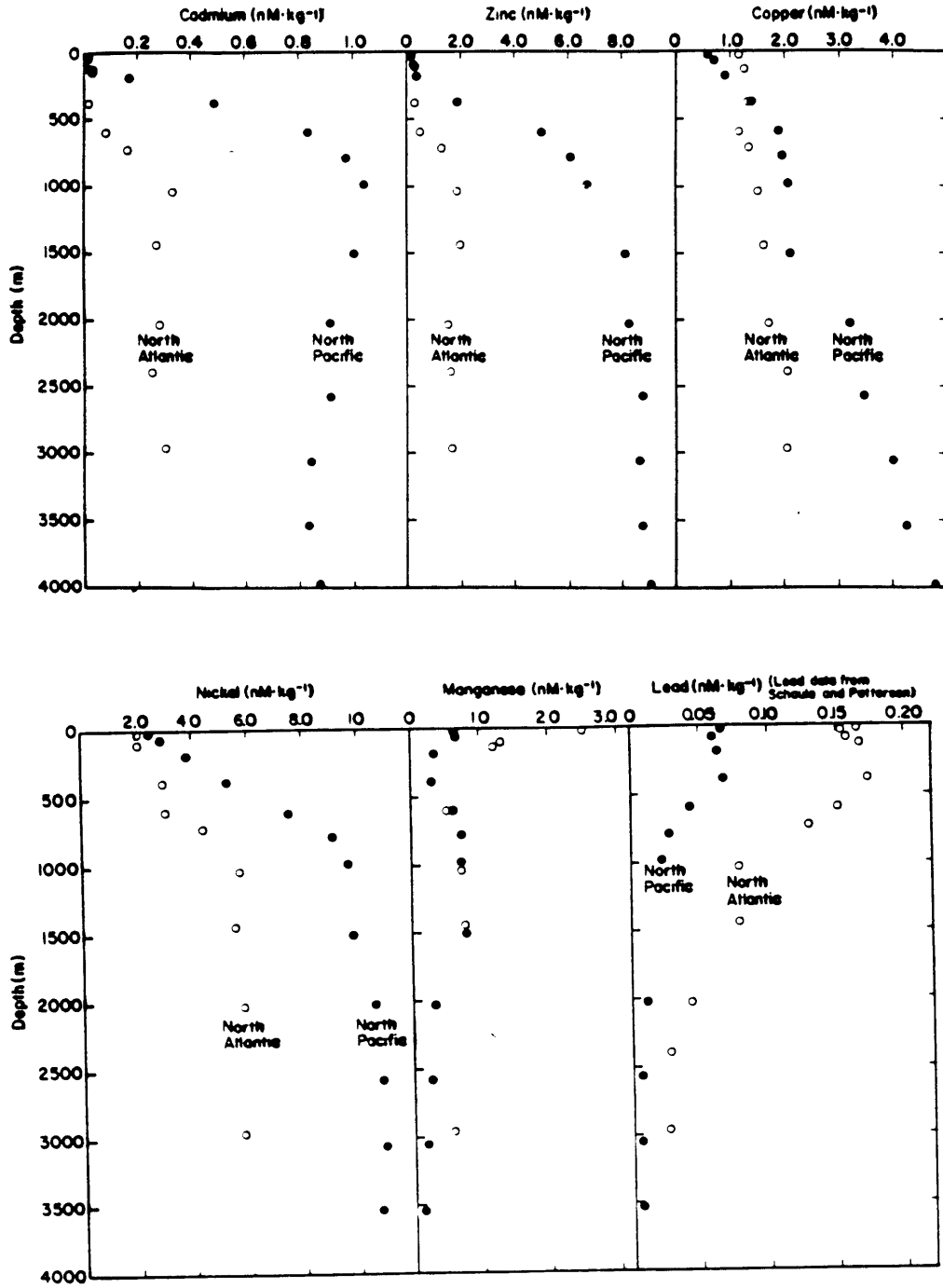
Fig. 5.7. Profiles of North Atlantic (34°06'N, 66°07'W) and North Pacific (32°41'N, 145°00'W) dissolved trace metals. After Bruland and Franks (1983).

adsorption control the dissolved/particulate partitioning for these elements. The correlation of dissolved profiles of these elements with those of major nutrient elements (Bruland, 1983) indicates that biological processes might be more important. These results suggest that the metal content of intermediate depth suspended particles is relatively insensitive to rather different biological provenances in surface water.

In contrast to the above nutrient-type elements, the total particulate content of Mn, Co, Cu, and Pb at 500-1500m is lower at the Pacific station by factors of 2.0, 1.6, 2.0, and 4.0, respectively (Fig. 5.6, Table 5.2). The corrections for refractory fractions of particulate Mn and Co at the Pacific station are large and are probably unreliable overestimates (see negative "excess" Co values calulated using average crustal ratios of Taylor, [1964], Fig. 5.5). A conservative correction for refractory ratios (estimating 25% refractory Mn and Co) increases the ratios to 3.0 for Mn and Co, 2.7 for Cu and 5.5 for Pb. The dissolved concentrations of Mn, Co, and Cu are likely to be about the same, or even somewhat higher in the Pacific (Fig. 5.7). It is known that the Pacific/Atlantic ratio for dissolved Cu is approximately 1.5 in this depth range (Bruland, 1980; Bruland and Franks, 1983). This inter-basin comparison is more difficult to make for Mn and Co, however, because dissolved profiles from the same Pacific station are not available and must be estimated from other California Current stations. Such extrapolations are uncertain because Mn and Co are short residence time elements whose concentrations are strongly dependent on local sources. The nearby stations of Martin, et al. (1985) and Knauer, et al., (1982) suggest that dissolved Mn and Co concentrations are about 0.5 nmol/kg and

30 pmol/kg in intermediate waters of the Pacific station, about the same as concentrations at the Sargasso Sea station (Jickells and Burton, 1988).

Thus the suspended particulate metal content of Mn, Co, and Cu is several times lower at the Pacific site, despite similar or somewhat higher dissolved concentrations (Table 5.2). The partitioning of these metals therefore appears not to be controlled simply by proportionality to dissolved concentrations. Of the metals considered here, only particulate Pb displays a rough correlation to its dissolved concentration at each station. This is consistent with the isotopic equilibration of Pb observed at the Sargasso Sea station (Chapter 4). It is important to note that this is based on 1984 dissolved Pb profiles in the Sargasso Sea (Boyle et al., 1986) and at a more southerly California Current Station (Vertex V, Martin et al., 1985). Concentrations in the Sargasso Sea have probably decreased in the 3-4 years between these measurements and the particulate metal profiles, because of the continuing decrease in North American aerosol Pb input (Boyle et al., 1986; Shen and Boyle, 1988). Pb concentrations at the Pacific station may be influenced by Japanese sources, and temporal concentration trends are not well established for this area.

The reason for the relatively low particulate Mn, Co, and Cu content of the Pacific particles is not known. However, sufficient information exists regarding the particulate distribution of Mn at other stations to propose several hypotheses for this element. (1) Sources of dissolved Mn to subsurface waters may be small, limiting the supply for oxidation to particulate Mn. It was suggested in Chapter 3 that ventilation of the

thermocline with high-Mn surface water might provide a source of elevated

particulate Mn in intermediate waters. It is not known whether

ventilation sources are smaller at the Pacific site. (2) Particulate Mn

may be strongly influenced by the activity of Mn-oxidizing bacteria

(Cowen and Bruland, 1985). Although it has been suggested that metal

deposits associated with bacteria are a ubiquitous open ocean phenomenon

(Cowen and Silver, 1984), the abundance of these organisms at these two

stations is not known. (3) Mn oxidation may be hindered at low

dissolved oxygen levels. Landing and Bruland (1987) observed lower

ratios of weak acid-soluble to refractory Mn in the oxygen minimum zone

at Vertex-I (500-1500m) in the northeast Pacific, and suggested that

reduction of particulate Mn to soluble Mn(II) occurred in this interval.

This process may also be responsible for the observed low particulate Mn

at the California Current station, where dissolved O_2 is less than 60 μM

throughout the intermediate waters (Fig. 5.8), compared to >150 μM at

Sargasso Sea O_2 minimum. The relative importance of these mechanisms is

not known, nor can other possibilities be ruled out (for instance,

enhanced competition of dissolved ligands with particle surface for

dissolved metals; Davis and Leckie, 1978; Coale, 1988).

Despite the difficulty in reconciling this evidence with a simple

adsorption model, we can calculate distribution coefficients (K_d, mol

metal per gram particles/mol metal per gram seawater) for these seven

metals at the two stations in order to determine whether the absolute or

relative magnitude of partitioning in the ocean is related to

observations in laboratory experiments. This is demonstrated for four

different depths at each station: surface, thermocline [500m], mid-water
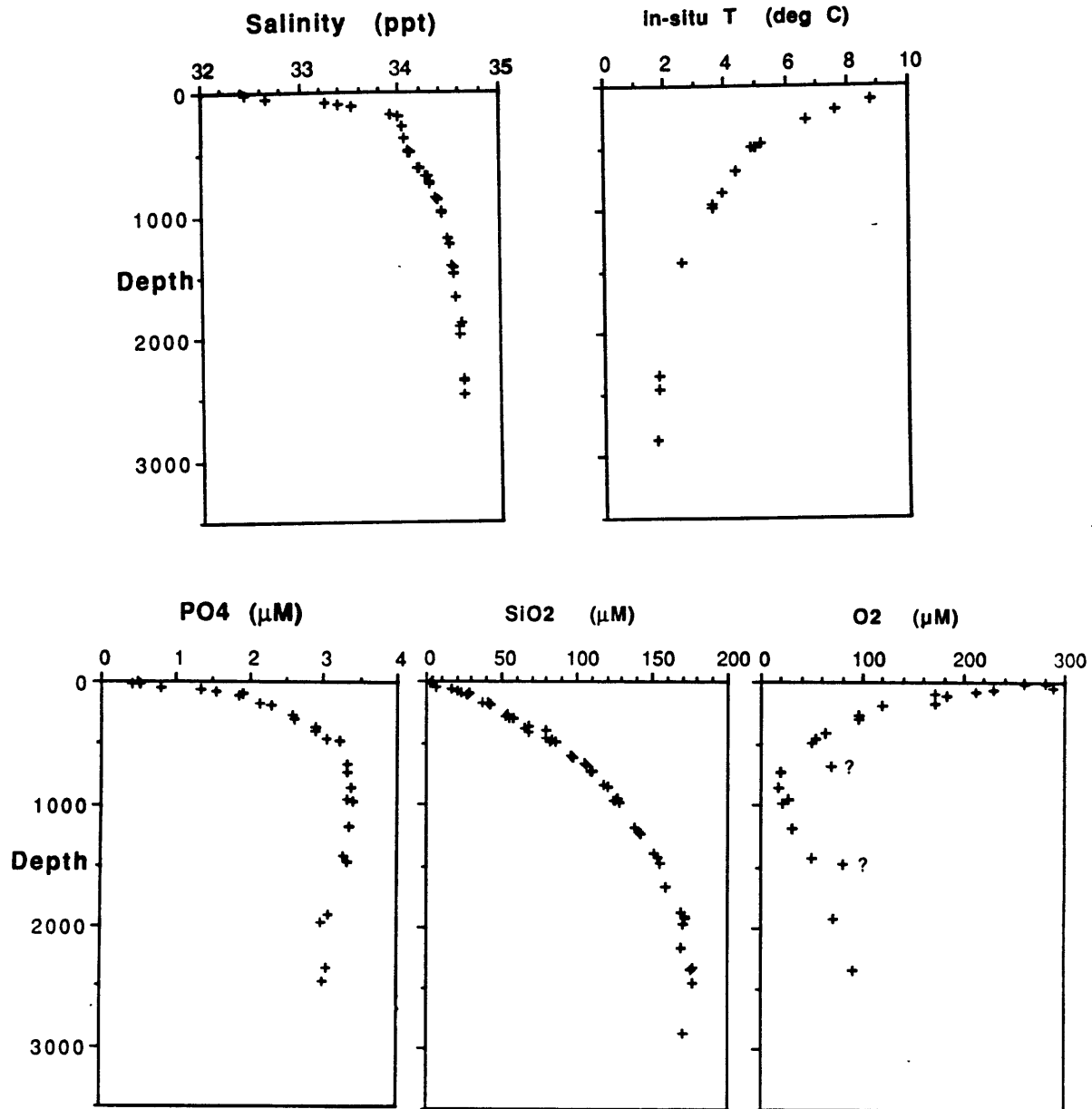
Fig. 5.8. Hydrographic data for Pacific station (41°00'N, 127°30'W).
Question marks indicate suspect data.

Table 5.3. Calculation of distribution coefficients at four depths for the northeast Pacific and Sargasso Sea stations.

Depth (m)	Element	Atlantic P(tot)	P(ex)	Pacific P(tot)	P(ex)	Atlantic diss	Pacific diss	Atlantic Kd(tot)	Kd(ex)	Pacific Kd(tot)	Kd(ex)
0	Zn	.1	.1	.6	.6	.04	.3	2.50	2.50	2.00	2.00
500		1.4	1.3	1.6	1.2	.4	4	3.50	3.25	.40	.30
1500		1.5	1.2	2	1.3	1.99	8	.75	.60	.25	.16
3000		1	.8	2.4	1.5	1.6	9	.62	.50	.27	.17
0	Cu	.3	.3	.15	.15	1.15	1.4	.26	.26	.11	.11
500		2.6	2.5	1.2	.85	1.23	1.6	2.11	2.03	.75	.53
1500		3.8	3.6	1.7	1.1	1.6	2	2.37	2.25	.85	.55
3000		2.8	2.6	3.2	2.6	2	3.5	1.40	1.30	.91	.74
0	Ni	.2	.2	.15	.15	2	4	.10	.10	.04	.04
500		1	.85	1.8	1.3	3	8	.33	.28	.23	.16
1500		1	.65	1.9	1.1	5.5	10.5	.18	.12	.18	.10
3000				2.6	1.6	5.75	10			.26	.16
0	Cd	.008	.008	.12	.12	.002	.08	4.00	4.00	1.50	1.50
500		.012	.011	.035	.032	.05	.9	.24	.22	.04	.04
1500		.008	.007	.011	.008	.27	1	.03	.03	.01	.01
3000		.006	.005	.008	.004	.3	.9	.02	.02	.01	.00
0	Pb	.02	.02	.02	.02	.06	.03	.33	.33	.67	.67
500		.35	.34	.1	.075	.11	.05	3.18	3.09	2.00	1.50
1500		.45	.37	.11	.07	.05	.01	9.00	7.40	11.00	7.00
3000		.31	.3	.22	.17	.025	.01	12.40	12.00	22.00	17.00
0	Mn	2	2	.5	.5	2.6	3	.77	.77	.17	.17
500		27	25	11	4	.5	.6	54.00	50.00	18	6.7
1500		28	24	12	3	.5	.4	56.00	48.00	30	7.5
3000		26	22	140	125	.5	.3	52.00	44.00	470	415
0	Co	.04	.04	.08	.08	.035	.2	1.14	1.14	.4	.4
500		.21	.17	.16	.04	.02	.05	10.50	8.50	3.2	.8
1500		.27	.16	.2	.04	.03	.03	9.00	5.33	6.7	1.3
3000		.23	.14	.4	.16	.035	.025	6.57	4.00	16	6.4

Key:

P(tot) = total particulate metal concentration in umol/g.
P(ex) = "excess" particulate metals concentration = P(tot) minus aluminosilicate metal, estimated from average crustal Me/Al ratios (Taylor, 1964)
diss = dissolved metal concentration in nmol/kg
Kd(tot)= (mol/g particle)/mol/g water), x 10^6
Kd(ex) = (mol excess metal/g particle)/mol/g water), x 10^6

Fig. 5.9. Calculated distribution coefficients (K_d, x 10^6) for four depths at Atlantic (circles) and Pacific (squares) stations. Values are calculated using total particulate metal content (filled symbols) and "excess" metal content (open symbols). Note that aluminosilicate correction for Mn and Co is not will constrained, so "excess" plots for these metals have large uncertainties (see text). Note scale change in Cd plot.
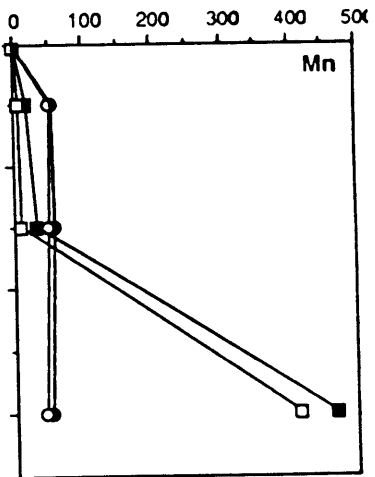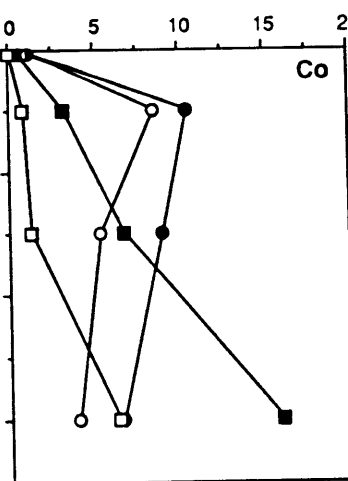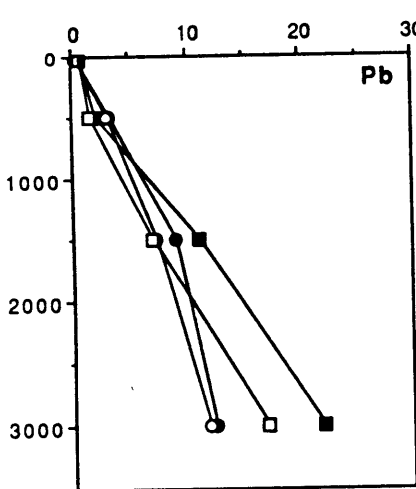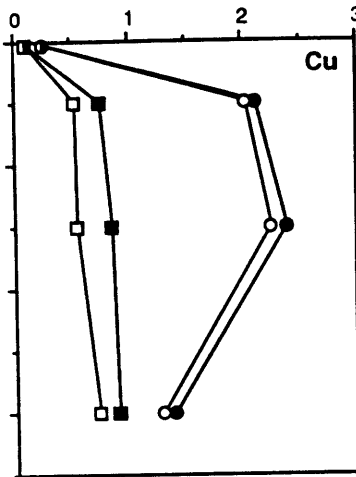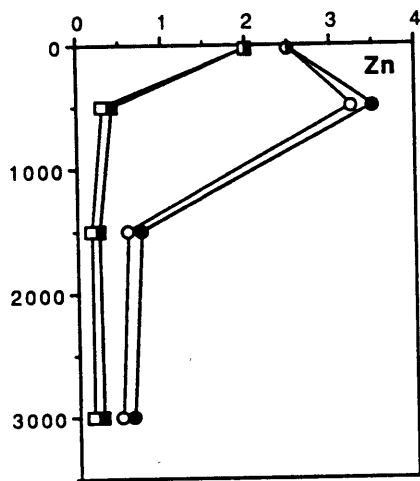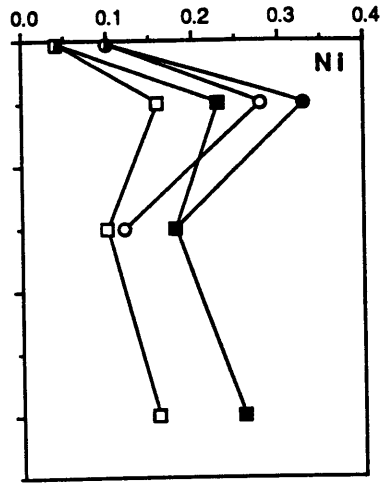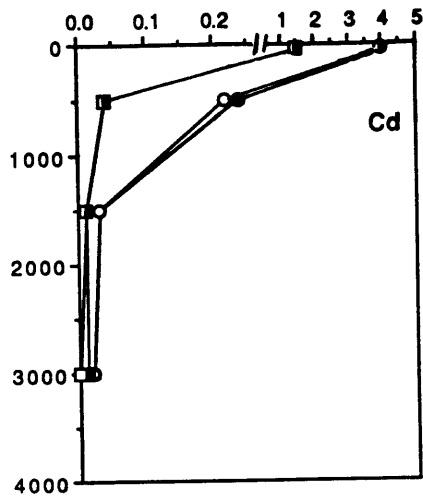
[1500m] and deep-water [3000m] (Table 5.3 and Fig. 5.9). The results show a trend of increasing K_d with depth, and generally lower K_d's at the Pacific station. However, as we have seen, the Atlantic/Pacific difference suggests that controls on metal partitioning, with the possible exception of Pb, have little to do with equilibrium constants for specific heterogeneous reactions. If we ignore the differences between the stations (< a factor of 5), the order of apparent particle affinity in the mid-water column (1500m) is Mn > Pb $\geq$ Co > Cu > Zn > Ni > Cd. This trend is very similar to that observed in laboratory adsorption studies (Li et al., 1984; Nyffeler et al., 1984), and suggests that, in an overall sense, the order of affinity and the _relative_ magnitude of the K_d differences for each element suggest that adsorptive tendencies of the individual elements are related to the degree of particle association in the ocean.

The magnitude of the laboratory-determined K_d's, however, are generally 1-3 orders of lower than observed in the ocean (Fig. 5.10). Reasons for this discrepancy are not known, but may be related to the "particle concentration effect", i.e. that apparent equilibrium K_d's determined in the laboratory are often found to be anti-correlated with the mass concentration of the adsorbent used (Honeyman et al., 1988; Santaschi, 1984). It is interesting to note that the radiotracer experiments which have given results closest to the natural K_d's found here used pure Mn oxide as the adsorbent/coprecipitant (Takematsu, 1987) or Mn-rich bottom sediments from MANOP site H (Nyffeler, 1984). However, because authigenic Mn comprises less than 1% of total suspended matter at our sites, the implied affinity of Mn oxides still falls short of
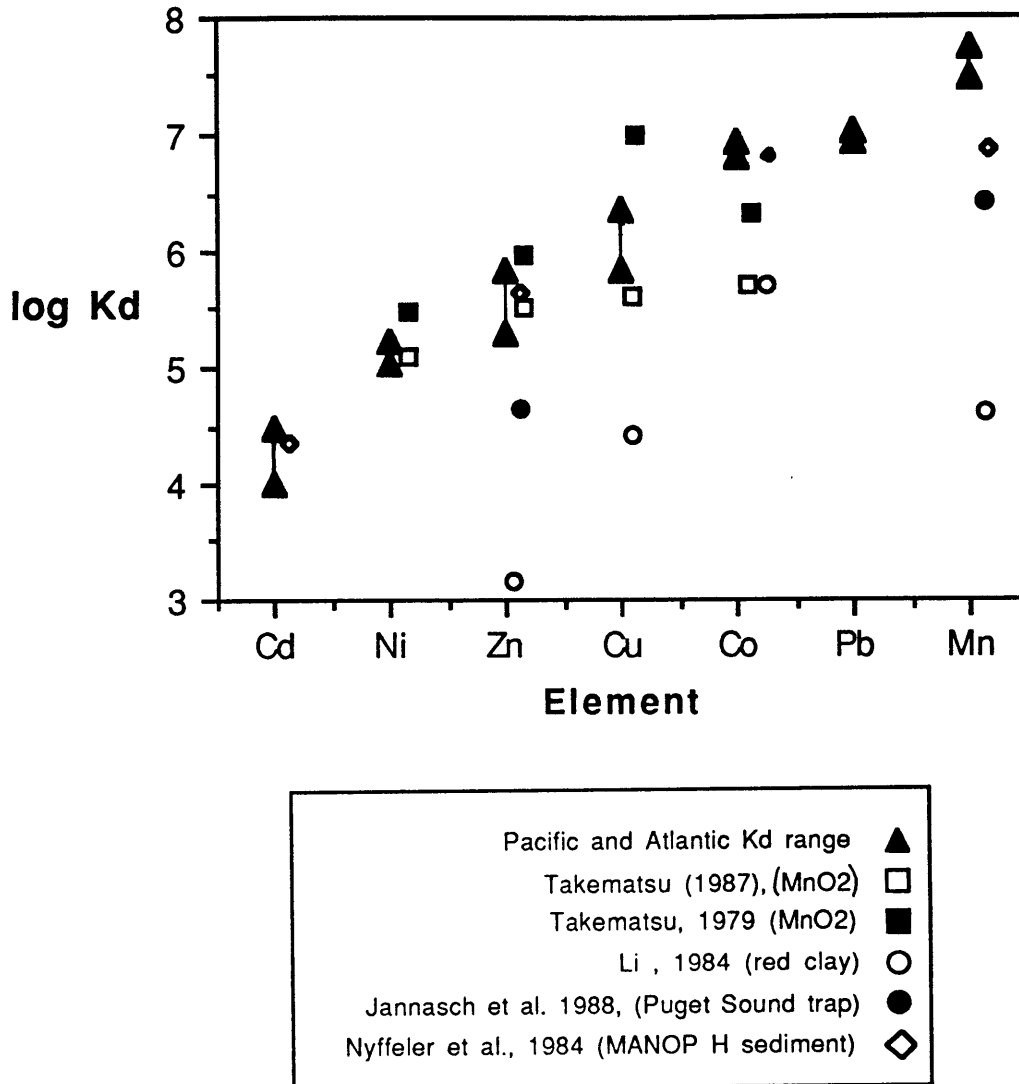
Fig. 5.10. Log K_d for trace elements at 1500m in Sargasso Sea and northeast Pacific (high and low represented by filled triangles) compared to equilibium distribution coefficients determined in laboratory uptake experiments using various natural and artificial solid phases.

explaining the observed K_d's by at least two orders of magnitude. This demonstrates the difficulty in ascribing the metal content of natural particles to a single carrier phase (Morel and Hudson, 1985).

It is clear that laboratory tracer experiments and current surface chemical models are not adequate to quantitatively predict metal partitioning or removal rates under natural oceanic conditions (Honeyman and Santschi, 1988). Variability in metal partitioning on the scale of one order of magnitude or less must be explained by mechanisms which do not appear to be accounted for by simple surface adsorption models.

5.4.3. Metal partitioning in the upper water column: influence of biological processes.

Particulate metal concentrations in surface waters (upper 100m) at the Atlantic and Pacific station are similar, except for Zn and Cd (Fig. 5.5). These two metals are enriched in surface water of the Pacific station by a factor of 5 for Zn (20 versus 4 pmol/l) and a factor of 10 for Cd (4.5 versus 0.4 pmol/l). Zn and Cd are the only metals of those examined which are not depleted in surface particles (although Zn content is depleted on a mol/g basis, see Fig. 5.6). This suggests a strong association with near-surface biological activity, as is indicated by their extremely depleted surface dissolved concentrations (Boyle, 1981; Bruland, 1980)(Fig. 5.7). A comparison of Cd and phosphorus distributions at the two stations demonstrates the influence of the biota on the particle/water partitioning in surface waters.

Profiles of dissolved and particulate Cd and P, and the Cd/P ratio for the two locations are shown in Fig. 5.11. The dissolved

Dissolved

▶ N. Atlantic
● N.E. Pacific

Cd (nmol/kg) **PO4 (µmol/kg)** **Cd/PO4 (nmol/µmol)**

Particulate

▶ N. Atlantic
● N.E. Pacific

Cd (pmol/l) **P (nmol/l)** **Cd/PO4 (nmol/µmol)**
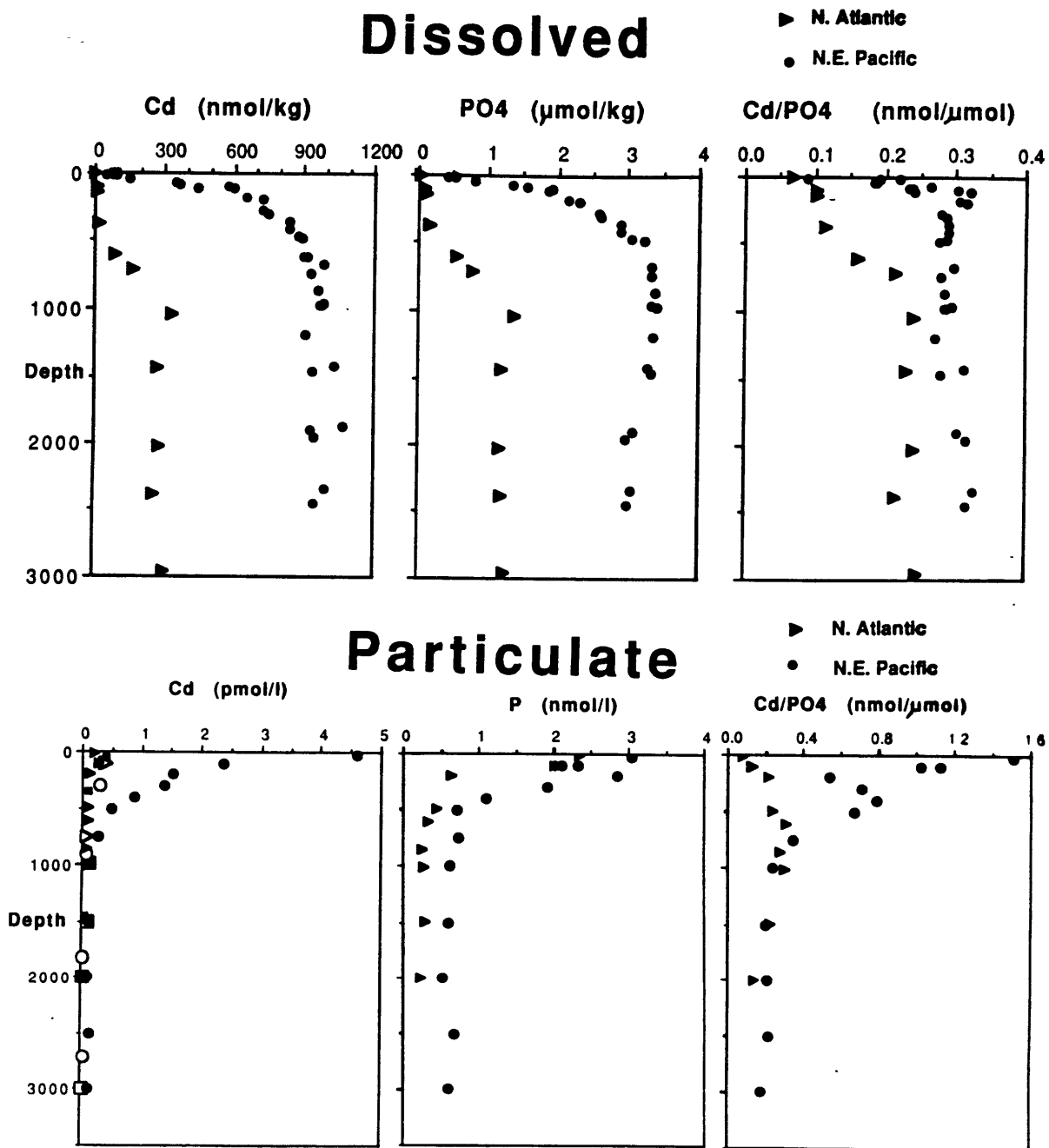
Fig. 5.11. Dissolved and particulate Cd, P, and Cd/P at Pacific (filled circles) and Atlantic (all other symbols) stations.

distributions reflect progressive enrichment of nutrients and
nutrient-type trace metals in the deep Pacific relative to the deep
Atlantic. Surface water at the Pacific site is enriched in nutrients and
Cd by more than an order of magnitude relative to the very depleted
central gyre surface water of the Sargasso Sea (Boyle et al., 1981;
Bruland and Franks, 1983). The dissolved Cd/P ratio is at a minimum in
surface waters of both stations, although the ratio for the Pacific
surface water is about twice that in the Sargasso Sea ($\sim$0.2 x 10^{-3} versus
0.1 x 10^{-3}). Deep water Cd/P is somewhat higher in the Pacific, as has
been noted previously (Boyle, 1988). Particulate P is only about 25%
higher in surface waters at the Pacific site, but the Cd/P ratio in
Pacific surface particles is more than an order of magnitude higher than
the Atlantic ratio (1.5 versus $\sim$0.1 x 10^{-3}). (This calculation assumes
that loss of particulate P due to filter rinsing was of similar magnitude
to that measured for Cd [$\sim$30%, see Appendix C]. This is not considered a
major source of uncertainty in the order of magnitude Atlantic/Pacific
difference seen here.)

How does such a large difference in the apparent uptake ratio of P
and its analog Cd come about? Published Cd/P ratios for plankton
demonstrate that planktonic Cd/P is not simply related to surface
dissolved Cd concentration or to nutrient supply. Reported Cd/P ratios
for plankton collected in surface waters with P and Cd concentrations
both higher and lower than at the Pacific site, vary from 0.2 to 0.9 x
10^{-3} with no systematic ratio to either dissolved constituent (Martin et
al., 1976; Knauer and Martin, 1981; Collier and Edmond, 1984).

The degree of fractionation of Cd and P between the particles and
the surface water is more likely the net result of the growth state of
the phytoplankton and the activity of zooplankton, bacteria, or other
hetertrophs. Boyle et al. (1981) and Collier and Edmond (1984)
parameterized metal fractionation relative to nutrients as a two-step
process. According to this model a fractionation relative to seawater
composition occurs when primary producers take up nutrients and metals
during growth, and a second fractionation occurs when consumers recycle
this material, leaving a residual which is removed as sinking biological
debris. In the upper 100m of the Sargasso Sea station, particulate Cd/P
is equal to the dissolved ratio, suggesting that these two process are in
approximate balance, and no net dissolved/particulate fractionation
occurs. In contrast, high particulate Cd/P in Pacific surface waters is
likely caused by a higher ratio of live organic matter to dead biological
debris.

The elevated particulate Cd/P ratio in the Pacific surface waters is
apparently carried into the thermocline as particles sink. Both Cd and P
are regenerated from particulate matter in the thermocline, and their
particulate concentrations decrease rapidly through this zone. At 200m,
the depth of the sub-surface particle maximum, particulate Cd/P exhibits
a minimum; conversely, the dissolved ratio indicates a slight maximum,
suggesting preferential regeneration of Cd in the particle maximum.
(This may indicate an advective influence on the Cd/P profile, at least
in the upper 200m, which cannot be assessed in this discussion of simple
vertical particulate transformation processes.) The particulate Cd/P
ratio only decreases to the dissolved ratio at 1000m. In light of the

striking surface Cd/P difference, it is surprising that the Pacific particulate ratio matches the Atlantic ratio at depths greater than 1000m, suggesting control which is independent of surface productivity (Fig. 5.11). Propagation of surface water particulate metal/nutrient ratios deep into the thermocline has not been observed previously. The Pacific data therefore suggests that dissolved Cd/P may be altered by dissolution of high Cd/P particles throughout the thermocline. This is a strictly one-dimensional interpretation; horizontal advection of water masses with Cd/P ratios unrelated to local particle flux are also likely. Nevertheless, it would be useful to know how widespread this phenomenon is, and whether advection of high Cd/P thermocline waters from similar high productivity regions to the central gyre could be related to the increased slope of the dissolved Cd/P regression in the deep Pacific versus the deep Atlantic (Bruland and Franks, 1983; Boyle, 1988).

5.5. CONCLUSION

Atlantic and Pacific particulate metal profiles provide a preliminary illustration that dissolved/particulate fractionation of some trace elements is determined by biological and chemical processes which cannot be understood in terms of simple surface chemical models.

In intermediate water, the particulate content of the nutrient-type metals Zn, Ni, and Cd is remarkably constant between these two regions of quite different surface productivity. Higher dissolved concentrations for these elements in the Pacific appear to have little effect on particulate distributions. The particulate content of Mn, Co, and Cu at the Pacific site is lower than observed in the Sargasso Sea, despite

similar dissolved concentrations. Of the metals studied, only Pb shows a dissolved/particulate fractionation which is similar at the two stations, even though absolute Pb concentrations differ by a factor of five. Additional studies of metal partitioning in other representative oceanographic regimes (for instance productive equatorial Pacific versus North Pacific central gyre) would be a valuable complement to this work.

REFERENCES

Bacon, M.P., Anderson, R.F. (1982) Distribution of thorium isotopes between dissolved and particulate forms in the deep sea, J. of Geophys. Res. 87, 2045-2056.

Balistrieri, L., Brewer, P.G. and Murray, J.W. (1981) Scavenging residence times of trace metals and surface chemistry of sinking particles in the deep ocean, Deep-Sea Res. 28A, 101-121.

Benjamin, M.M. and J.O. Leckie (1980) Multiple-site adsorption of Cd, Cu, Zn, snd Pb on amorphous iron oxydroxide, J. Colloid Interface Sci. 79, 209-221.

Berger, W.H., Fischer, K., Lai, C. and Wu, G. (1987) Ocean productivity and organic carbon flux, Part I: Overview and maps of primary production and export production. SIO Reference Series 87-30. University of California, Scripps Institution of Oceanography, La Jolla, California.

Billett, D.S.M., Lampitt, R.S., Rice, A.L., and Mantoura, R.F.C. (1983) Seasonal sedimentation of phytoplankton to the deep-sea benthos, Nature 302, 520-522.

Bishop, J.K.B.and M.Q. Fleisher (1987) Particulate manganese dynamics in gulf stream warm-core rings and surrounding waters of the N.W. Atlantic, Geochim. Cosmochim. Acta 51, 2807-2827.

Boyle, E.A., Huested, S.S. and Jones, S.P. (1981) On the distribution of copper, nickel, and cadmium in the surface waters of the North Atlantic and North Pacific Ocean. J. Geophys. Res. 86, 8048-8066.

Boyle, E.A., Chapnick, S.D., and Shen, G.T. (1986) Temporal variability of lead in the western North Atlantic, J. Geophys. Res. 91, 8573-8593.

Boyle, E.A. (1988) Cadmium: Chemical tracer of deepwater paleoceanography, Paleocean. 3, 471-489.

Bruland, K.W., (1980) Oceanographic distributions of cadmium, zinc, nickel, and copper in the North Pacific, Earth Planet. Sci. Lett. 47,176-198.

Bruland, K.W., and Franks, R.P. (1983) Mn, Ni, Cu, Zn, and Cd in the western North Atlantic, in Trace Metals in Sea Water, C.S. Wong, E.Boyle, K.W. Bruland , T.D. Burton, E.D. Goldberg, eds., Nato Conf. Series, Plenum Press, pp. 395-414.

Bruland, K.W. (1983) Trace elements in sea-water, in Chemical Oceanography Vol. 8, J.P. Riley, R. Chester, eds., Academic Press, pp.158-220.

Campbell, A.C., German, C., Palmer, M.R., and Edmond, J.M. (1988) Preliminary report on the chemistry of hydrothermal fluids from the Escanaba Trough. EOS, Trans. Am. Geophys. Union 69, 1271.

Coale, K. and Bruland, K.W. (in press).

Cochran, J.K., Livingston, H.D., Hirschberg, D.J. and Surprenant, L.D. (1987) Natural and anthropogenic radionuclide distributions in the northwest Atlantic Ocean, Earth Planet. Sci. Lett. 84, 135-152.

Collier, R. and Edmond, J. (1984) The trace element geochemistry of marine biogenic particulate matter, Prog. Oceanog. 13, 113-199.

Cowen, J.P. and Silver, M.W. (1984) The association of iron and manganese with bacteria on marine macroparticulate material, Science 224, 1340-1342.

Cowen, J.P. and Bruland, K.W. (1985) Metal deposits associated with bacteria: implications for Fe and Mn marine biogeochemistry, Deep-Sea Res. 32, 253-272.

Craig, H. (1974) A scavenging model for trace elements in the deep sea, Earth Planet. Sci. Lett. 23, 149-159.

Davis, J.A. and Leckie, J.O. (1978) Effect of adsorbed complexing ligands on trace metal uptake by hydrous oxides. Environ. Sci. Tech. 12, 1309-1315.

Deuser, W.G., Ross, E.H. and Anderson, R.F. (1981) Seasonality in the supply of sediment to the Deep Sargasso Sea and implications for the rapid transfer of matter to the deep ocean, Deep-Sea Res. 28, 495-505.

Deuser, W.G., (1986) Seasonal and interannual variations in deep-water particle fluxes in the Sargasso Sea and their relation to surface hydrography, Deep-Sea Res. 33, 225-246.

DSDP (1970) Initial Reports of the Deep Sea Drilling Project, Volume V. Washington (U.S. Government Printing Office), pp. 165-202.

Flament, P., Armi, L. and Washburn, L. (1985) The evolving structure of an upwelling filament, J. Geophys. Res. 90, 11765-11778.

Goldberg, E.D., (1954) Marine geochemistry 1. chemical scavengers of the sea, J. Geol. 62, 249-265.

Honeyman, B.D., Balistrieri, L.S. and Murray, J.W. (1988) Oceanic trace metal scavenging: the importance of particle concentration, Deep-Sea Res. 35, 227-246.

Honeyman B.D. and Santschi, P.H. (1988) Metals in aquatic systems, Environ. Sci. Tech. 22, 862-871.

Hunter, K.A. (1983) The adsorptive properties of sinking particles in the deep ocean, Deep-Sea Res. 30, 669-675.

Jannasch, H.W., Honeyman, B.D., Balistrieri, L.S. and Murray, J.W. (1988) Kinetics of trace element uptake by marine particles, Geochim. Cosmochim. 52, 567-577.

Jickells, T.D. and J.D. Burton (1988) Cobalt, copper, manganese and nickel in the sargasso sea, Marine Chem. 23, 131-144.

Knauer, G.A., and Martin, J.H. (1981) Phosphorus-cadmium cycling in northeast Pacific waters, J. Mar. Res. 39, 65-78.

Knauer, G.A., Martin, J.H. and Gordon, R.M. (1982) Cobalt in north-east Pacific waters. Nature 297, 49-51.

Lal, D. (1977) The oceanic microcosm of particles, 198, 997-1009.

Landing, W.M. and Bruland, K.W. (1987) The contrasting biogeochemistry of iron and manganese in the Pacific Ocean, Geochim. Cosmochim. Acta 51, 29-43.

Lerman, A., Lal, D. and Dacey, M.F. (1974) Stokes settling and chemical reactivity of suspended particulates in natural waters. In Suspended Solids in Water (ed. R.J. Gibbs), pp. 17-47. Plenum Press, New York.

Li, Yuan-Hui, Burkhardt, L., Buchholtz, M. O'Hara, P. and Santschi, P.H. (1984) Partition of radiotracers between suspended particles and seawater, Geochim. Cosmochim. Acta 48, 2011-2019.

Martin, J.H., Bruland, K.W. and Broenkow, W.W. (1976) Cadmium transport in the California Current. In Marine Pollutant Transfer (eds. H. Windom and R.A. Duce), pp. 159-184. Lexington Books, Lexington Mass.

Martin, J.H., Knauer, G.A., and Broenkow, W.W. (1985) VERTEX: the lateral transport of manganese in the northeast Pacific, Deep-Sea Res. 32, 1405-1427.

Mooers, C.N.K. and Robinson, A.R. (1984) Turbulent jets and eddies in the California Current and inferred cross-shore transports, Science 223, 51-53.

Morel, G.M.M. and Hudson, R.J.M. (1984) The geobiological cycle of trace elements in aquatic systems: Redfield revisited, in Chemical Processes is Lakes, W. Stumm, ed., Wiley-Interscience, New York, pp. 251-281.

Murray, J.W. (1975) The interaction of metal ions at the manganese dioxide-solution interface, Geochim. Cosmochim. Acta 39, 505-519.

Nelson, T.A., Klinkhammer, G.P., Trefry, J.H. and Trocine, R.P. (1986) Real-time observation of dispersed hydrothermal plumes using nephelometry: Examples from the Mid-Atlantic Ridge. Earth Planet. Sci. Lett. 81, 245-252.

Nyffeler, U.P., Li, Y.H., and Santschi, P.H. (1984) A kinetic approach to desribe trace-element distribution between particles and solution in natural aquatic systems, Geochim. Cosmochim. Acta 48, 1513-1522.

Oakley, S.M., Nelson, P.O. and Williamson, K.J. (1981) Model of trace-metal partitioning in marine sediments, Environ. Sci. Technol. 15, 474-480.

Peng, T.-H. and Broecker, W.S. (1987) C/P ratios in marine detritus, Global Biochem. Cycles 1, 155-161.

Redfield, A.C., Ketchum, B.H. and Richards, F.A. (1963) The influence of organisms on the composition of sea water. In: The Sea: Vol. 2, M.N. Hill, ed., Wiley Interscience, New York.

Santschi, P.H. (1984) Particle flux and trace metal residence time in natural waters, Limnol. Oceanogr. 29, 1100-1108.

Schindler, P.W. (1975) Removal of trace metals from the oceans: a zero order model, Thalassia Jogoslavica 11, 101-111.

Shen, G.T. and Boyle, E.A. (1988) Thermocline ventilation of anthropogenic lead in the Western North Atlantic, J. Geophys. Res. 93, 15715-15732.

Takahashi, T., Broecker, W.S., and Langer, S. (1985) Redfield ratio based on chemical data from isopycnal surfaces. J. Geophys. Res. 90, 6907-6924.

Takematsu, N. (1987) Ultimate removal of trace elements from seawater and adsorption. J. Earth Sci. 35, 227-248.

Taylor, S.R., (1964) Abundance of chemical elements in the continental crust: a new table, Geochim. Cosmochim. Acta 28, 1273-1285.

Trocine, R.P. and Trefry, J.H. (1988) Distribution and chemistry of suspended particles from an active hydrothermal vent site on the Mid-Atlantic Ridge at 26°N. Earth Planet. Sci. Lett. 88, 1-?.

Turekian, K.K. (1977) The fate of metals in the ocean, Geochim. Cosmochim. Acta 41, 1139-1144.

Whitfield, M.and Turner, D.R. (1987) The role of particles in regulating the composition of seawater, Aquatic Surf. Chem. 457-493.

CHAPTER 6

FURTHER INVESTIGATION OF PARTICULATE TRACE METALS:

PRELIMINARY RESULTS

6.1. <u>INTRODUCTION</u>

Two additional studies were carried out which are to some degree
complementary to the main objectives of the thesis research. A short
cruise from Woods Hole, Massacusetts to Bermuda (Oceanus 197) enabled
four stations to be sampled for suspended particulate matter. One cast
of 2-3 pumps was made at each station. The objective of the study was to
determine trends in particle composition from shelf water, across the
Gulf Stream, and into the Sargasso Sea, and to broadly quantify the
horizontal variability in particulate metal distributions at a few depths
within the Sargasso Sea. This would allow some assessment of whether the
Bermuda station was representative of distributions in the Sargasso Sea
in general.

The second study involved sampling of a dispersed hydrothermal
particulate plume at the Trans-Atlantic Geotraverse (TAG) hydrothermal
field on the mid-Atlantic ridge. The object was to identify
compositional changes in the metal content of plume particulate material
with increasing distance and mixing from the source of the venting
hydrothermal fluid from which the particles precipitated. It was hoped
that interactions between fresh hydrothermal precipitates and dissolved
metals in seawater could be distinguished from the trends of metal

Table 6.1 Transect stations, Oceanus 197

Station number	Sampling date	Coordinates	bottom depth
1	6 April, 1988	40°09'N, 70°01'W	118m
2	7 April, 1988	37°59'N, 68°11'W	4410m
3	8 April, 1988	35°58'N, 66°31'W	4950m
4	9 April, 1988	33°46'N, 65°20'W	?
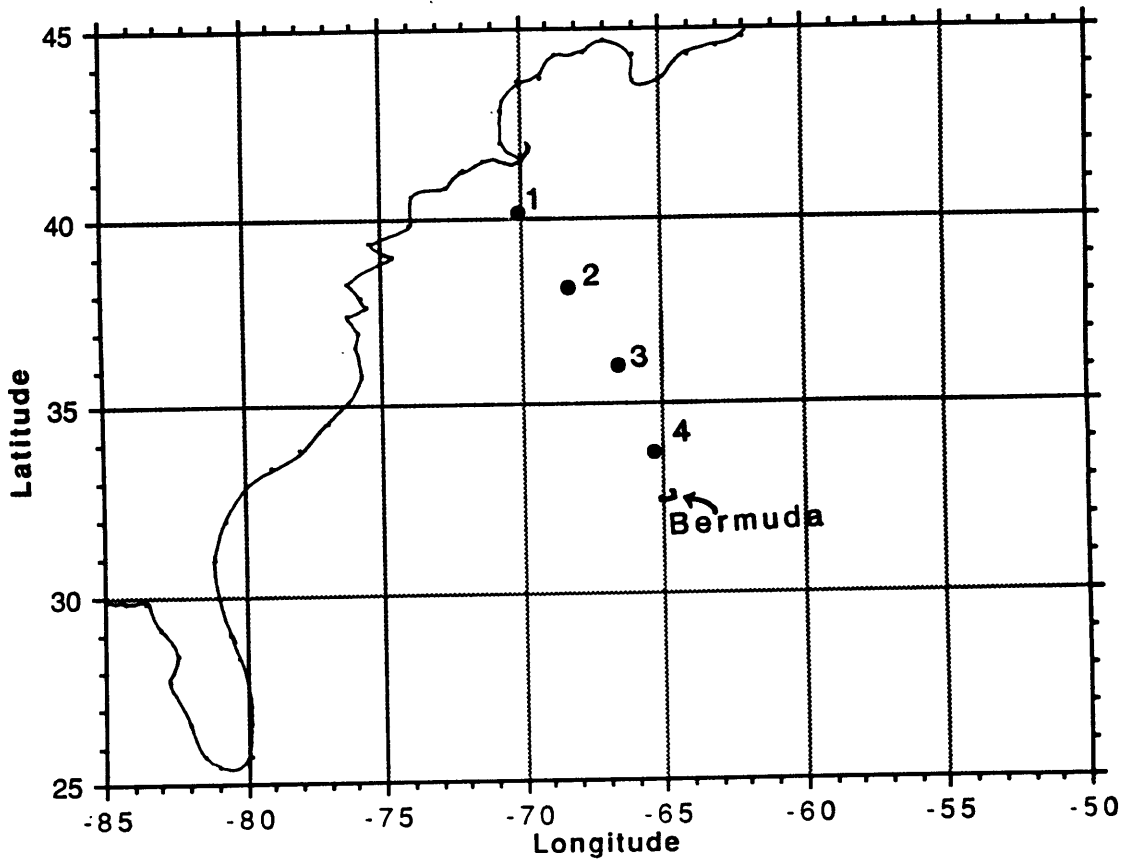
Fig. 6.1 Oceanus 197 station locations.

composition with increasing age and dilution of the fresh hydrothermal precipitates.

Each of these studies is briefly described in this chapter. While low sampling density only allows broadly stated and preliminary interpretations to be made, the results are useful guides for future investigations.

6.2. A transect of stations from the North American Shelf to Bermuda

Four stations approximately evenly spaced between Cape Cod, Massachusetts and Bermuda were occupied over a three-day period in April, 1988 (Table 6.1, Fig. 6.1). Station 1 was located in shelf water, station 2 in the Gulf Stream, and 3 and 4 in the Sargasso Sea. For each station, <53 μm suspended mass, Al, Zn, Cu, Cd, and Pb were determined, using methods outlined in Chapter 2. The uniformity of the temperature structure in the upper water column at station 3, station 4, and an occupation of the Bermuda station at the end of the transect (see Chapter 3) is evident from XBT profiles (Fig. 6.2). The temperature profile at the Gulf Stream station is clearly distinguishable from the Sargasso Sea profiles (Fig. 6.2). Figures 6.3 and 6.4 present the vertical particulate metal profiles for each station, with the metal concentrations expressed per volume of seawater and per dry weight of particulate matter, respectively.

The most important finding is that, in general, stations within the Sargasso Sea have suspended particulate metal distributions virtually indistinguishable from the Bermuda profile. Small differences in suspended mass concentration between station 3 and 4 (17% at 50m, 40% at

Fig. 6.2 Temperature profiles for Stations 2-4, plus 5 (Bermuda station)
from expendable bathythermographs. Replicate XBT's were fired at
Stations 2-4.

Temperature (deg C),   XBT
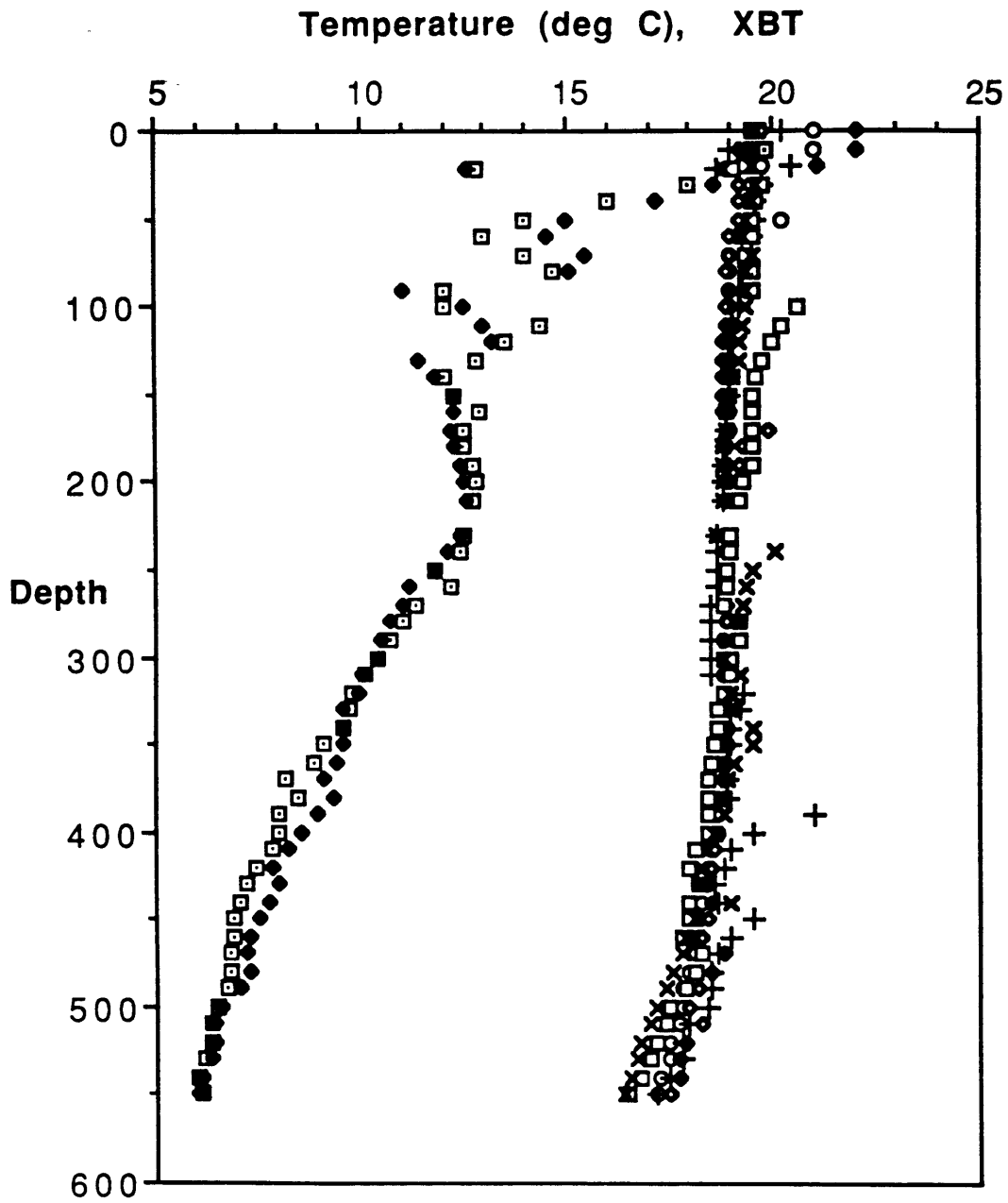
Station 2

Station 3

Station 4

Station 5

171

Fig. 6.3 Profiles of <53μm suspended particulate mass and metal
concentrations, expressed per liter seawater, for stations 1-4.

Suspended particulate matter, <53 um (ug/l)

Al (nmol/l)

Zn (pmol/l)

Cu (pmol/l)

Cd (pmol/l)

Pb (pmol/l)
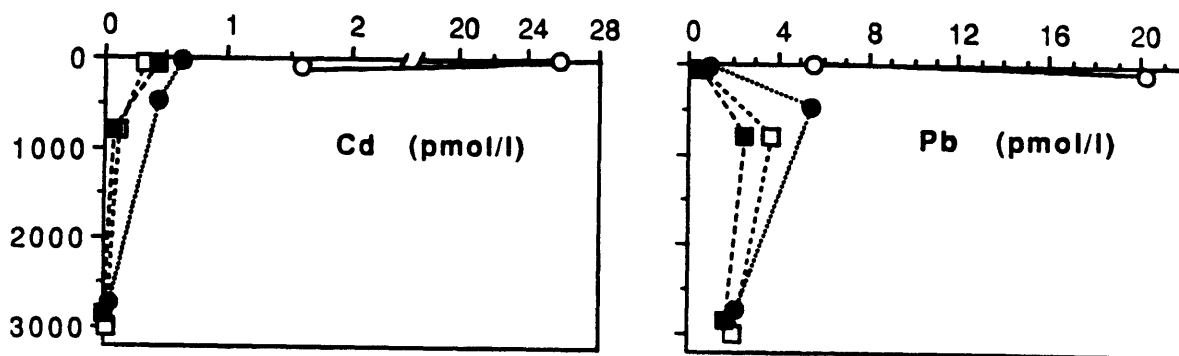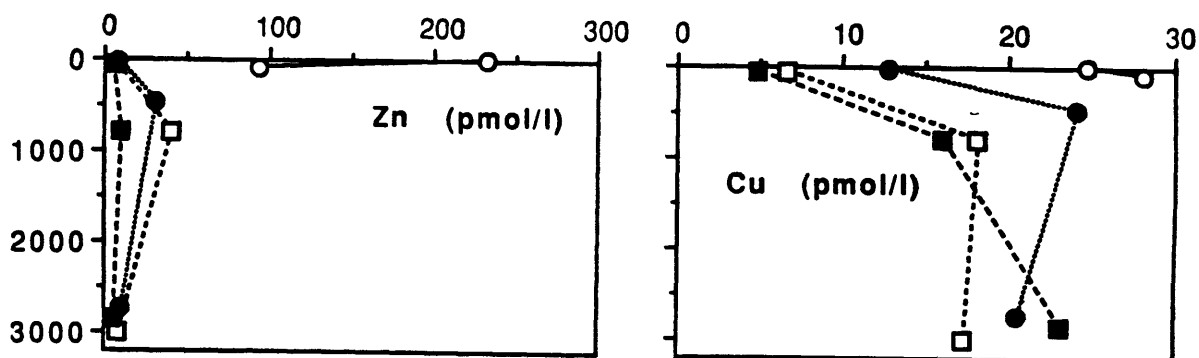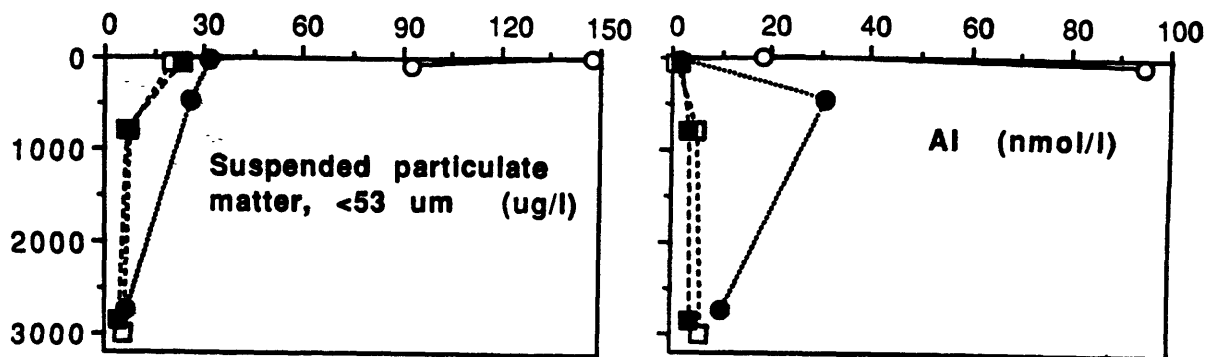
Station 1 (shelf)
Station 2 (Gulf Stream)
Station 3 (Sargasso)
Station 4 (Sargasso)
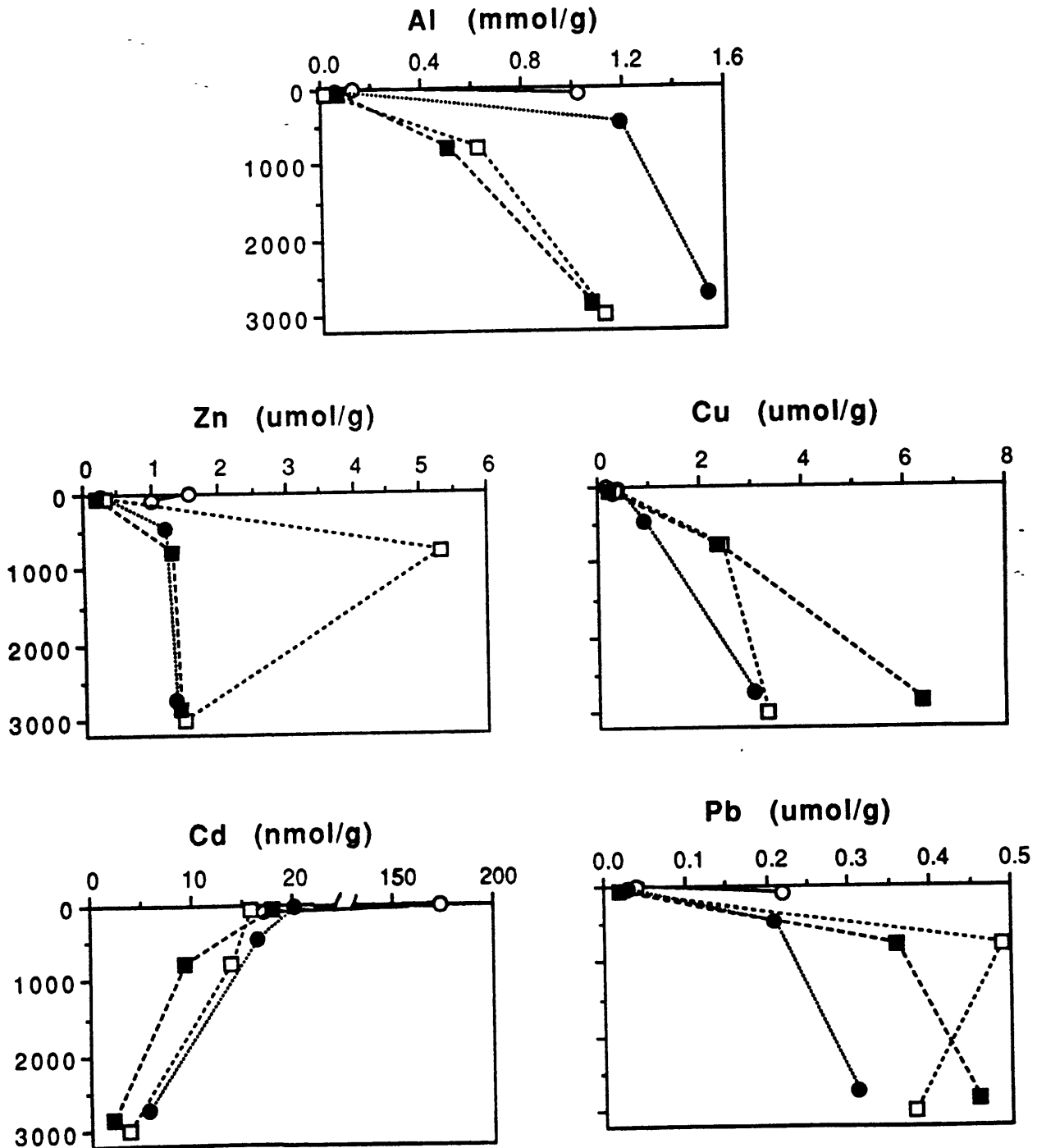
Fig. 6.4 Profiles of <53μm suspended particulate mass and metal concentrations, expressed per gram of dry particulate matter.

~3000m) can be attributed to variability in surface biological structure and influence of nepheloid layer particles. When normalized to particle mass (Fig. 6.4), the metal concentrations are identical within measurement error, with the following exceptions: particulate Zn and Pb are apparently enriched at ~800m at station 3, and Cu is higher at ~3000m at station 4. The differences are less than a factor of two for Pb and Cu. The reason for the five-fold enrichment of Zn in the lower thermocline at station 3 is not known; contamination cannot be ruled out.

Station 2, which appears to be on the northern edge of the Gulf Stream (compare XBT profile with T profiles measured by Bishop and Fleisher, 1987), shows substantially higher suspended mass concentrations at the upper two sampling depths (Fig. 6.3). However, metal <u>content</u> of particles at this station (Fig. 6.4) was not significantly different from the Sargasso Sea stations with the exception of Al. The increased aluminosilicate content of the suspended matter is consistent with the energetic western boundary current and proximity to sources of resuspended continental slope sediments.

The shelf station has a still higher suspended mass concentration, (by a factor of 3-5 compared to Sargasso stations) and consequently higher particulate metal concentrations than the other stations. This is due to increased productivity and sediment resuspension in the shelf waters. Nevertheless, metal concentrations per weight particulate matter are not outside the range of concentrations seen at other stations, except for the Cd concentration at 10m in the shelf water. Even at the high mass concentration of 90 μg/l, 30m above the bottom, particulate Al indicated only ~30% aluminosilicate by weight, about the same as in the

deep Sargasso samples. Station 1 particles at 10m depth were enriched in Zn and Cd by factors of 5 and 10, respectively, relative to near-surface samples at the open ocean stations. This is about the same degree of enrichment seen in surface particles at the California Current station (Chapter 5).

Overall, the results indicate very little variability in particulate metal concentration in the northwest section of the Sargasso Sea, and a relatively small range (< order of magnitude) of particulate metal content (per particle mass) from a boundary region to the open ocean. A quantification of particulate metal transport across the Gulf Stream would require more extensive sampling and better control on hydrographic parameters at the sampling stations. Particulate trace metal distributions at the Bermuda station appear to be representative of a large region of the oligotrophic central gyre.

6.3. Particulate metal distributions in a dispersed hydrothermal plume at the TAG site, Mid-Atlantic Ridge

Samples of suspended particulate matter were collected from within and nearby a buoyant hydrothermal plume at the TAG site, Mid-Atlantic Ridge. A single RAPPID pump was deployed 50-100m above or below a CTD package or a larger filtration/real-time sensing device (Simpson et al., 1987). Positioning of the pump and other equipment packages was generally guided by real-time transmissometer readings, and by a partial transponder navigation net. Attempts were made to sample as closely as possible to the suspected plume source, a hydrothermal mound located approximately at 26°08′N, 44°49′W. However, navigational problems
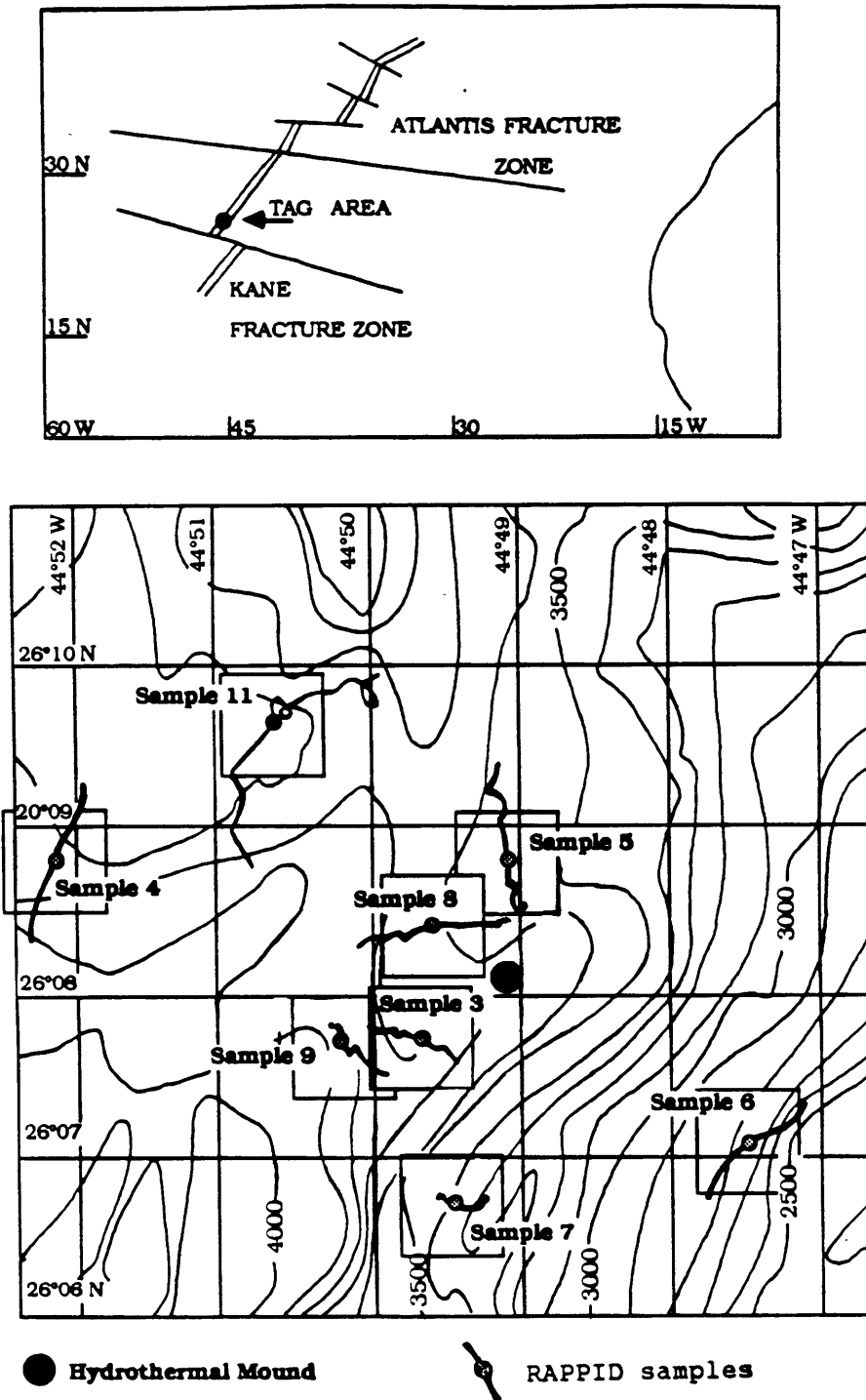
Fig. 6.5 TAG hydrothermal area and detail of approximate RAPPID pump sample locations (lines through points indicate approximate ship drift during pumping). Navigation was generally by satellite fixes and dead reckoning. Other sampling stations (FIDO pump, CTD) shown as well.

generally limited positioning to within ~ 2 km of intended sampling

locations (Fig. 6.5). Thus the samples were collected from the

relatively far-field, laterally-spreading portion of the plume, centered

at about 3300m depth, ~300-400m above the median valley floor. Eleven

samples were collected, three from stations located ~100km east and west

of the ridge (as ambient background controls), and eight from within the

valley walls.

Suspended mass concentration varied from 7-30 μg/l for background to

most concentrated plume sample. The small range indicates that plume

samples were all relatively dilute. Particulate Fe was taken as an

indication of the fraction of hydrothermally-derived particles in each

sample. While this was not necessarily directly related to proximity to

the plume source, (since ship drift frequently caused the pump to

integrate particulate matter from more and less intense portions of the

plume within one sample), samples up to 35 wt% Fe were collected.

Analysis of trace metal content (per g dry particulate matter) versus Fe

content indicate that Fe-enriched samples were also enriched (relative to

ambient background particles) in Zn, Cu, Cd, and Co by factors up to 40,

100, 50, and 8, respectively (Fig. 6.6). In contrast, particulate

content of Mn, Ca, and Al varied by only a factor of 2, in no systematic

relation to Fe content (Fig. 6.6). It was concluded that Ca and Al were

predominantly associated with ambient particulate matter ($CaCO_3$ and

aluminosilicates). Mn is highly enriched in vent fluid, but apparently

is oxidized only very slowly. No appreciable precipitation of Mn oxide

was apparent in the plume particles. Zn, Cu, Cd, and Co are associated

with the hydrothermal source.

Fig. 6.6 Regressions of particulate metals versus particulate Fe in samples from in and near TAG hydrothermal plume.

Al vs. Fe (per mass particulate)
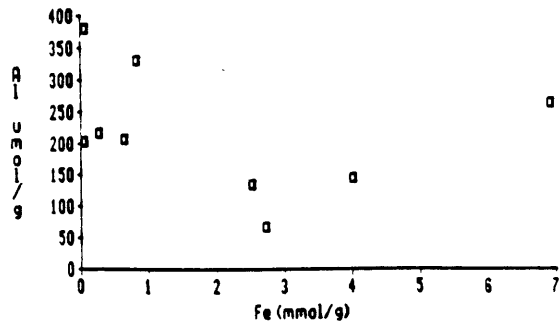
Ca (as CaCO3) vs. Fe (per mass particulate)
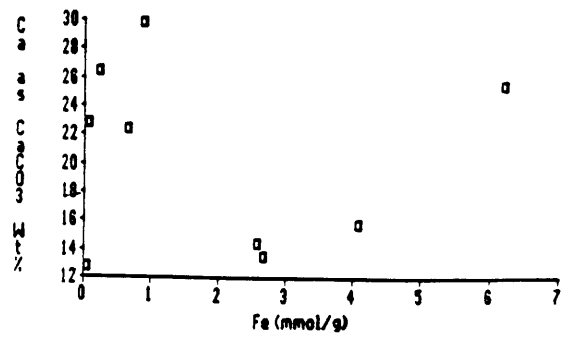
Mn vs. Fe (per mass particulate)
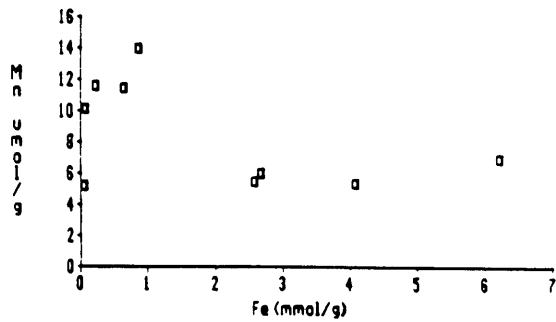
Co vs. Fe (per mass particulate)
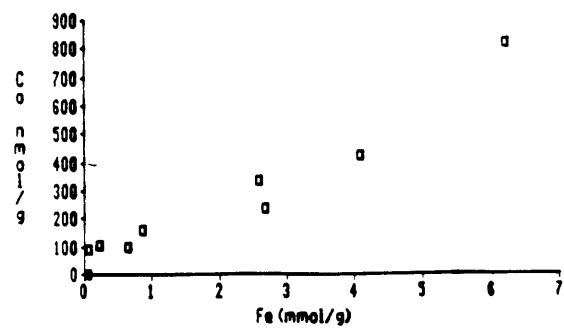
Cd vs. Fe (per mass particulate)
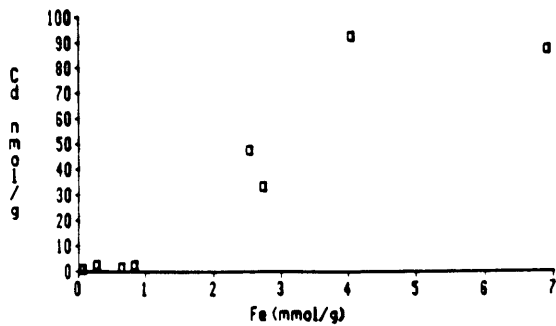
Zn vs. Fe (per mass particulate)
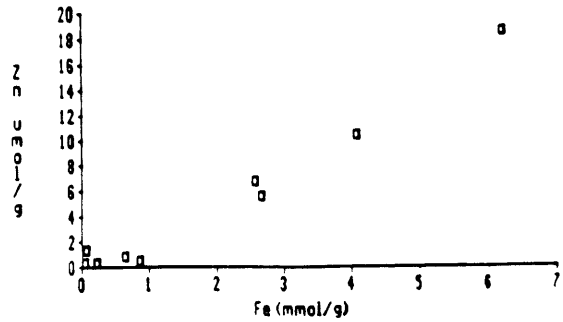
Cu vs. Fe (per mass particulate)
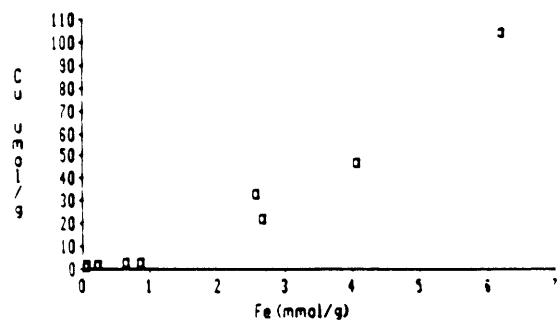
Fig. 6.7 Plots of metal/Fe ratio versus reciprocal of particulate Fe
concentration. Straight line indicates conservative behavior with
respect to particulate Fe. Note concave up lines for Cd, Zn, and Cu.

Al/Fe

Ca/Fe

Mn/Fe (x10E-3)

Co/Fe (x10E-6)

Cd/Fe (x10E-6)

Zn/Fe (x10E-3)

Cu/Fe (x10E-3)
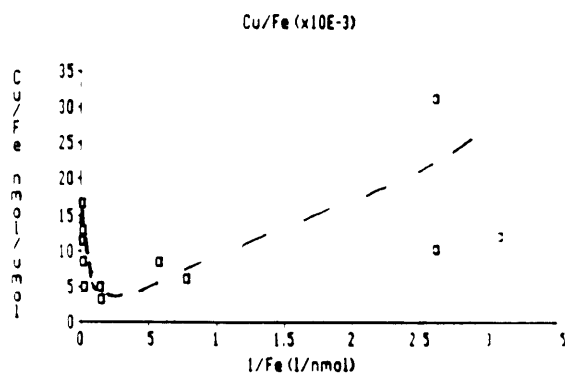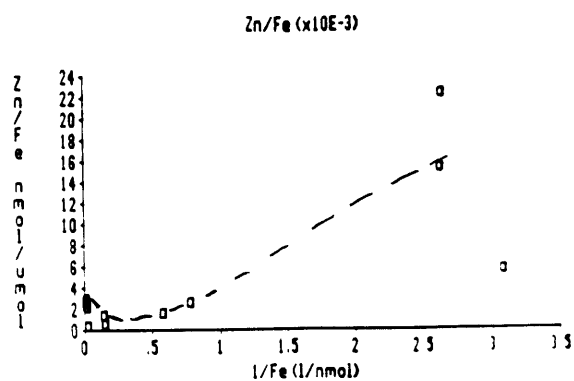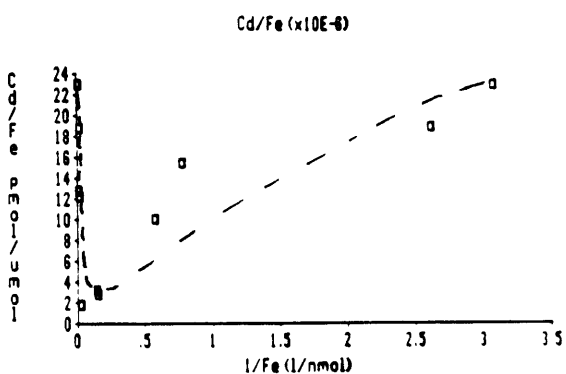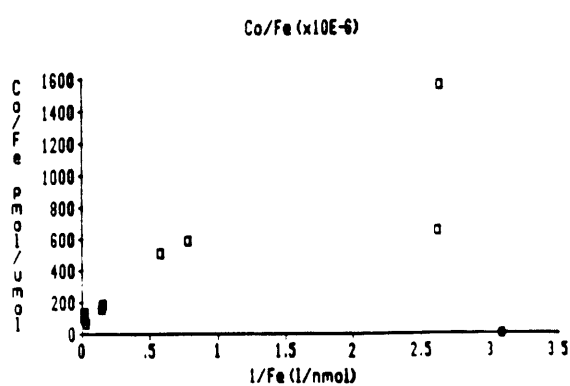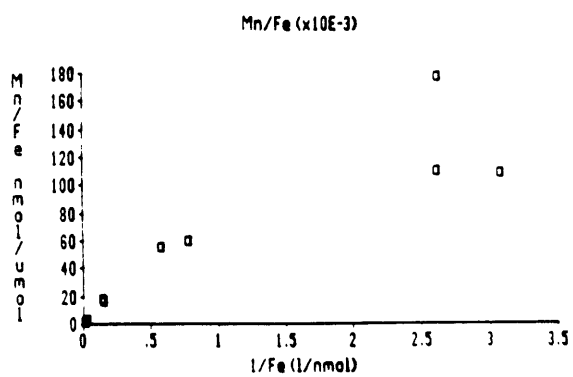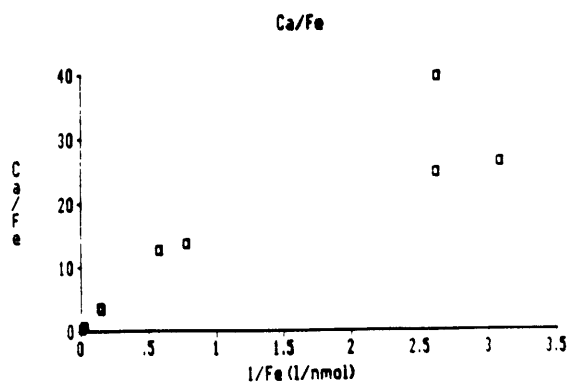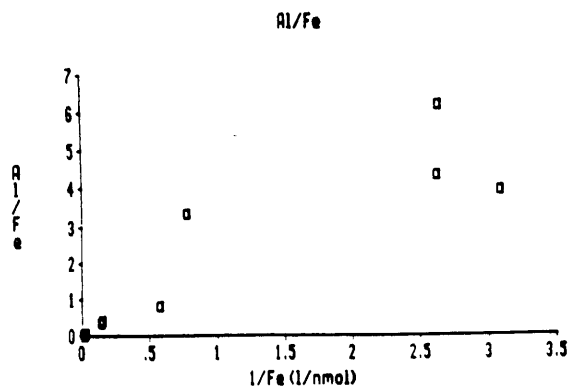
In a previous study of particle chemistry at the TAG site (Trocine and Trefry, 1988), particulate Fe was seen to vary linearly with total suspended matter and dissolved Mn, suggesting conservative mixing with little loss to dissolution or settling. Defining behavior for the other metals relative to Fe therefore provides an estimate of the degree and direction of non-conservative behavior within the plume. In order to identify processes other than mixing which alter metal content of plume particles, the data was modeled as a two-component mixing process, with particulate Fe as the independent variable. The results of this model are most graphically obvious in plots of metal/Fe ratio plotted against the reciprocal of the particulate Fe concentration (Fig. 6.7). Conservative behavior relative to particulate Fe is indicated by linearity of this regression. The results (Fig. 6.7) indicate a loss of Cd and, to a lesser extent, Zn and Cu, relative to Fe within this portion of the plume. In contrast, plots for Co, Mn, Ca, and Al appear approximately linear.

The observation that the Cd/Fe, Cu/Fe and Zn/Fe ratios all display minima at Fe concentrations equivalent to ~5 wt% Fe indicates that phases rich in these metals are somehow being lost during mixing. This could occur through dissolution, differential settling, loss to solution during oxidation of metal sulfides, or desorption of metals adsorbed to Fe oxides during very early stages of plume mixing. Particulate Co, in contrast, appears to remain tightly associated with Fe during mixing in this portion of the plume. If scavenging of seawater metals is occurring within the plume, any particulate metal contribution from this source is obscured by loss processes within this far-field regime. The results

complement the near-field work of Trocine and Trefry (1988) and suggest that transformations of metal composition within the plume are occurring not only immediately upon mixing in the upward flowing portion of the plume, but on time scales of hours-days and distance scales of kilometers in the more dispersed portion of the plume.

6.4. Conclusions

These results serve to illustrate the range of particulate metal environments in the North Atlantic. Hydrothermal precipitates can be viewed as an extreme exogenous source of particles to the deep water column. Distant from such perturbations, the particulate metal concentration in deep waters of the North Atlantic appears to be relatively constant.

REFERENCES

Bishop, J.K.B. and M.Q. Fleisher (1987) Particulate manganese dynamics in Gulf Stream warm-core rings and surrounding waters of the N.W. Atlantic. Geochim. Cosmochim. Acta, 51, 2807-2825.

Simpson, W.R., T.J.P. Gwilliam, V.A. Lawford, M.J.R. Fasham and A.R. Lewis (1987) In situ deep water particle sampler and real-time sensor package with data from the Madeira Abyssal Plain. Deep-Sea Res., 34, 1477-1497.

Trocine, R.P. and Trefry, J.H. (1988) Distribution and chemistry of suspended particles from an active hydrothermal vent site on the Mid-Atlantic Ridge at 26°N. Earth Planet. Sci. Lett. 88, 1-15.

CHAPTER 7

GENERAL CONCLUSION

In this research, samples of suspended particulate matter were collected for trace metal analysis from the full water column of an oligotrophic central-gyre station in the Sargasso Sea and a second station in the California Current, northeast Pacific. To collect relatively large samples, and to ensure freedom from metal contamination, a new in situ filtration method was devised. The samples were analyzed for major constituent elements and the trace metals Mn, Co, Pb, Zn, Cu, Ni, and Cd in order to investigate the role of suspended particulate matter in the marine geochemistry of these trace elements. Sampling in two distinct oceanographic regimes provided an opportunity to test the effect of particle composition and dissolved metal distributions on dissolved/particulate trace metal partitioning.

The first finding of this study was that particulate concentrations of most of the trace metals investigated were at least several times lower than previous estimates for intermediate and deep waters in the North Atlantic. The smooth profile shapes and consistency of the results from one station occupation to another lend confidence to the validity of the measurements. At the Bermuda station, concentrations of particulate metals generally increase with depth in the upper water column to values which are less than 5% of the total (dissolved plus particulate) concentrations for Cu, Zn, and Pb, and less than 1% for Ni and Cd. Deep water particulate concentrations of Al, Fe, Mn, and Co are ~10-50% of total. The measurements demonstrated at the outset of this research that

the new sampling and analytical method allowed the first realistic assessment of the role of fine, slowly-sinking particles in the marine geochemistry of these trace elements.

The analysis of a number of different trace elements, as well as major elements comprising the principal bulk phase components, provided the opportunity to investigate element associations which might suggest processes that control the trace metal content of marine particles. The Sargasso Sea results indicate a surprising correlation between profile shapes for particulate Co, Pb, Zn, Cu, and Ni and the shape of the particulate Mn profile. All showed surface depletion and a relative maximum at ~500m. This result suggests an important role for the formation of authigenic Mn in determining the particulate concentrations of other trace metals in open ocean sub-surface waters. The importance of other phases, such as organic particle coatings or authigenic Fe phases, in regulating particulate metal content cannot be ruled out, but bulk particle composition data revealed no evidence to support such control.

The mean concentrations of non-refractory particulate Mn, Co, and Cu at intermediate depths at the Pacific station were 3-5 times lower than observed in mid-waters at the Sargasso Sea station. This correlation further supported a role for Mn phases in determining the uptake of Co and Cu onto suspended particles. The reasons for the difference in particulate Mn concentration at the two stations were not unequivocally determined, but likely possibilities appear to be (1) low oxygen concentrations at the Pacific station may be maintaining the net production of oxidized Mn at low levels, and/or (2) an advective source

of dissolved Mn via ventilation of thermocline waters with higher latitude surface water may provide a source for Mn oxidation in the Sargasso Sea main thermocline.

In addition to this apparent association of some metals with inorganic particulate components, the importance of biological processes in controlling particulate metal content was evident for Cd and Zn. Both metals were enriched in surface particulate matter at the relatively more productive Pacific site. This was probably the result of a less "reworked" biogenic particle population at the Pacific site, i.e. a larger fraction of living particles producing metal partitioning more representative of uptake fractionation during organism growth than of net growth/recyling processes. The effect of surface biological processes was evident throughout the upper water column at the Pacific station; the Cd/P ratio in the surface suspended particles, which was an order of magnitude higher than at the Sargasso station, decreased with depth, but remained elevated relative to the Sargasso profile, and relative to the dissolved Cd/P ratio, to about 1000m. In the deeper water column, the particulate Cd/P ratio, and the particulate Cd, Ni, and Zn content were remarkably similar at the two stations, despite the differences in surface productivity and in dissolved concentrations of these metals. This suggested a behavior different from Mn, Co or Cu. Therefore, at these two stations, the deep particulate content of the "nutrient-type" metals appears to be relatively independent of differences in bulk particle composition, and of biological activity in overlying surface waters.

To investigate the relationship between trace metals associated with fine suspended particles and the total vertical flux of metals observed in the deep ocean, a simple particle interaction/flux model was constructed for the Sargasso Sea station. The complexities of oceanic particle interactions were simplified by classifying particulate matter into only two size classes: small suspended particles represented by the samples collected by in situ filtration, and large fast-sinking particles/aggregates which dominate the sinking flux and are sampled with sediment traps. The flux due to the removal of suspended particulate trace metals was calculated from the particulate metal concentrations measured in this study, and the small particle residence time estimated by comparing deep suspended and sinking particulate ^{230}Th. A comparison of this calculated flux to the total sediment trap flux measured in deep water at this station reveals that interactions between suspended and sinking particles contribute less than 30% of the total observed flux for all of the metals examined here, with the exception of Cu (40%) and Cd (50%). This result suggests that, while suspended particles may be removed largely by aggregation onto faster-sinking large particles, these large particles carry a complement of metals from surface waters which is greater than the contribution via deep ocean suspended particles. To the extent that the Sargasso station can be considered representative of the oligotrophic central gyre ocean, the implication is that metal removal in the oceans is controlled largely by processes occurring at the ocean boundaries (e.g surface waters, in this case), and may be only secondarily dependent on the degree or mechanism of metal/particle interactions in the ocean interior.

An assumption inherent in this model is that small suspended particles, rather than large aggregates, dominate interactions with dissolved metals because of their abundance and available surface area. If this is true, it would be instructive to know how rapidly dissolved/particulate exchange occurs relative to the residence time of the suspended particles. This question was investigated by measuring stable Pb isotope ratios and the ratio of total Pb to ^{210}Pb in suspended particles and in seawater at the Sargasso Sea station. Vertical variations in the isotopic composition of the dissolved Pb pool were almost perfectly matched throughout the upper 2000m by the composition of Pb in suspended particles, suggesting that isotopic equilibration occurs faster than the particles are removed. This indicates that the partitioning of Pb between dissolved and suspended particulate phases in the open ocean is not controlled by particle residence time, but must instead be determined by the Pb binding capacity of the particles. It is not known whether rapid exchange occurs for other metals as well. The comparison of particulate and dissolved metal distributions at the two stations revealed that Pb was the only element of those investigated which showed similar dissolved/particulate fractionation at different dissolved concentration. Thus Pb behavior may resemble that of Th, but may be a poor analog for dissolved/particulate exchange processes for other trace elements.

Further investigation of scavenging processes by careful collection and analysis of suspended particulate matter would be fruitful. For example, analysis of rare earth elements in similarly collected samples would clarify the role of _in situ_ scavenging in establishing the relative

concentrations of this coherent group of elements in the ocean. The results of the Pb isotope study could be tested for other elements with appropriate isotopic systematics. For instance, with sufficient analytical sensitivity, a similar study could be carried out with neodymium isotopes to determine whether equilibration occurs for elements which are less particle-reactive than Pb. A natural extension of this work is to sample a central-gyre station in the North or South Pacific, where particle composition might be similar to that found at the Sargasso station, but dissolved metal distribution would resemble the California Current station.

APPENDIX A

Northwest Atlantic suspended particulate data

Table A.1. Particulate elemental composition, Sargasso Sea, 1986-87,
(per volume seawater)

Cruise	Depth (m)	Volume (liters)	Mass Conc ug/l	Zn pmol/l	Cu pmol/l	Co pmol/l	Pb pmol/l
EN 148	980	607	7.23	9.39	15.1	1.86	2.54
		607					2.60
		607					2.50
	1500	450	10.37	10.58	13.8	1.78	3.73
		450					3.87
		450					3.91
	2000	697	5.72	5.37	12.9	1.28	1.87
		697					1.54
		697					2.12
	2990	765	5.06	4.99	14.2	1.16	1.50
		765					1.46
		765					1.74
	4000	562	10.46	14.80	11.9	3.01	1.65
		562					1.64
		562					1.74
EN-157	300	241	18.46	9.09	8.1	.51	.83
		241					.95
		241					1.04
0.4um	300	120	20.80	8.92	11.9	.30	.75
	905	710	6.87	7.35	13.5	1.66	2.37
		710	6.87	6.96	14.2	1.70	2.06
		710					2.30
		710					2.21
	1810	733	4.91	4.97	11.1	1.09	1.42
		733					1.69
		733					1.68
	2715	951	6.38	9.06	13.4	1.13	1.56
		951					1.49
		951					1.54
	3800	548	11.29	12.76	16.0	2.85	1.44
		548					1.26
		548					1.48
WE 9-87	100	415	19.13	4.24	3.4	.65	.96
		415	19.13	7.45	4.0	.65	.99
		415					.98
	750	1026	6.47	15.89	23.8	1.92	2.12
		1026	6.47	8.64	14.5	1.47	2.13
		1026					2.27

Table A.1. (continued)

Cruise	Depth (m)	Cd pmol/l	PO4 nmol/l	Mn pmol/l	Ca nmol/l	Al nmol/l	Fe nmol/l
EN 148	980	.118		192.8	29.4	3.51	1.48
	1500	.090		228.9	34.3	6.07	2.18
	2000	.027		122.1	17.3	3.92	1.32
	2990	.029		132.0	16.7	3.32	1.42
	4000	.044		210.0	21.2	25.62	7.47
EN-157	300	.287		81.3	61.2	1.15	.24
0.4um	300	.297		90.8	48.5	.71	.09
	905	.077		159.6	22.2	3.51	1.20
		.065		152.8	24.4	2.82	1.17
	1810	.033	.371	103.3	15.4	3.11	1.17
	2715	.055	.315	126.4	19.1	3.39	1.16
	3800	.037	.336	186.3	15.8	23.72	6.35
WE 9-87	100	.359		7.9	33.3	.96	.42
	100	.395		10.0		1.59	.47
	750	.101		168.8	26.2	3.70	1.35
	750	.082		137.6		2.69	1.04

Table A.2.   Particulate elemental composition, Sargasso Sea, 1986-87,
(per gram dry particles)

Cruise	Depth (m)	CaCO3 Wt. %	Est.Al-Si Wt. %	Zn umol/g	Cu umol/g	Co nmol/g	Pb nmol/g
EN 148	980	40.7	13.1	1.30	2.09	257.3	350.7
							359.8
							346.1
	2000	30.2	18.5	.94	2.26	223.2	326.0
							268.3
							371.2
	2990	33.0	17.7	.99	2.80	229.7	296.8
							289.1
							343.3
	4000	20.3	66.1	1.42	1.14	287.4	158.2
							156.5
							166.7
EN-157	300	33.2	1.7	.49	.44	27.9	45.0
							51.7
							56.2
0.4um	300	23.3	.9	.43	.57	14.4	36.1
	905	32.4	13.8	1.07	1.96	242.0	344.5
		35.6	11.1	1.01	2.06	248.2	299.4
							334.3
							322.0
	1810	31.4	17.1	1.01	2.25	222.2	288.9
							344.4
							341.7
	2715	29.9	14.3	1.42	2.10	176.3	243.9
							234.0
							240.6
	3800	14.0	56.7	1.13	1.42	252.1	127.7
							111.5
							130.9
WE 9-87	100	17.4	1.4	.22	.18	34.0	50.4
			2.2	.39	.21	34.0	51.6
							51.0
	750	40.5	15.5	2.45	3.67	296.7	326.8
			11.2	1.33	2.24	227.4	329.8
							350.9

Table A.2.   (continued)

Cruise	Depth (m)	Cd nmol/g	Mn umol/g	Ca mmol/g	Al mmol/g	Fe mmol/g
EN 148	980	16.28	26.64	4.07	.49	.20
	2000	4.79	21.34	3.02	.68	.23
	2990	5.73	26.07	3.30	.66	.28
	4000	4.17	20.07	2.03	2.45	.71
EN-157	300	15.54	4.41	3.32	.06	.01
0.4um	300	14.26	4.37	2.33	.03	
	905	11.16	23.24	3.24	.51	.17
		9.54	22.25	3.56	.41	.17
	1810	6.78	21.03	3.14	.63	.24
	2715	8.60	19.81	2.99	.53	.18
	3800	3.28	16.50	1.40	2.10	.56
WE 9-87	100	18.77	.41	1.74	.05	.02
		20.65	.53		.08	.02
	750	15.66	26.08	4.05	.57	.21
		12.73	21.27		.42	.16

Table A.3. Particulate elemental composition, Sargasso Sea, 1988,
(per volume seawater)

Cruise	Depth (m)	Volume (liters)	Mass Conc ug/l	incl >53um	Est.Corg nmol/l	Zn pmol/l	Cu pmol/l	Ni pmol/l	Co pmol/l	Pb pmol/l
WE 3-88	10	224	25.98	31.78	746	4.46	7.05	4.9	1.03	.47
										.94
										1.00
	100	361	16.96	22.26	448	7.26	7.98	7.2	1.02	.96
										1.69
										1.01
	200	760	8.97	10.17	150	8.43	10.79			1.83
								6.8	1.68	1.80
								9.7		1.62
	494	1053	8.35	9.85	129	11.74	21.66	8.3	1.79	2.76
						10.97				3.04
						11.58				2.87
	608	1094	6.58	7.28	93	9.04	16.69	8.0	2.09	2.54
										2.36
										2.61
	861	1182	5.60	6.00	77	7.93	15.97	6.0	1.76	2.07
										2.02
										2.35
	1013	1026	5.85	6.35	76	6.62	15.24	7.0	1.61	2.04
										2.12
										2.01
	1483	1529	5.88	6.88	80	8.40	16.75	5.4	1.60	2.44
										2.39
										2.34
	2000	1342	4.75	5.35	31	7.12	18.30	4.6	1.24	2.28
										2.30
										2.41
OC 197 Sta. 1	10	65	147.69			232.31	24.62			5.54
	88	289	92.39			93.08	28.03			20.21
Sta. 2	20	141	31.21			8.51	12.77			.99
	468	775	25.81			30.97	24.00			5.39
	2724	757	6.74			8.98	20.48			2.11
Sta. 3	50	197	19.80			6.09	6.60			.46
	783	1124	7.47			39.59	18.06			3.67
	3000	1181	5.25			7.79	17.27			1.99
Sta. 4	50	207	23.19			4.83	4.83			.53
	790	1203	6.82			8.89	16.04			2.47
	2847	1263	3.64			5.15	23.12			1.67
Sta. 5	50	148	41.89		926		6.42	5.4	1.01	1.30
										1.38
										2.67
	330	957	8.88		129	12.24	17.17	7.8	1.83	3.09
										2.32
										2.57
	1450	1199	4.67		49	7.03	17.91	4.6	1.27	2.27
										2.21
										1.89

Table A.3. (continued)

Cruise		Depth (m)	Cd pmol/l	PO4 nmol/l	Mn pmol/l	Si,opal nmol/l	Ca nmol/l	Al nmol/l	Fe nmol/l
WE 3-88		10	.188	2.335	52.2	10.3	70.5	1.08	.31
					60.4				
					65.4			1.45	
		100	.265	2.008	47.6	17.3	47.4	.93	.25
				2.075	53.7				
					51.9				
		200	.129	.618	193.7	4.4	47.9	1.03	.39
		494	.098	.425	224.3	5.3	42.0	2.52	.85
		608	.092	.304	206.3	3.5	32.7	3.14	.80
		861	.066	.239	131.6	3.3	24.3	4.01	1.09
		1013	.075	.254	139.3	5.6	26.7	3.60	1.20
		1483	.061	.278	162.6	5.5	26.1	3.56	1.16
		2000	.029	.208	137.0	5.0	23.2	4.97	1.36
								4.52	
								5.10	
OC 197	Sta. 1	10	25.692					18.46	
		88	1.592					94.81	
	Sta. 2	20	.631					1.84	
		468	.425					30.71	
		2724	.038					10.30	
	Sta. 3	50	.315					.41	
		783	.103					4.72	
		3000	.019					5.89	
	Sta. 4	50	.420					1.69	
		790	.064					3.42	
		2847	.008					3.91	
	Sta. 5	50	.388		16.7	59.3	146.4	2.16	.28
		330	.099		241.6	12.4	43.0	1.82	.50
		1450	.038		130.9	5.2	20.5	4.05	1.19

Table A.4. Particulate elemental composition, Sargasso Sea, 1988,
(per gram dry particles)

Cruise	Depth (m)	CaCO3 Wt. %	Al-Si Wt. %	opal Wt. %	org.mat. Wt. %	Zn umol/g	Cu umol/g	Ni umol/g	Co nmol/g	Pb nmol/g
WE 3-88	10	27	1.1	2.8	69	.17	.27	.19	39.5	18.2
										36.3
			1.5							38.7
	100	28	1.5	7.1	63	.43	.47	.42	60.4	56.9
										99.8
										59.8
	200	53	3.1	3.4	40	.94	1.20			203.7
			3.2					.76	187.8	201.1
			4.5					1.09		180.8
	494	50	8.1	4.4	37	1.41	2.59	.99	215.0	330.8
						1.31				364.5
						1.39				344.4
	608	50	12.9	3.7	34	1.37	2.54	1.22	318.1	386.0
										358.1
										397.2
	861	43	19.3	4.2	33	1.42	2.85	1.07	314.4	369.8
										360.6
										419.4
	1013	46	16.6	6.8	31	1.13	2.61	1.20	274.9	349.2
										361.9
										343.9
	1483	44	16.3	6.5	33	1.43	2.85	.91	272.7	414.8
										406.5
										398.1
	2000	49	28.2	7.4	16	1.50	3.85	.97	260.2	479.6
			25.6							484.8
			28.9							506.0
OC 197 Sta. 1	10					1.57	.17			37.5
	88					1.01	.30			218.7
Sta. 2	20					.27	.41			31.8
	468					1.20	.93			209.0
	2724					1.33	3.04			313.7
Sta. 3	50					.31	.33			23.1
	783					5.30	2.42			491.7
	3000					1.48	3.29			379.0
Sta. 4	50					.21	.21			22.9
	790					1.30	2.35			362.2
	2847					1.41	6.35			458.7
Sta. 5	50	35	1.4	10.0	53	.08	.16	.13	24.6	31.4
										33.4
										64.7
	330	50	5.7	10.0	35	1.41	1.98	.90	210.5	355.4
										267.4
										295.3
	1450	44	23.4	7.7	25	1.51	3.84	.98	271.4	486.1
										474.1
										405.5

Table A.4. (continued)

Cruise		Depth (m)	Cd nmol/g	PO4 umol/g	Mn umol/g	Si,opal mmol/g	Ca mmol/g	Al mmol/g	Fe mmol/g
WE 3-88		10	7.22	89.9	2.01	.40	2.72	.04	.012
					2.32				
					2.52			.06	
		100	15.63	118.4	2.81	1.02	2.80	.05	.015
				122.4	3.16				
					3.06				
		200	14.38	69.0	21.60	.49	5.34	.12	.044
								.12	
								.17	
		494	11.73	50.9	26.87	.63	5.04	.30	.101
		608	13.94	46.2	31.34	.53	4.96	.48	.122
		861	11.77	42.6	23.52	.60	4.34	.72	.195
		1013	12.75	43.5	23.81	.97	4.56	.61	.205
		1483	10.44	47.3	27.66	.93	4.44	.61	.198
		2000	6.19	43.7	28.82	1.05	4.89	1.05	.287
								.95	
								1.07	
OC 197	Sta. 1	10	173.96					.12	
		88	17.23					1.03	
	Sta. 2	20	20.23					.06	
		468	16.45					1.19	
		2724	5.69					1.53	
	Sta. 3	50	15.90					.02	
		783	13.81					.63	
		3000	3.71					1.12	
	Sta. 4	50	18.12					.07	
		790	9.39					.50	
		2847	2.17					1.07	
	Sta. 5	50	9.40		.40	1.44	3.55	.05	.007
		330	11.34		27.81	1.43	4.95	.21	.058
		1450	8.16		28.04	1.10	4.38	.87	.255

Table A.5. Particulate ^{210}Pb and ^{206}Pb/^{207}Pb, Bermuda, 1987-88

Cruise	Depth	Pb-210 dpm/100kg	Pb/Pb-210 pmol/dpm	Pb 206/207
WE 9-87	750	.236	926	
WE 3-88	10	.224	379	
	100	.218	498	1.1902
	200	.312	558	1.1933
	494	.347	838	1.1965
	608	.265	941	1.1948
	861	.240	898	1.1889
	1013	.249	827	1.1877
	1483	.298	798	1.1876
	2000	.343	680	1.1854
EN 157	300			1.1895
	905			1.1912
	1810			1.1862
	2715			1.1903
	3800			1.1959

APPENDIX B

Northeast Pacific station: suspended particulate
and hydrographic data

Table B.1.   Particulate elemental composition, Pacific, June 1988, (per volume seawater)

Cruise	Depth (m)	Volume (liters)	Mass Conc ug/l	Est.Corg nmol/l	Zn pmol/l	Cu pmol/l	Ni pmol/l	Co pmol/l	Pb pmol/l
AII 118	30	186	34.92	1444	22.80	4.78	5.4	2.31	.68
									.57
									.81
	100	271	24.31	848	25.76	8.23	8.5	1.96	1.31
									1.42
									1.39
	183	427	40.51	851	67.61	29.41	67.9	7.66	5.37
									4.88
									5.03
	287	456	28.37	677	42.28	18.42	38.8	4.23	1.83
						20.79			3.57
						31.86			3.68
	397	675	15.76	367	28.16	17.79	22.8	2.49	1.74
									1.67
									1.81
	491	537	12.71	270	21.79	15.57	23.8	2.18	1.30
							21.2		1.28
									1.23
	686	722	12.21	192	25.24	18.70	24.1	2.19	1.18
									1.31
									1.22
	983	896	11.61	257	19.75	13.46	19.2	1.86	.89
									.80
									.95
	1439	667	10.42	169	20.82	17.30	19.3	2.22	1.09
									1.34
									.90
	1918	1235	8.60	134	19.86	24.44	19.0	2.06	1.23
									1.34
									1.36
	2353	1096	13.22	205	33.59	36.48	32.8	4.33	2.36
									2.41
									2.22
	2872	745	13.46	182	29.77	41.93	34.1	5.60	2.93
						42.35			2.72
						43.33			3.18

Table B.1. (continued)

Cruise	Depth (m)	Cd pmol/l	PO4 nmol/l	Mn pmol/l	Ca nmol/l	Al nmol/l	Fe nmol/l
AII 118	30	4.591	3.04	17.3	1.9	.27	.10
	100		2.11				
		2.361	2.32	231.7	17.6	8.12	2.40
	183	1.524	2.84	544.0	37.6	60.42	18.92
	287	1.359	1.91	237.3	27.6	34.65	10.29
				261.6		37.94	
				280.3		42.32	
	397	.877	1.11	180.6	31.3	14.16	4.36
	491	.479	.72	138.5	18.5	16.20	4.47
	686	.256	.73	128.8	15.1	22.58	6.02
	983	.149	.62	116.5	12.4	15.51	5.27
	1439	.118	.59	142.1	8.7	20.39	5.89
	1918	.108	.52	354.1	7.4	17.17	5.27
	2353	.149	.67	1368.9	6.1	28.47	9.00
	2872	.109	.60	1887.9	3.9	32.21	9.68
	2872			1914.0		33.83	
	2872			2029.7		30.34	

Table B.2. Particulate elemental composition, Pacific, June 1988,
(per gram dry particles)

Cruise	Depth (m)	CaCO3 Wt. %	Est.Al-Si Wt. %	Est. Orgm Wt. %	Zn umol/g	Cu umol/g	Ni umol/g	Co nmol/g	Pb nmol/g
AII 118	30	.5	.2	99.3	.65	.14	.15	66.2	19.6
									16.3
									23.2
	100	7.3	9.0	83.7	1.06	.34	.35	80.5	53.7
									58.5
									57.4
	183	9.3	40.3	50.4	1.67	.73	1.68	189.1	132.6
									120.5
									124.1
	287	9.7	33.0	57.3	1.49	.65	1.37	149.2	64.6
			36.1	63.9		.73			125.9
			40.3	59.7		1.12			129.7
	397	19.9	24.3	55.9	1.79	1.13	1.45	157.9	110.6
									105.6
									115.0
	491	14.6	34.4	51.0	1.71	1.22	1.87	171.4	102.1
							1.67		100.8
									97.1
	686	12.3	49.9	37.7	2.07	1.53	1.97	179.3	96.8
									107.5
									100.1
	983	10.7	36.1	53.2	1.70	1.16	1.65	160.6	76.8
									69.0
									81.8
	1439	8.3	52.8	38.8	2.00	1.66	1.86	212.9	105.0
									128.7
									86.3
	1918	8.7	53.9	37.4	2.31	2.84	2.21	239.2	143.4
									155.6
									158.0
	2353	4.7	58.1	37.2	2.54	2.76	2.48	327.8	178.5
									182.4
									167.9
	2872	2.9	64.6	32.4	2.21	3.12	2.53	416.0	217.5
			67.9	32.1		3.15			202.0
			60.9	39.1		3.22			236.6

Table B.2. (continued)

Cruise	Depth (m)	Cd nmol/g	PO4 umol/g	Mn umol/g	Ca mmol/g	Al mmol/g	Fe mmol/g
AII 118	30	131.47	87.1	.5	.05	.01	.003
	100	97.13	95.3	9.5	.73	.33	.099
			86.8				
	183	37.63	70.1	13.4	.93	1.49	.467
		47.90	67.3	8.4	.97	1.22	.363
				9.2		1.34	
	287			9.9		1.49	
	397	55.61	70.7	11.5	1.99	.90	.276
	491	37.70	56.2	10.9	1.46	1.27	.352
	686	20.96	60.1	10.6	1.23	1.85	.494
	983	12.86	53.6	10.0	1.07	1.34	.454
	1439	11.29	56.5	13.6	.83	1.96	.565
	1918	12.58	60.9	41.2	.87	2.00	.613
	2353	11.30	51.0	103.5	.47	2.15	.681
	2872	8.12	44.3	140.3	.29	2.39	.719
				142.2		2.51	
				150.8		2.25	

Table B.3. Pacific hydrographic data (plus dissolved Cd).

	depth m	Salinity ppt	in-situ T deg C	Cd pM	PO4 µM	SiO2 µM	O2 mM
1	0			78		3.4	
2	10	32.439		46	0.52	3.7	260.5
3	15			79	0.41	3.5	281.1
4	20					2.7	
5	40			145	0.79	6.3	288.3
6	40	32.656		150	0.81	7.0	
7	65			352	1.33	16.6	229.4
8	84	33.253		364	1.55	20.4	211.1
9	90			574	1.90	22.8	171.7
10	90					28.4	
11	96	33.392				23.0	
12	110	33.538	8.77	518	1.86	26.5	183.3
13	173					41.0	
14	177	33.923		654	2.15	37.8	170.6
15	193	33.984	7.62	721	2.29	42.2	119.6
16	270	34.025	6.69	722	2.59	53.5	96.7
17	288					52.3	
18	295					58.0	
19	308			744	2.60	55.1	95.5
20	363	34.060		833	2.88	68.5	
21	387					65.2	
22	393					80.0	
23	407			837	2.89	68.5	63.0
24	461	34.087	5.20	873	3.04	80.0	54.2
25	479	34.110				83.8	
26	481	34.097				82.8	
27	486	34.091	5.03	888	3.23	81.9	49.1
28	491		4.85			85.6	
29	600	34.185				96.2	
30	610	34.200		914		97.1	
31	666	34.285				105.7	
32	676	34.274	4.33	985	3.33	106.1	68.4
33	723	34.301				109.5	
34	733	34.302		925	3.33	110.9	19.1
35	847	34.370				118.5	
36	857	34.371	3.90	960	3.39	119.9	16.5
37	953	34.420	3.62	979	3.34	126.6	26.4
38	959	34.410				124.7	
39	973	34.426				126.1	
40	974	34.425	3.57	972	3.40	128.5	22.0
41	1187	34.473		908	3.36	138.9	31.3
42	1221					141.3	
43	1231	34.491				142.2	
44	1400	34.521				151.7	
45	1419	34.538				154.1	
46	1429	34.540	2.55	1031	3.29	153.6	49.9
47	1467	34.540		933	3.33	154.6	80.3
48	1666	34.562				159.4	
49	1876	34.607		1065		169.3	
50	1899	34.602				171.2	
51	1909	34.602		929	3.07	171.7	70.9
52	1961	34.590		942	2.98	170.7	
53	2154					169.7	
54	2333	34.632				176.9	
55	2343	34.626	1.80	988	3.04	175.0	90.3
56	2454	34.630	1.81	943	2.99	176.9	
57	2862		1.70			170.7	

APPENDIX C

Analyses of filter rinsing solutions (Zn and Cd): Bermuda and Northeast
Pacific stations

Table C.1. Zn and Cd in filter rinse solutions, Bermuda

Cruise	Depth (m)	Rinse vol (1)	Zn rinse nM	Cd rinse pM	%Zn lost	%Cd lost
WE 3-88	200	.130	.6	40	1.2	5.3
	10	.135	2.2	100	29.7	32.1
	494	.145	6.4	0	7.5	0.0
	100	.130	4.9	150	24.3	20.4
	1013	.115	1.8	150	3.0	22.5
	608	.140	3.3	190	4.7	26.5
	861	.135	6.3	230	9.1	39.9
	1483	.130	7.0	240	7.1	33.3
	2000	.115	8.1	210	9.7	61.1
OC 197	50	.125	5.1	310	138.6	67.5
	350	.085	10.8	610	7.8	55.0
	1450	.140	19.5	520	32.4	159.3
	dip,1200m	.140	3.8	0		
WE 3-88	Rinse bl1	.115	.6	0		
	Rinse bl2	.070				
OC 197	Rinse bl1	.070	.4	0		
	Rinse bl2	.075	2.0	0		

Table C.2.   Zn and Cd in filter rinse solutions, Northeast Pacific

Cruise	Depth (m)	Rinse vol (1)	Zn rinse nM	Cd rinse pM	%Zn lost	%Cd lost
AII 118	500	.130	4.1	820	4.6	41.4
	1000	.145	8.6	520	7.0	56.4
	1500	.115	6.7	700	5.5	102.5
	2000	.150	9.0	160	5.5	18.0
	750	.115	11.2	340	7.1	21.2
	2500	.150	4.6	160	1.9	14.7
	100	.105	5.5	1130	8.3	18.5
	200	.140	6.0	840	2.9	18.1
	30	.120	10.9	1790	30.8	25.2
	400	.165	4.5	1740	3.9	48.5
	300	.130	8.7	1560	5.9	32.7
	3000	.160	7.4	1700	5.3	334.2
	dip blk	.090	6.4	270		

APPENDIX D

TAG hydrothermal area: particulate data

Table D.1. Particulate elemental composition, TAG hydrothermal plume and off-axis samples.

Location:cast	Depth meters	Volume liters	Mass ug/l	Zn pmol/l	Cu pmol/l	Co pmol/l	Cd pmol/l	Mn pmol/l	Ca nmol/l	Al nmol/l	Fe nmol/l
TAG:3	3290	240	21.8	145.83	707.5	7.08	1.03	118.3	30.8	2.92	55.00
:4	3290	428	8.2	4.39	22.8	1.23	.02	112.1	23.7	2.71	6.82
:5	3315	188	25.3	261.70	1159.0	10.59	2.34	132.4	39.5	3.67	101.60
:6	2610	488	6.8	2.93	14.5	.87	.02	96.3	21.8	1.45	1.74
:7	3375	432	10.9	9.19	33.7	1.09	.02	125.9	24.7	2.25	6.99
:8	3355	270	28.9	167.41	658.1	6.85	.95	177.0	40.0	1.96	78.52
:9	3340	223	14.1	293.27	1630.5	12.83	1.24	109.9	40.4	3.68	97.31
:11	3330	287		19.06	200.5	2.91	.07	125.1	29.1	2.68	40.31
26N,46W:12	1815	419	6.2	1.81	3.9	0.00	.01	34.8	8.5	1.26	.32
" : unrinsed		419	6.2	8.50	12.0	.59	.01	67.5	15.2	2.36	.38
26N,42W:14	2000	413		3.44	8.0	.75	.02	77.2	17.5	4.29	1.28
	3300	230		5.78	3.9	.25		42.2	9.4	1.65	.38

Location:cast	Depth meters	Zn/Fe x10E-3	Cu/Fe x10E-3	Co/Fe x10E-6	Cd/Fe x10E-6	Mn/Fe x10E-3	Al/Fe	Ca/Fe
TAG:3	3290	2.65	12.9	129	18.8	2.2	.05	.56
:4	3290	.64	3.3	180	2.7	16.4	.40	3.47
:5	3315	2.58	11.4	104	23.0	1.3	.04	.39
:6	2610	1.68	8.3	500	10.0	55.3	.84	12.54
:7	3375	1.31	4.8	156	3.1	18.0	.32	3.54
:8	3355	2.13	8.4	87	12.1	2.3	.03	.51
:9	3340	3.01	16.8	132	12.8	1.1	.04	.42
:11	3330	.47	5.0	72	1.8	3.1	.07	.72
26N,46W:12	1815	5.59	12.0	0	22.8	107.4	3.90	26.18
" : unrinsed		22.25	31.3	1556	18.8	176.9	6.19	39.79
26N,42W:14	2000	2.68	6.2	581	15.5	60.2	3.34	13.64
	3300	15.11	10.2	659		110.2	4.32	24.57